UNIVERSITAT ROVIRA i VIRGILI

International Erasmus Mundus Master in

QUATERNARY AND PREHISTORY

Erasmus Mundus

Paleoecology and dietary habits of cave bear lineage through stable isotopes analyses ($\delta^{13}C$ and $\delta^{18}O$) and dental microwear on *Ursus deningeri* from Vallparadís Section (Terrassa, Vallès-Penedès Basin, NE Iberian Peninsula)

VÍCTOR VIZCAÍNO VARO

Supervisor/s: JOAN MADURELL-MALAPEIRA, FLORENT RIVALS, CARLOS TORNERO, BIENVENIDO MARTÍNEZ-NAVARRO

Academic year 2022/2023

I would like to thank all my supervisors, who put the effort and time so that I learn the useful methodologies here applied to make insights about dietary habits of the past. I also thank family and friends for any support provided.

Cover illustration: Leonardo Sorbelli

Content

Abstract

Dietary habits for the cave bear lineage have been studied previously for the Early Pleistocene ursids from Dmanisi (1.8 Ma) and Orce sites (1.6 – 1.2 Ma), and their diet was found to be omnivorous with a substantial consumption of meat and fish in both cases. The present study represents the chronological continuation of these previous published works. Therefore, here we present a multiproxy approach using two methods, namely tooth microwear, and stable isotopes analyses ($\delta^{13}C$ and $\delta^{18}O$) on tooth enamel, both performed on *Ursus deningeri* from levels EVT7/CGR7 (0.86 Ma) and EVT12 (1.07-0.99 Ma) from the Vallparadís Section (NE Iberian Peninsula). For the isotopic analyses we used the former species and other eight more taxa of carnivores and ungulates, with a total of 112 samples, while five lower first molars were analyzed for dental microwear and compared with extant and extinct bears. These combined methodologies provide complementary data since microwear studies yield information about the diet of last days/weeks of the individual while stable isotopes analyses give data from the tooth growth time. Our preliminary results indicate a diet for *U. deningeri* based on C3 plants regarding the stable isotopes analyses, and an omnivorous diet based on the dental microwear analyses. Our study provides information about the paleoecology of ursids from the '*Early to Middle Pleistocene Transition*' in the Vallparadís Section, although further research with a wider sampling regarding the dental microwear analyses will be necessary for a more complete understanding and interpretation of the diet of this species.

Keywords*:* Ursus deningeri, *Vallparadís Section*, *stable isotopes*, *dental microwear*, *Early Pleistocene.*

1. Introduction

1.1. Aims of this work

This work represents the necessary continuation on previous works recently published by our research team and focused on the dietary patterns of Early Pleistocene ursids and specifically trying to decipher when, where and why the cave bear lineage started their adaptation towards a herbivorous diet (Medin et al., 2017, 2019).

In Medin et al., (2017), they studied the Late Villafranchian carnivore guild from Orce sites: Venta Micena, that dates from 1.6-1.5 Ma (Martínez-Navarro, 1991; Oms et al., 2000); Barranco León, with a chronology of 1.43 ± 0.38 Ma (Toro-Moyano et al., 2013); Fuente Nueva-3, that dates from 1.19 ± 0.21 Ma (Duval et al., 2012). Among the studied carnivore assemblage, they focused on the ursid material (*Ursus etruscus*) whose dietary habits were analyzed through a multiproxy approach by using dental morphology and microwear. The results showed a clear omnivorous diet in the three studied sites, regarding the morphologically analyzed bunodont dentition and the tooth microwear, close to that from the extant brown bear (*Ursus arctos*).

Surprisingly, the isotopic data from Venta Micena specimens showed some divergent results (Palmqvist & Arribas, 2001; Palmqvist et al., 2003; Mendoza et al., 2005; Palmqvist et al., 2008a; Palmqvist et al., 2008b). High values of $\delta^{15}N$, typical from species with a hypercarnivorous diet, were recorded for *U. etruscus*. This has been interpreted as a regular consumption of fish given the paleoenvironment of the site, which is interpreted as a saline lake with an enrichment of $\delta^{15}N$ due to the thermal springs (García-Aguilar et al., 2014, 2015), although other interpretations for these $\delta^{15}N$ signatures have been proposed. The also high $\delta^{18}O$ values recorded in *U. etruscus* showed a low water dependence.

It is relevant to note that the above mentioned isotopic data are based on bone collagen, whose conservation is practically nil from 50-100 ka BP (Clementz, 2012; Saarinen et al., 2022).

Later, Medin et al., (2019) presented data based on dental microwear and morphometrics of *U. etruscus* from Dmanisi (Georgia), where early *Homo* is first recorded out of Africa, with a chronology of 1.85-1.77 Ma (Gabunia et al., 2000; Vekua et al., 2002; Lordkipanidze et al., 2007). The results showed that *U. etruscus* was clearly opportunistic and had an omnivorous behavior. They concluded the coexistence of *U. etruscus* and early *Homo* resulted in an overlapping in feeding resources since the omnivorous behavior of both taxa, and even then, it was not enough for the ecological exclusion of each other.

Here we present a multiproxy analysis through dental microwear analysis of *U. deningeri* from the Early-Middle Pleistocene (1.2-0.6 Ma) site of Vallparadís Section (Vallès-Penedès Basin, NE Iberian Peninsula), and a stable isotopes analysis on 9 species including *U. deningeri*, ungulates and other carnivorans from the same site, thus allowing us to perform a general study of the fossil mammal assemblage, concerning both diet and habitat of the individuals of layer EVT12 (MIS31) and EVT7 (MIS21). Starting from the assumption that there is an ecological change between these two layers, already tested through other works (Strani et al., 2019; Sorbelli et al., 2021), it is a good opportunity for confirming these published studies with both isotopic and microwear data of European Early Pleistocene chronologies.

1.2. Stable isotope analyses

The aim of the stable isotope analyses is to register the ratio of heavy isotopes in relation to the light isotopes that are present in the organic tissues such as bone collagen, teeth collagen or bioapatite in the enamel, which have attached to the organisms along their whole lives in several ways. By knowing these ratios or signatures (δ), it is possible to infer dietary habits, environments, or mobility behaviours of different species through analysing $\delta^{13}C$, $\delta^{18}O$, and $\delta^{15}N$ among others (Bocherens et al., 1994; Cerling et al., 1997; Kohn & Cerling, 2002; Kohn, 2010; Bedaso et al., 2013).

Stable isotopes analyses have been widely used during the last decades in order to reconstruct the ecology, birth seasonality or mobility of both Pleistocene and Holocene ecosystems (Balasse, 2002; Tornero et al., 2013, 2016, 2018; Balasse et al., 2016;

González-Guarda et al., 2017; Ramírez-Pedraza et al., 2019; Szabó et al., 2021), and for reconstructing the diet of extinct taxa (Macfadden et al., 1999; Merceron et al., 2006, 2013; Souron et al., 2012, 2013; Bibi et al., 2013; Metcalfe et al., 2013; Souron, 2017, 2018). Cave bear (*Ursus spelaeus*) is one of the most iconic species from the European Late Pleistocene, and its coeval presence in karstic environments with species from the genus *Homo* has made of this species an even more interesting taxon to study. Several insights from its diet have been published since the 90's decade (Bocherens et al., 1990, 1994, 1997, 2006, 2011, 2014; Fernández-Mosquera et al., 2001; Bocherens, 2004, 2015, 2019; Richards et al., 2008; Pérez-Rama et al., 2011; Robu et al., 2013, 2018; Münzel et al., 2014; Krajcarz et al., 2016; Ramírez-Pedraza et al., 2019; Naito et al., 2020).

Both carbon and oxygen isotopic data can give different kind of information, and so is the interpretation that the researchers can obtain from them. In the case of stable carbon isotopes, it is possible to reconstruct the diet of an individual, influenced by the photosynthetic pathway (C_3 and C_4) used by plants that are consumed by animals, and it is related to a specific type of landscape or ecological conditions. This has allowed to set up a dichotomy of C_4-feeders and C_3-feeders constantly used in works based on the study of diets of mammals through tooth enamel stable carbon isotopes (Bocherens et al., 1996; Cerling et al., 1997, 2015; Koch, 1998; Sponheimer & Lee-Thorp, 2003; Merceron et al., 2006, 2013; Levin et al., 2008; Bedaso et al., 2013; Uno et al., 2018).

The C_3 modern plants using photosynthetic pathway (including most trees, woody shrubs, bushes, herbs, and grasses) have an average isotopic composition of -28.5‰ (global range -20 to -37‰), with -23‰ as the maximum value recommended for typical C_3 plants and a cut-off of -31.5‰ for closed-canopy forests (Kohn, 2010). In this work, we have used the average $\delta^{13}C$ value of -27‰ for modern C_3 plants. Modern plants employing C_4 photosynthetic pathway (tropical grasses and sedges) have an average isotopic composition of -12‰ (global range -10 to -14‰) (Cerling & Harris, 1999; Kohn & Cerling, 2002). The Crassulacean acid metabolism (CAM) plants can have $\delta^{13}C$ values corresponding to both C_3 and C_4 plants.

Instead, by analyzing the $\delta^{18}O$ it is possible to distinguish between obligate and non-obligate drinkers, with the possibility of making inferences about precipitation source, humidity, temperature, and plant water (Kohn, 1996). Evaporation reflects a positive

effect on $\delta^{18}O$, so areas with strong aridity and water deficit are ^{18}O-enriched. Thus, the difference between oxygen isotopic values from obligate drinkers and non-obligate drinkers is influenced by aridity (Roberts et al., 2018). Regarding oxygen isotopic values, this work is only based on the distinction between obligate and non-obligate drinkers and the conclusions about the aridity that we can obtain from that. In addition, nitrogen isotopic data ($\delta^{15}N$) gives information about the trophic level of the individuals of an assemblage (Bocherens et al., 1997), but dealing with Early Pleistocene chronologies makes it tough to analyze because of its poor conservation.

Stable isotopes analyses can be applied to organic and inorganic tissues of the studied individual. Given the scarcity of well-preserved soft tissues, such as collagen, of Pleistocene-aged remains, researchers are limited to work with bioapatite, specifically tooth enamel, when dealing with Early Pleistocene-aged or older remains (Clementz, 2012).

In this sense, the isotopic data from this work are taken from tooth enamel (hydroxylapatite) from an Early Pleistocene large mammal assemblages. In these old chronologies (around 1-1,5 Ma), to make a stable isotopic analyses sampling tooth enamel gives a more valid and reliable result than sampling bone collagen, which has some limitations. In Saarinen et al., (2022) they make an statement about the limit that entails the use of this methodology in such an old chronology. Such old chronologies should imply that the percentage of bone collagen is not well-preserved, so the idea of performing a stable isotopes analysis through samples taken from bone collagen from a >1 Ma site, is tough to prove. Thus, this work displays a more reliable *modus operandi*, since we understood this site can only offer reliable isotopic data by using hydroxilapatite samples.

Here we chose to work with both carbon and oxygen stable isotopes from tooth enamel, since the analyse of carbonate (CO_3), which is structurally integrated into the enamel mineral lattice, entails an easier chemical preparation, and provides isotopes of 2 elements (C and O) than in the analyse of phosphate (PO_4), which provides just results for oxygen stable isotopes.

1.3. Dental microwear analyses

Occlusal surfaces of teeth can be studied through a microscopic approach, to quantify the different kinds of marks that food can leave on the enamel. This methodology can give information about the last days or weeks of the individual before its death (Grine, 1986; Teaford & Oyen, 1989), shedding light about the diet and the that could have had the animal and the moment before its death, since researchers can make insights from this data considering the seasonality. Thus, a lot of researchers have specialized in this approach, letting them to study the paleoecology of several groups of animals, including humans.

The study of these marks generated by the process of mastication has been carried out through different type of microscopes. In this work, we have used the stereomicroscope, which is a good choice concerning issues such as cost and time (Solounias & Semprebon, 2002), but other studies have been performed using the scanning electron microscope or SEM (Rensberger, 1978; Walker et al., 1978; Ryan, 1979; Grine, 1981), or the use of the scanning confocal microscopy for analyzing dental microwear textures (Ungar et al., 2003, 2010; Scott et al., 2005; Kubo et al., 2017).

The earliest studies of dental microwear were carried out in the 1950s, when the study consisted of the observation and comprehension of the masticatory apparatus movements of herbivores and omnivores when gnawing (Butler, 1952; Mills, 1955; Barnicoat, 1957; Baker et al., 1959; Dahlberg & Kinzey, 1962; Field & Purves, 1964; Cutress & Healy, 1965; Healy & Ludwig, 1965; Ludwig et al., 1966; Healy, 1967; Healy et al., 1967).

Later, the studies based on this methodology started to reach more precise conclusions. Grine (1981) made an observation of both *Paranthropus robustus* and *Australopithecus africanus* molars, which led him to differentiate the diet according to the number of different marks (scratches and pits). In the case where the predominant marks were scratches, which was found to be *Australopithecus africanus*, the individual was related to a diet based on abrasive and soft food such as leaves. Instead, when the predominant marks were pits, which was *Paranthropus robustus*, the specimen was thought to have a diet based on hard food such as seeds. This was posteriorly supported

by Teaford and Walker (1984), adding more information to accurate into the diet distinction.

The method in question gained reliability with the creation of some databases of extant groups of animals, to be able to compare the results of the counting of the marks of occlusal surfaces of extinct species teeth with those from the database. The advantage of knowing the current ecology and diet of extant species let the scientific community to proceed with a more than safe reference. For example, Solounias and Semprebon (2002) made this kind of database with data from extant ungulates, helping to the comparison with fossil ungulates.

The analysis through stereomicroscope started to be used in the 2000's, allowing the low-magnification observation of marks (Semprebon et al., 2004). Since then, dietary studies have been carried out for several groups (e. g., Bovidae (Rivals & Deniaux, 2003), Camelidae (Semprebon & Rivals, 2010), Antilocapridae (Semprebon & Rivals, 2007), Cervidae (Rivals & Semprebon, 2017), and proboscideans (Rivals et al., 2012, 2019)).

Carnivorans, both extant and fossils, are less analyzed through dental microwear. First studies were focused on dietary habits of machairodontine *Smilodon fatalis* by using SEM (van Valkenburgh et al., 1990; Anyonge, 1996). Later, Dewar (2004) used the low-magnification stereomicroscopy to study Paleogene carnivorans, although diet of more fossil carnivores has been studied (Goillot et al., 2009; Stynder et al., 2012).

Pinto-Llona & Andrews (2001) presented the first dental microwear analysis on ursids, focusing on *U. spelaeus* feeding behavior, study continued in Pinto-Llona (2006; 2013). However, low-magnification stereomicroscopy on ursids was first used in Peigné et al., (2009), where they determine dietary habits of *U. spelaeus* from Belgium. Consequently, more dental microwear data were published, using different available methodologies (Donohue et al., 2013; Münzel et al., 2014; Jones & DeSantis, 2016; Medin et al., 2017, 2019; Peigné & Merceron, 2019; Stynder et al., 2019; Ramírez-Pedraza et al., 2019, 2020; Ramírez Pedraza et al., 2022), in addition to necessary reference database (Pappa et al., 2019).

1.4. Ursidae

Looking at the etymology of the word itself, the name of the order Carnivora refers to a determined kind of diet (from latin, *caro* means "meat" and *vorare* means "to devour"). Then, it would make sense that the animals grouped within this order had a carnivorous diet. However, not all of them are a good representant of this kind of feeding, finding some examples in the family Ursidae for this reason these taxa are several times known as carnivorans, not carnivores. Ursids, commonly named "bears", are a family placed in the order Carnivora, where we can observe a high diversity in their type of diet.

The family of Ursidae is nowadays represented by 8 species, placed in different genera and subfamilies. These species are the brown bear (*Ursus arctos*), the American black bear (*Ursus americanus*), the Asian black bear (*Ursus thibetanus*), the polar bear (*Ursus maritimus*), the giant panda (*Ailuropoda melanoleuca*), the sun bear or Malayan bear (*Helarctos malayanus*), the spectacled bear or Andean bear (*Tremarctos ornatus*), and the sloth bear or Indian bear (*Melursus ursinus*).

These species represent the mentioned diversity in the diet within the ursids, corresponding to the also diverse geographical distribution of each of them. The brown bear (*U. arctos*), with a body weight of 135-545 kg and occasionally reaching 725 kg in Kamchatka (Macdonald, 2009), is nowadays considered to concern 16 subspecies, such as the Grizzly bear (*U. a. horribilis*). It is the most widely distributed species, occupying Europe, Near East, Asia and North America, and also its diet is the most diverse within Ursidae, being significant for the development of brown bear ecological behaviour (Gende & Quinn, 2004; Bojarska & Selva, 2012). The black bear (*U. americanus*), with a body weight of 60-225 kg (Macdonald, 2009), which inhabits the American continent, including the wholeness of North America and part of Central America, also presents a mixed diet including meat and fish, insects, roots and fruit, with a soft mast predominance (Frary et al., 2011). The sun bear (*H. malayanus*) is the smallest ursid, with a body mass of 27-65 kg (Macdonald, 2009). However, it is one of the largest mammals of the Bornean rainforest, inhabiting the forested areas of South East Asia, with a soft mast diet based on insects, fruit, honey and casually meat (Wong, 2002;

Fredriksson & Wich, 2006; Fredriksson, 2012). The Asiatic black bear (*U. thibetanus*), with a body mass of 60-200 kg, rarely more than 200 kg (Macdonald, 2009), can be also broadly considered as a generalist regarding the diet, just like *U. arctos*, with a marked flexibility in both exploitation and composition of food, consuming a wide range of available food depending on the season and the region (Huygens et al., 2003; Furusaka et al., 2017; Panthi et al., 2019). Living in the mountain regions of South East Asia, bases its diet on fruit, insects, leaves and stems, with a hard mast predominance despite the dietary seasonality (Steinmetz & Garshelis, 2008; Koike et al., 2012). The spectacled bear (*T. ornatus*), with a body weight of 100-175 kg, rarely more than 200 kg (Macdonald, 2009), is the only bear that inhabits South America, in the Cordillera de los Andes, and is fed by fruit, insects, some rodent, corn and berries (Peyton, 1980).

The previously mentioned species are considered omnivorous, with their respective particularities and preferences, especially the case of *U. arctos* due to its wide range of geographical distribution. However, there are some ursid species with a specialized diet.

The giant panda (*A. melanoleuca*), with a body weight of 100-150 kg (Macdonald, 2009), which inhabits in the forests of South-Central China, has a strictly herbivorous diet based on bamboo stems and leaves, uncommonly feeding on small mammals (Macdonald, 2009). In the other extreme there is the polar bear (*U. maritimus*), the largest of the world's bear species, with a body mass of 400-600 kg (Macdonald, 2009). This species displays a circumpolar distribution in the northern hemisphere, occurring in Asia, North America and Europe. Regarding the diet, they are specialized in a hypercarnivorous diet, mainly feeding on seal meat and fish. Instead, the sloth bear (*Melursus ursinus*), with a body mass of 80-145 kg, rarely more than 190 kg , which is found in lowland ecosystems such as those from India, Nepal, Sri Lanka and Bhutan (Macdonald, 2009). Concerning its insectivorous diet, it is mainly based on termites and ants (Joshi et al., 1997).

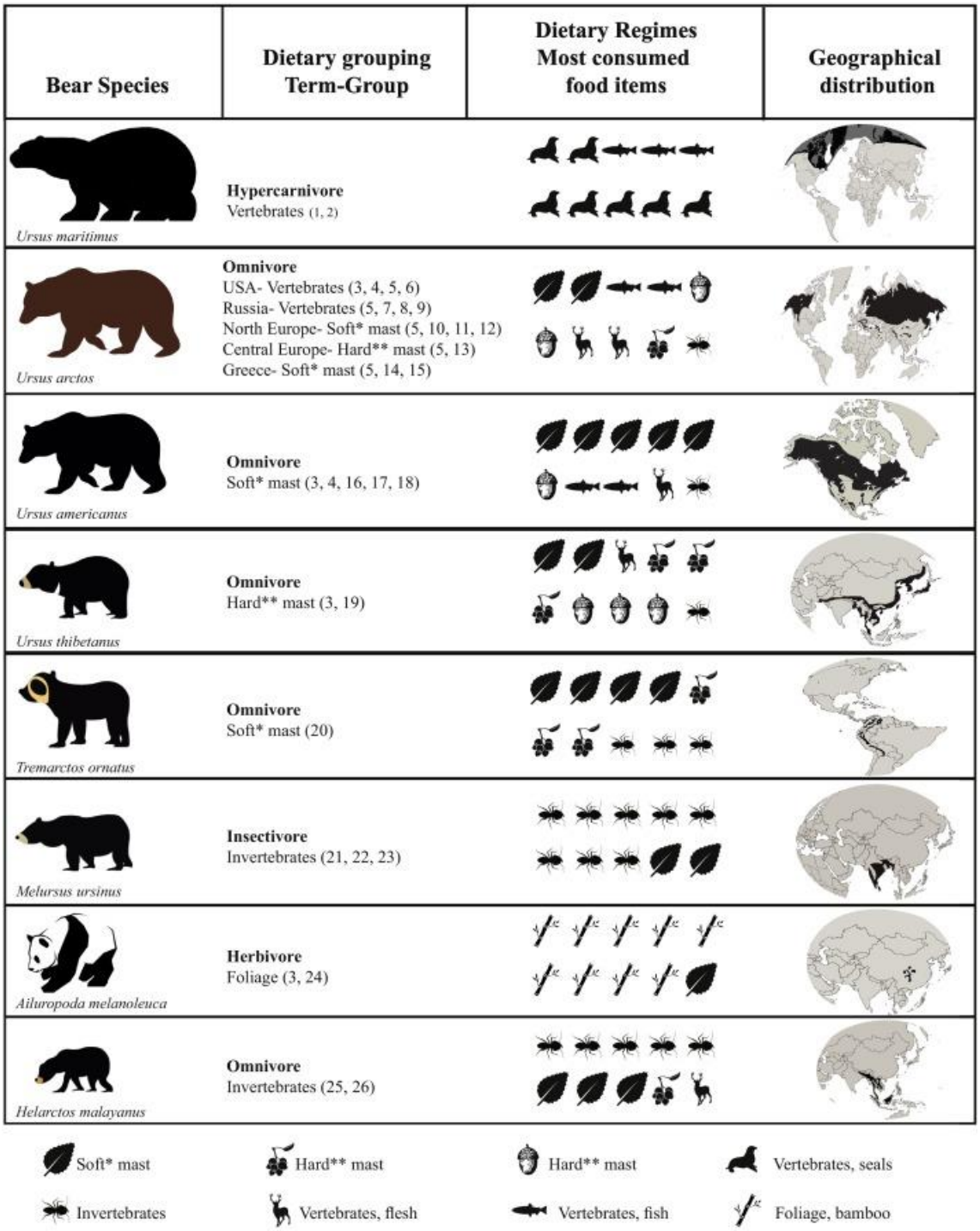

Fig. 1. Dietary groupings of the key food items consumed by each extant bear species, including their dietary regimes (with symbols) and their geographical distribution. Soft mast: fibres food, including leaves and fruits with no seeds. Hard mast: berries and fruits with seeds as well as nuts. Extracted from Pappa et al., (2019).

2. The Vallparadís Section

The Vallparadís Section is composed of two paleontological sites, called Cal Guardiola and Vallparadís Estació, located in the western and eastern bank, respectively, of the Torrent de Vallparadís, in the town of Terrassa (Vallès-Penedès Basin, Northeastern Iberian Peninsula) (Madurell-Malapeira et al., 2010, 2017). Overall, the Vallparadís Section witnessed several excavations with a span from 1997 until 2008, recovering more than 30.000 large mammal remains in the most rich layers of each site (Madurell-Malapeira et al., 2017).

Fig 2. Excavation of the layer EVT7 of the Vallparadís Estació site during February 2006.

In 1997, Cal Guardiola was started to be excavated, with a good result concerning the quantity and quality of the specimens. More than 3.000 remains, both belonging to macromammals and plants (Mijarra et al., 2007), were recovered in the western bank-located site (Madurell-Malapeira et al., 2009).

Later, in 2005, during an urbanistic intervention in which a railway station for Ferrocarrils de la Generalitat de Catalunya was under construction, the researchers realised the potential the new accidental excavation could have, since they did a paleontological intervention in order to recover as much remains as possible. In this scenario, the systematic excavation lasted 3 years, until 2008, having recovered more than 30.000 remains including small and large mammals, and plants (Alba, Aurell, et al., 2008; Alba, Moyà-Solà, et al., 2008; Madurell-Malapeira et al., 2009).

Fig. 3. One of the richest squares found during the excavation of layer EVT12 of the Vallparadís Estació site during December of 2007. In the image it is possible to see three different equid crania and another one from *Megaloceros* sp.

2.1. Geological setting

The Vallparadís Section is located in the Vallès-Penedès Basin, which is a 15 km wide and 100 km long half-graben with a NE-SW direction, parallel to the coastline of Catalonia and to the Catalan Coastal. This basin was formed in the late Oligocene, during

the rifting of the Western Mediterranean (Cabrera & Calvet, 1996; Roca et al., 1999; Cabrera et al., 2004). The faults are present in both NW and SE margins of the basin, but with a more pronounced activity in the NW margin, as there is a Neogene master normal fault present in it (Cabrera & Calvet, 1996).

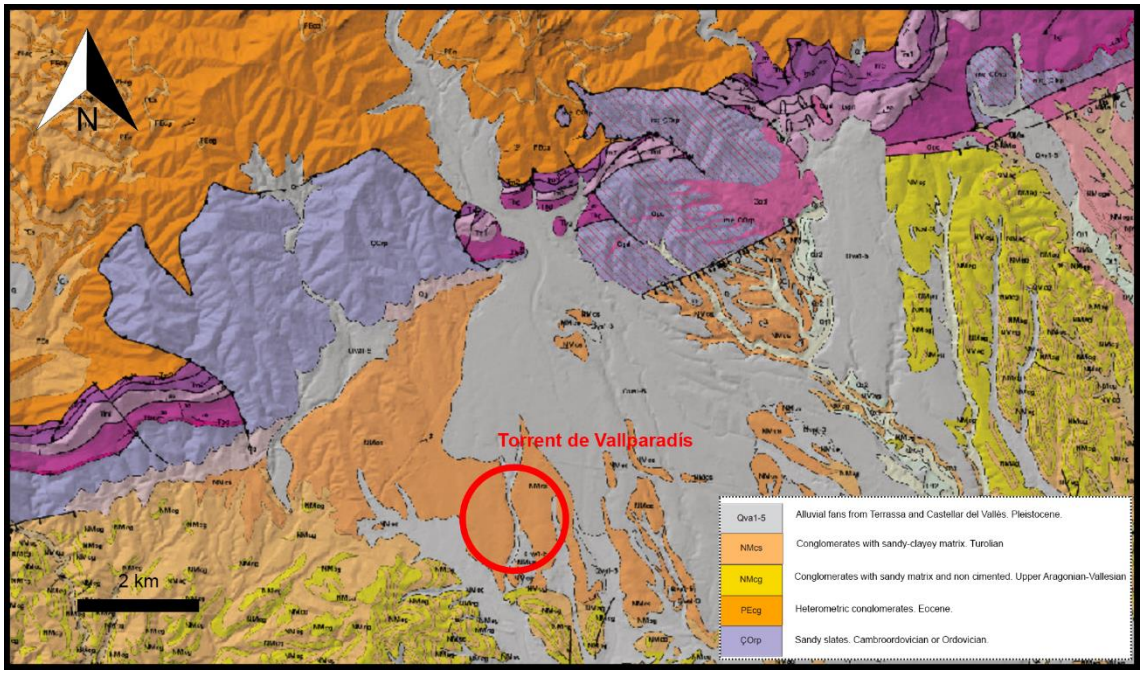

Fig 4: Geological map of Terrassa, with the Vallparadís area indicated in red.

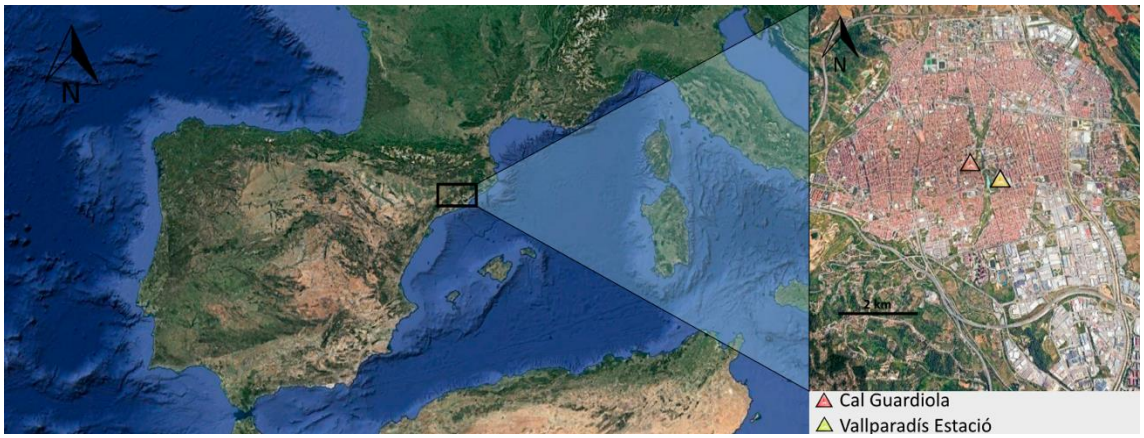

Fig 5: a) Map of the Iberian Peninsula showing the location of the composite site Vallparadís Section. b) Map of the town Terrassa showing both sites Cal Guardiola and Vallparadís Estació, located in each riverbank of Torrent de Vallparadís.

The material that fills the basin is clastic sediments which are Neogene and Quaternary in age, and mostly coming from the erosion suffered in the Paleozoic, Mesozoic and Paleogene rocks found in the Catalan Coastal Ranges (Agustí et al., 1997).

The marine Early Pliocene units which developed over erosive surfaces were covered by Pleistocene-Holocene terraces (de Mas, 1984; Martinell, 1988; Agustí et al., 1997).

Fig. 6. Excavation of layer EVT7 of Vallparadís Estació during the beginning of 2007.

2.2. Layers

The whole sequence in the Vallparadís Section comprises more than ten layers with a thickness of close to 20 meters. The geological, sedimentological, biochronological, magnetostratigraphical data and the absolute dating methods performed evidence a chronology from 1.1 to 0.6 Ma to most of the sequence with an isolated Late Pleistocene layer EVT1 (Madurell-Malapeira et al., 2010; Minwer-Barakat et al., 2011; Duval et al., 2015a).

Despite practically all the studied layers had fossil content, most of the unearthed remains come from layers CGRD2 and CGRD7 of Cal Guardiola, and layers EVT12, EVT7 and EVT3 of Vallparadís Estació site, with a total amount of more than 30.000 large

mammals remains recovered from these layers (Madurell-Malapeira et al., 2017). Remains from layers CGRD7, EVT7 and EVT12 have been used for this work.

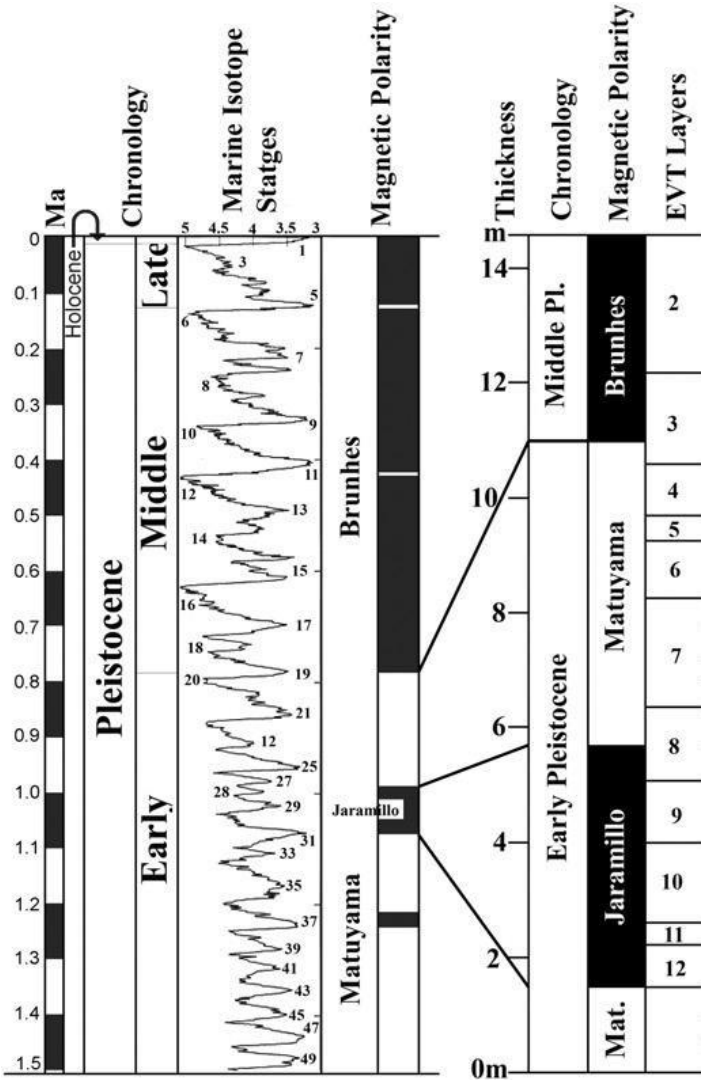

Fig. 7. Chronological range of the different layers of Vallparadís Estació.

2.2.1. Layer CGRD2

The layer CGRD2 from Cal Guardiola corresponds to a pre-Jaramillo subchron interval, with an approximate age of ca. 1.2-1.1 Ma (Madurell-Malapeira et al., 2010, 2014, 2017). 937 specimens of large mammals were recovered during the 1997 field survey which correspond to the following species (Madurell-Malapeira et al., 2010, 2014, 2017; Sorbelli et al., 2021): *Pachycrocuta brevirostris, Ursus deningeri, Canis mosbachensis, Vulpes alopeoides, Mammuthus meridionalis*, *Hippopotamus antiquus, Bison*

schoetensacki, *Dama vallonnetensis, Megaloceros savini, Stephanorhinus hundsheimensis, Equus altidens*.

2.2.2. Layer CGRD7

Layer CGRD7 corresponds to a post-Jaramillo interval of Matuyama chron (ca. 0.99-0.78 Ma). A number of 748 remains of large mammals were recovered, with the following identified species (Madurell-Malapeira et al., 2010, 2014, 2017; Sorbelli et al., 2021): *Macaca sylvanus* cf. *Florentina, Homotherium crenatidens, Panthera gombaszoegensis, Lynx pardinus, Pachycrocuta brevirostris, Ursus deningeri, Canis mosbachensis, Mammuthus meridionalis*, *Hippopotamus antiquus, Sus strozzi, Bison schoetensacki*, , *Megaloceros savini, Dama vallonnetensis, Equus altidens* and *Stephanorhinus hundsheimensis*.

Fig. 8. *Hippopotamus antiquus* skeleton from the layer CGRD7 of Cal Guardiola.

2.2.3. Layer EVT12

Layer EVT12 corresponds to the Jaramillo subchron (1.07-0.99 Ma) and probably corresponds to the interglacial stage MIS31. More than 2400 vertebrate remains were

unearthed from this layer (Strani et al., 2019), with the following faunal list (J. M.-M. unpublished data): *Macaca sylvanus, Megantereon* sp., *Lynx pardinus, Pachycrocuta brevirostris, Ursus deningeri, Canis (Xenocyon) lycaonoides, Canis mosbachensis, Vulpes alopecoides, Meles meles, Mammuthus meridionalis, Hippopotamus antiquus, Sus strozzi, Megaloceros savini, Dama vallonnetensis, Caproleus* sp.*, Bison schoetensacki,* Bovidae indet., *Stephanorinhus hundsheimensis* and *Equus altidens.*

2.2.4. Layer EVT7

Layer EVT7 corresponds to the post-Jaramillo interval of the Matuyama chron (0.99-0.78 Ma), with an absolute dating of 0.858 ± 0.087 Ma using ESR method (Duval et al., 2015b), probably related with the interglacial stage MIS21, (Strani et al., 2019). This layer yielded 20.286 vertebrate remains with the following faunal list (Madurell-Malapeira et al., 2010, 2014, 2017; Boscaini, 2014; Sorbelli et al., 2021): *Macaca sylvanus* cf. *florentina*, *Panthera fossilis, Panthera gombaszoegensis, Puma pardoides, Lynx pardinus, Pachycrocuta brevirostris, Ursus deningeri, Canis (Xenocyon) lycaonoides, Canis mosbachensis, Vulpes alopecoides, Meles meles, Mammuthus meridionalis*, *Hippopotamus antiquus, Sus strozzi Megaloceros savini, Dama vallonnetensis, Caproleus sp. Bison schoetensacki*, Bovidae indet., Caprini indet., *Equus altidens, Stephanorhinus hundsheimensis, Iberomys huescarensis*, *Eliomys quericinus*, *Apodemus* cf. *sylvaticus*, *Stenocranius gregaloides*, *Mimomys savini* and *Hystrix refossa*.

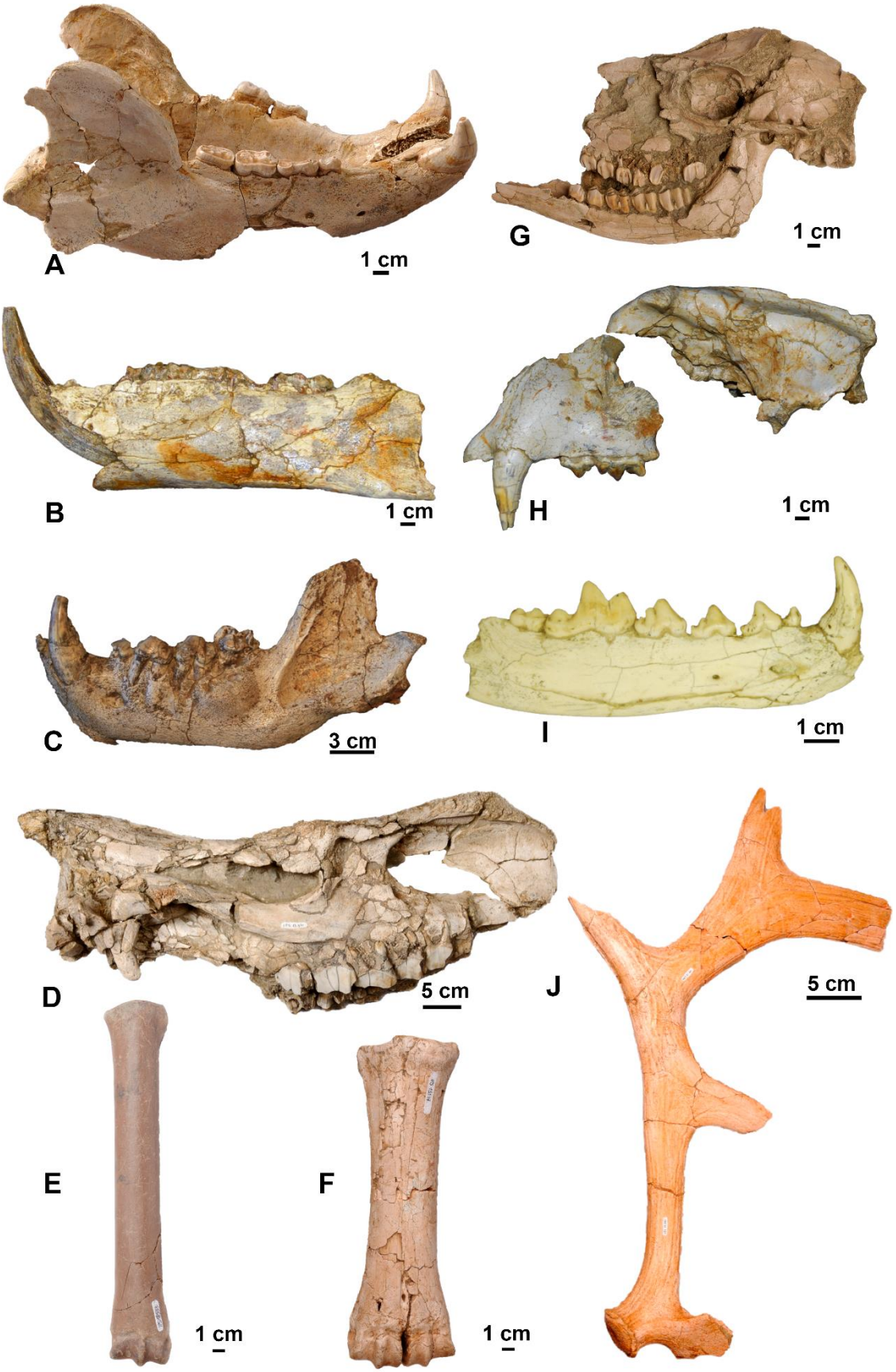
A
1 cm
G
1 cm
B
1 cm
H
1 cm
C
3 cm
I
1 cm
D
5 cm
J
5 cm
E
1 cm
F
1 cm

Fig. 9. Large mammals remains from Vallparadís Section. **A**: *Ursus deningeri* mandible of layer CGRD7 of Cal Guardiola (IPS14950); **B**: *Sus strozzi* left hemimandible from layer EVT7 of Vallparadís Estació in buccal view (IPS107041c) ; **C**: *Pachycrocuta brevirostris* left hemimandible from the layer EVT12 of Vallparadís Estació in buccal view (EVT24641); **D**: *Stephanorhinus hundsheimensis* cranium from the CGRD7 layer of Cal Guardiola in lateral view (IPS13371); **E**: *Equus altidens* right metatarsal from the layer CGRD2 of Cal Guardiola (IPS18533); **F**: *Bison schoetensacki* right metacarpal from the layer CGRD7 of Cal Guardiola (IPS13547); **G**: *Dama vallonnetensis* cranium from the layer CGRD7 of Cal Guardiola in lateral view (IPS14911); **H**: *Panthera gombaszoegensis* partial cranium from the layer EVT7 of Vallparadís Estació in lateral view (EVT20122 + EVT20156); **I**: *Canis mosbachensis* right hemimandible from the layer EVT12 of Vallparadís Estació in buccal view (EVT24342); **J**: *Megaloceros savini* antler from the CGRD7 layer of Cal Guardiola (IPS13370).

3. Material and methods

Different specimens coming from the Vallparadís Section has been used for each analysis, as well as the respective sample selection and methodology. Here are described the materials for stable isotope and dental microwear analyses, the criteria for its selection, and the methodology followed until reaching the results in both cases.

Fig. 10. *Ursus deningeri* cranium from layer EVT12 from Vallparadís Estació. Picture: Joan Madurell-Malapeira.

3.1. Stable isotopes analyses

3.1.1. Sample selection

In order to carry out the stable isotopes analyses of this work, we have taken a total amount of 112 samples, all of them belonging to dental remains. Since the aim of the work is to understand the changes in the *U. deningeri* diet between the layers

EVT7/CGRD7 (MIS21) and the layer EVT12 (MIS31), the samples have been chosen for having a similar number of samples from each layer.

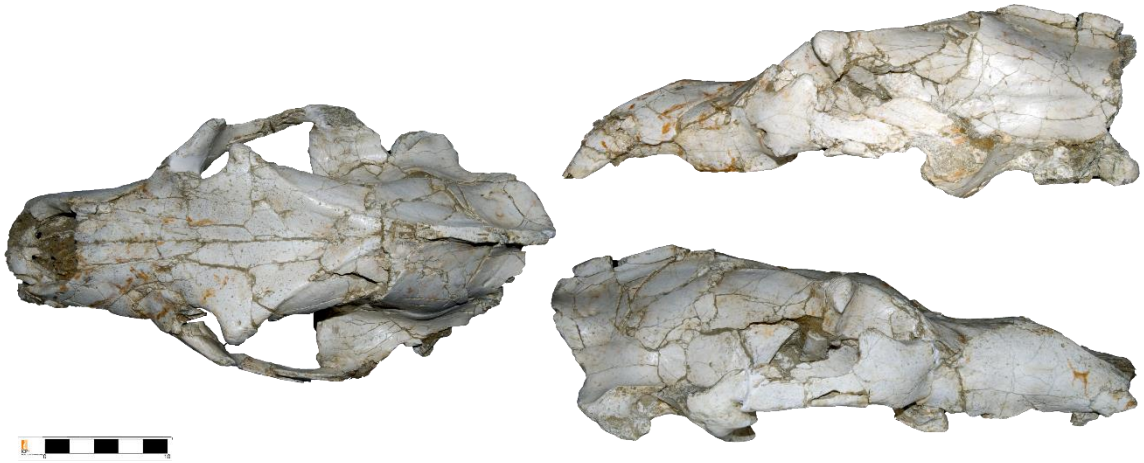

Fig. 11. *Ursus deningeri* cranium from layer EVT7 from Vallparadís Estació. Picture: Joan Madurell-Malapeira.

In this way, we have tried to take an approximate total of 10 samples from each species, and an equative number coming from each layer (Table 1). Thus, we took enamel samples from 9 different species, including the taxon this work is focused on, to put its data in a well-constructed background. The breakdown of the samples is the following: 31 samples of *Ursus deningeri*, 25 from EVT7 and 6 from EVT12; 13 samples of *Pachycrocuta brevirostris brevirostris*, 6 from EVT7 and 7 from EVT12; 11 samples of *Canis mosbachensis*, 6 from EVT7 and 5 from EVT12; 11 samples of *Equus altidens* 5 from EVT7 and 6 from EVT12; 11 samples of *Bison schoetensacki*, 6 from EVT7 and 5 from EVT12; 12 samples of *Dama vallonnetensis*, 7 from EVT7 and 5 from EVT12; 6 samples of *Mammuthus meridionalis*, all of them from EVT7; 6 samples of *Hippopotamus antiquus*, 5 from EVT7 and 1 from EVT12; 11 samples of *Stephanorhinus hundsheimensis*, 6 from EVT7 and 5 from EVT12.

Table 1. Specimens and layers used for stable isotopes analyses.

Museum Nº	Sample	Species	Layer
IPS110438	1	*Ursus deningeri*	EVT12
IPS110439	2	*Ursus deningeri*	EVT7
IPS110421	3	*Ursus deningeri*	EVT7
IPS110411	4	*Ursus deningeri*	EVT7
IPS110428	5	*Ursus deningeri*	EVT7

IPS110431	6	*Ursus deningeri*	EVT7
IPS110423	7	*Ursus deningeri*	EVT7
IPS110414	8	*Ursus deningeri*	EVT7
IPS110424	9	*Ursus deningeri*	EVT7
IPS110445	10	*Ursus deningeri*	EVT7
IPS110446	11	*Ursus deningeri*	EVT7
IPS110427	12	*Ursus deningeri*	EVT7
IPS110440	13	*Ursus deningeri*	EVT7
IPS114657	14	*Ursus deningeri*	EVT7
IPS110418.15	15	*Ursus deningeri*	EVT7
IPS110418.19	16	*Ursus deningeri*	EVT7
IPS110418.1	17	*Ursus deningeri*	EVT7
IPS114661	18	*Ursus deningeri*	EVT7
IPS110418.2	19	*Ursus deningeri*	EVT7
IPS110418.22	20	*Ursus deningeri*	EVT7
IPS110418.24	21	*Ursus deningeri*	EVT7
IPS110418.4	22	*Ursus deningeri*	EVT7
IPS110418.17	23	*Ursus deningeri*	EVT7
IPS110418.7	24	*Ursus deningeri*	EVT7
IPS110418.13	25	*Ursus deningeri*	EVT7
IPS110429	26	*Ursus deningeri*	EVT7
IPS127733	27	*Dama vallonnetensis*	EVT7
EVT 22998	28	*Stephanorhinus hundsheimensis*	EVT12
EVT3270	29	*Dama vallonnetensis*	EVT7
EVT9730	30	*Dama vallonnetensis*	EVT7
EVT9319	31	*Dama vallonnetensis*	EVT7
EVT25416-62	32	*Dama vallonnetensis*	EVT12
EVT18714	33	*Dama vallonnetensis*	EVT7
EVT5817	34	*Equus altidens*	EVT7
EVT17388	35	*Mammuthus meridionalis*	EVT7
EVT933	36	*Dama vallonnetensis*	EVT7
IPS127732	37	*Dama vallonnetensis*	EVT12
EVT20736	38	*Mammuthus meridionalis*	EVT7
EVT23386	39	*Stephanorhinus hundsheimensis*	EVT12
EVT15121	40	*Dama vallonnetensis*	EVT7
EVT25416-43	41	*Dama vallonnetensis*	EVT12
EVT15225	42	*Stephanorhinus hundsheimensis*	EVT7
EVT21098	43	*Stephanorhinus hundsheimensis*	EVT7
EVT20435	44	*Stephanorhinus hundsheimensis*	EVT7
EVT9548	45	*Stephanorhinus hundsheimensis*	EVT7
EVT2993	46	*Mammuthus meridionalis*	EVT7
EVT4204	47	*Stephanorhinus hundsheimensis*	EVT7
EVT9241	48	*Stephanorhinus hundsheimensis*	EVT7
EVT3324	49	*Bison schoetensacki*	EVT7
EVT4389	50	*Bison schoetensacki*	EVT7
EVT22786	51	*Stephanorhinus hundsheimensis*	EVT12

EVT9993	52	*Bison schoetensacki*	EVT7
EVT5943	53	*Bison schoetensacki*	EVT7
EVT3097	54	*Equus altidens*	EVT7
EVT333	55	*Equus altidens*	EVT7
EVT4991	56	*Equus altidens*	EVT7
EVT22790	57	*Stephanorhinus hundsheimensis*	EVT12
EVT24822	58	*Bison schoetensacki*	EVT12
EVT10662	59	*Equus altidens*	EVT7
EVT22509	60	*Ursus deningeri*	EVT12
EVT25384	61	*Ursus deningeri*	EVT12
EVT25378	62	*Ursus deningeri*	EVT12
EVT20711B	63	*Ursus deningeri*	EVT12
EVT24458	64	*Pachycrocuta brevirostris*	EVT12
EVT20711F	65	*Ursus deningeri*	EVT12
EVT18545	66	*Pachycrocuta brevirostris*	EVT12
EVT25454	67	*Pachycrocuta brevirostris*	EVT12
EVT23308	68	*Stephanorhinus hundsheimensis*	EVT12
EVT23584	69	*Dama vallonnetensis*	EVT12
EVT22896	70	*Pachycrocuta brevirostris*	EVT12
EVT25193	71	*Pachycrocuta brevirostris*	EVT12
EVT22918	72	*Pachycrocuta brevirostris*	EVT12
EVT23340	73	*Hippopotamus antiquus*	EVT12
EVT22945	74	*Pachycrocuta brevirostris*	EVT12
EVT24342	75	*Canis mosbachensis*	EVT12
EVT22398	76	*Canis mosbachensis*	EVT12
EVT22767	77	*Pachycrocuta brevirostris*	EVT7
EVT24612	78	*Canis mosbachensis*	EVT12
EVT23045	79	*Pachycrocuta brevirostris*	EVT7
EVT1679	80	*Pachycrocuta brevirostris*	EVT7
EVT25003	81	*Canis mosbachensis*	EVT12
EVT25504	82	*Canis mosbachensis*	EVT12
EVT6312	83	*Pachycrocuta brevirostris*	EVT7
EVT13840	84	*Canis mosbachensis*	EVT7
EVT13921	85	*Canis mosbachensis*	EVT7
EVT23056	86	*Pachycrocuta brevirostris*	EVT7
EVT5003	87	*Canis mosbachensis*	EVT7
EVT9113	88	*Canis mosbachensis*	EVT7
EVT21325	89	*Pachycrocuta brevirostris*	EVT7
EVT6924	90	*Canis mosbachensis*	EVT7
EVT400a	91	*Canis mosbachensis*	EVT7
EVT24185	92	*Equus altidens*	EVT12
EVT24460	93	*Equus altidens*	EVT12
EVT24043	94	*Bison schoetensacki*	EVT12
EVT23859	95	*Equus altidens*	EVT12
EVT14038e	96	*Equus altidens*	EVT12
IPS127734	97	*Dama vallonnetensis*	EVT12

EVT14038b	98	*Bison schoetensacki*	EVT12
EVT14038c	99	*Bison schoetensacki*	EVT12
EVT14038c2	100	*Bison schoetensacki*	EVT12
EVT3156	101	*Mammuthus meridionalis*	EVT7
EVT24261	102	*Equus altidens*	EVT12
EVT5871	103	*Hippopotamus antiquus*	EVT7
EVT476	104	*Hippopotamus antiquus*	EVT7
EVT1193	105	*Hippopotamus antiquus*	EVT7
EVT21890	106	*Mammuthus meridionalis*	EVT7
EVT6010	107	*Bison schoetensacki*	EVT7
EVT2612	108	*Bison schoetensacki*	EVT7
EVT786	109	*Hippopotamus antiquus*	EVT7
EVT6889	110	*Hippopotamus antiquus*	EVT7
EVT25483	111	*Equus altidens*	EVT12
EVT11733	112	*Mammuthus meridionalis*	EVT7

3.1.2. Methodology

In this work, the analyses have been performed on $\delta^{13}C$ and $\delta^{18}O$ from tooth enamel. The possibility of performing the study based on bone collagen have been totally ruled out, since nowadays it is not possible to extract it with the scientific community current tools.

Once the selection has been done, the samples surface has been cleaned with a tungsten abrasive drill bit. Then, samples of enamel have been removed by drilling with a diamond bit. A rotary hand drill with a diamond-tipped dental burr was used to recover enamel from an area of the tooth as large as possible to avoid seasonal bias at the time of mineralization. We have carried out this process to obtain a certain measurement of enamel from the specimens, which ranges in 2-8 mg. Powder samples have been taken from the part of the crown with more enamel content, mostly buccal side, taking care of not drilling dentine or cement, which is abundant in equids teeth. This protocol has been performed at the Laboratory of Research Module B of the Universitat Autònoma de Barcelona and at the Museu de l'Institut Català de Paleontologia Miquel Crusafont, Sabadell.

Fig. 12. *Mammuthus meridionalis* selected specimens from EVT7.

Fig. 13. Process of drilling for obtaining powdered enamel samples at the Laboratory of Research Module B of Universitat Autònoma de Barcelona.

Subsequently, powdered enamel samples have been chemically treated at the Biomarkers Laboratory of the Institut Català de Paleoecologia Humana i Evolució Social (IPHES-CERCA). We followed the protocol established in Thorpe & Van der Merwe (1987), later modified by Koch et al., (1997), Balasse (2002), and Tornero et al., (2013), in order to remove the exogen carbonates that remain in the sample. That means that samples have been chemically treated in 0.1M acetic acid [CH_3COOH] (0.1 mL solution/0.1 mg sample) for 4 hours. Later, samples have been freeze-dried and rinsed with distilled water 5 times. The last proportion of water has been removed by evaporation in an oven at 70 °C for 48 hours.

Fig. 14. *Bison schoetensacki* specimen powdered enamel sample at the Laboratory of Universitat Autònoma de Barcelona.

After the described chemical treatment, samples have been sent to the Environmental Isotope Laboratory, University of Arizona, United States. There, an automated carbonate preparation device (KIEL-III) coupled to a gas-ratio mass spectrometer (Finnigan MAT 252) measured the $\delta^{13}C$ and $\delta^{18}O$ values of tooth enamel bioapatite.

$\delta^{H}X_{sample}=[(R_{sample}-R_{standard})/R_{standard}]x1000$, where X is the element, H is the mass of the rare, heavy isotope, and $R=^{13}C/^{12}C$, or $^{18}O/^{16}O$. $\delta^{13}C$ and $\delta^{18}O$ values are expressed in the Vienna-Pee Dee Belemnite (VPDB) standard. Accuracy and precision of the

measurements were checked using two internal laboratory calcium carbonate standards (RC-1 and CECC) normalized to NBS18 and NBS19 international standards. A total of 16 RC-1 and CECC samples were measured (RC-1 expected values +2.83‰ for $\delta^{13}C$; CECC expected values −20.78‰ for $\delta^{13}C$). The mean analytical precision of RC-1 was +0.01‰ for $\delta^{13}C$ values and +0.02‰ for $\delta^{18}O$.

Atmospheric CO_2 has been changing over time (Tipple et al., 2010) with a consequent influence on the carbon values of plants during its fixation in the photosynthesis process (Farquhar et al., 1989). To make a comparison between the carbon values of present-day plants with those consumed by animals in the past, it is crucial to perform corrections. In our work, we have corrected by ~ +1.5 the $\delta^{13}C$ values of modern plants, due to the difference between the pre-Industrial $\delta^{13}CCO_2$ value of ~ -6.5‰ established for the Plio-Pleistocene (Tipple et al., 2010) and the $\delta^{13}CCO_2$ value of ~ -8‰ at the time the reference collection of modern plants was collected (Kohn, 2010). When plants are consumed, a fixation occurs in the tooth enamel of the animals, a process of isotopic fractionation (Krueger & Sullivan, 1984; Koch, 1998; Cerling & Harris, 1999; Passey et al., 2005).

3.2. Dental microwear analyses

3.2.1. Sample selection

Dental microwear analyses have been performed using teeth of *U. deningeri*, the upper fourth premolar (P4) and the lower first molar (m1). Samples have been selected with the same criterion as we used for stable isotopes analyses, but only *U. deningeri* teeth were chosen for this proxy. Due to the bad preservation and advanced age of some specimens from Vallparadís Section, including craniums and mandibles, we have only been able to use a total of 5 dental remains for dental microwear analyses. However, we still have sampled all the available P4 and m1 in the assemblage, what means an equative number of specimens for each layer, being 1 sample from CGRD7 and 2 from EVT7, which have the same chronology, and 2 samples from EVT12.

3.2.2. Methodology

Once selected the teeth we were going to use, we have proceeded to make the replicas to perform the analyses. In this purpose, the protocol established by (Solounias & Semprebon, 2002) and (Semprebon et al., 2004) has been accurately followed. Firstly, the occlusal surface of all samples has been cleaned with acetone, thereby eliminating either remain that might act as a pollutant for the analysis. Then, the surface has been cleaned with 96° ethanol. The next step has been the realization of casts, made of high-resolution dental silicone (vinylpolysiloxane). We have covered the teeth surface with the mentioned material, using an application gun, taking care of building a wall, around the crown of the teeth to create a container for later pouring the epoxy resin. Then, after 10-20 minutes of waiting for the silicone to set, we have removed the molds from the teeth, from then on, having only to work with them. Later, molds have been filled with the epoxy resin, giving as result the positive of the teeth after 48h of setting.

These molds have been analysed under a Zeiss Stemi 2000C stereomicroscope at 35x magnification.

Carnivores are known to possess carnassial teeth, which develop an advanced function in the masticatory activity. Focusing on the m1 in ursids, it can be separated into two main areas, depending on its function. The mesial part is called the slicing area, while the distal part is termed the grinding area. The slicing area is placed in the cusps set called trigonid, which consists of 1) paraconid, 2) protoconid, 3) metaconid. Furthermore, grinding area occupies the talonid, which consists of 1) entoconid, 2) hipoconid, 3) hipoconulid.

In addition, within the occlusal surface we can distinguish two different types of surfaces: facets and non facets. Facet surfaces are related with direct contact between upper and lower teeth, and it is the area where the wear is visible *de visu*. Instead, non facet surfaces are not directly related with this contact, showing normally different microwear results than that from facet surfaces.

For this work, all kind of surfaces have been used, except in specimen 14950, since the individual seemed to be very old, and all the tooth consisted of facet surfaces.

The dental microwear analyses from this work has been also performed following the methods and features classification present in (Solounias & Semprebon, 2002) and (Semprebon et al., 2004). It consists of the quantification of different kind of marks in a reticle of 0.16 mm^2:

- Scratches: elongated scars. They can appear as 1) fine scratches (FS), which, as its name suggests, are fine and slightly deep; 2) coarse scratches (CS), wider and deeper than fine scratches; 3) hypercoarse scratches (HCS), which are even deeper and darker than coarse scratches; 4) cross scratches (XS), which are the minority of the total scratches that are perpendicularly oriented as to the most of it.
- Scratch width score: value that depends on the kind of scratches that prevail on the analysed surface. A value of (0) is related to a surface where fine scratches are prevalent; (1) is assigned to a relative equivalent of mix of fine and coarse scratches; (2) is related to a surface where coarse scratches are prevalent; (3) is related to the presence of hypercoarse scratches.
- Pits: round scars. They can appear as 1) small pits (SP), which present a white brilliant color under the microscope; 2) large pits (LP), which are deeper and larger than small pits, and present a darker color under microscope; 3) puncture pits (PP), which are much deeper than large pits, with a very simmetric and regular surface; 4) gouges (G), whose irregular edges are their most identifiable feature.

Microphotographs of the analysed surfaces have been taken with a Blackfly S digital camera and the Kivy Mic Capture Z as the software. In order to achieve a complete depth of field, we merged the different images taken from various focal planes and produced one single image with Helicon Focus 7, and for inserting the scale we used ImageJ.

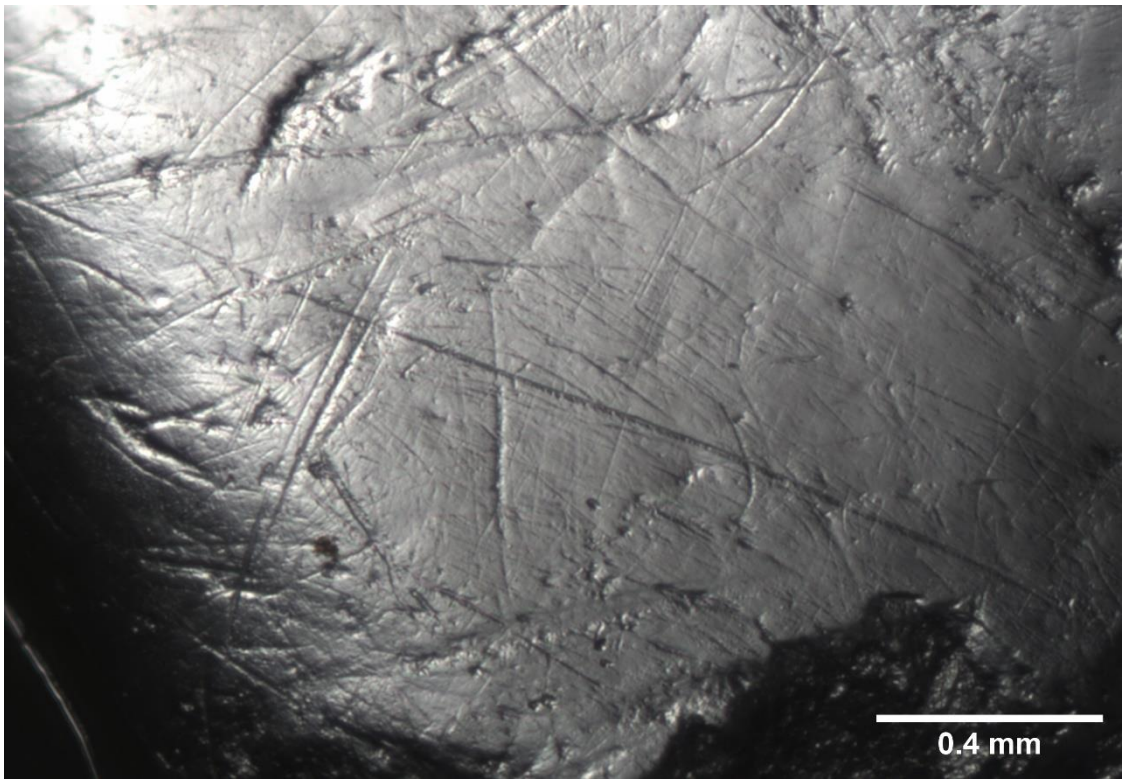

Fig. 15. Scratches and pits in the occlusal surface of an upper first molar (M1) of specimen IPS110442.

4. Results

4.1. Stable isotopes analyses ($\delta^{13}C$ and $\delta^{18}O$)

The $\delta^{13}C$ values of all taxa measured in Vallparadís Section range from -15.6 to -7.8‰ with a mean of -12.4 ± 1.3‰ (*n* = 112) (Tables 3-6; Fig. 16 and 17). *Pachycrocuta brevirostris* (*n* = 13; range = -13.2 to -10.1‰; mean = -12.1 ± 1‰), *Ursus deningeri* (*n* = 31; range = -15.6 to -12.1‰; mean = -13.7 ± 0.8‰), *Canis mosbachensis* (*n* = 11; range = -13.1 to -11.79‰; mean = -12.4 ± 0.4‰), *Hippopotamus antiquus* (*n* = 6; range = -13.3 to -12.1‰; mean = -12.8 ± 0.4‰), *Mammuthus meridionalis* (*n* = 6; range = -13.6 to -11.3‰; mean = -12.2 ± 0.9‰), *Stephanorhinus hundsheimensis* (*n* = 11; range = -12.8 to -11.4‰; mean = -12.0 ± 0.4‰), *Dama vallonnetensis* (*n* = 12; range = -13.0 to -9.5‰; mean = -11.8 ± 0.8‰), *Equus altidens* (*n* = 11; range = -13.3 to -8.3‰; mean = -12.0 ± 1.3‰), *Bison schoetensacki* (*n* = 11; range = -12.5 to -7.8‰; mean = -10.4 ± 1.7‰).

The $\delta^{18}O$ values of all taxa range from -5.3 to 1.6‰ with a mean of -2.9 ± 1.3‰ (*n* = 112) (see Table 2). *Pachycrocuta brevirostris* (*n* = 13; range = -4.6 to -1.5‰; mean = -3.5 ± 0.8‰), *Ursus deningeri* (*n* = 31; range = -5.0 to -0.8‰; mean = -2.9 ± 1.0‰), *Canis*

mosbachensis (*n* = 11; range = -2.8 to 1.6‰; mean = -1.2 ± 1.5‰), *Hippopotamus antiquus* (*n* = 6; range = -5.0 to -3.7‰; mean = -4.5 ± 0.5‰), *Mammuthus meridionalis* (*n* = 6; range = -5.0 to -1.4‰; mean = -3.5 ± 1.2‰), *Stephanorhinus hundsheimensis* (*n* = 11; range = -4.5 to -2.7‰; mean = -3.7 ± 0.6‰), *Dama vallonnetensis* (*n* = 12; range = -4.6 to 0.0‰; mean = -2.2 ± 1.4‰), *Equus altidens* (*n* = 11; range = -5.3 to -1.5‰; mean = -3.3 ± 1.1‰), *Bison schoetensacki* (*n* = 11; range = -4.4 to 0.4‰; mean = -2.8 ± 1.4‰).

Table 2. Carbonate hydroxylapatite $\delta^{13}C$ and $\delta^{18}O$ values from Vallparadís Section mammal assemblage.

Sample	Species	Layer	$\delta^{13}C$	$\delta^{18}O$	C SD	O SD
1	*U. deningeri*	EVT12	-13.9	-2.7	0.05	0.10
2	*U. deningeri*	EVT7	-15.4	-2.0	0.06	0.04
3	*U. deningeri*	EVT7	-14.2	-2.4	0.02	0.01
4	*U. deningeri*	EVT7	-12.9	-4.1	0.04	0.07
5	*U. deningeri*	EVT7	-14.1	-3.3	0.01	0.09
6	*U. deningeri*	EVT7	-15.6	-3.7	0.02	0.03
7	*U. deningeri*	EVT7	-13.6	-3.6	0.06	0.23
8	*U. deningeri*	EVT7	-13.9	-4.9	0.06	0.02
9	*U. deningeri*	EVT7	-12.9	-3.9	0.02	0.06
10	*U. deningeri*	EVT7	-12.9	-3.1	0.03	0.03
11	*U. deningeri*	EVT7	-13.5	-4.6	0.01	0.06
12	*U. deningeri*	EVT7	-13.5	-3.7	0.02	0.04
13	*U. deningeri*	EVT7	-12.5	-2.1	0.04	0.01
14	*U. deningeri*	EVT7	-12.8	-2.6	0.01	0.01
15	*U. deningeri*	EVT7	-14.7	-5.0	0.06	0.31
16	*U. deningeri*	EVT7	-13.8	-2.7	0.25	0.21
17	*U. deningeri*	EVT7	-13.8	-2.9	0.01	0.05
18	*U. deningeri*	EVT7	-12.4	-0.8	0.03	0.01
19	*U. deningeri*	EVT7	-13.7	-2.6	0.02	0.04
20	*U. deningeri*	EVT7	-14.3	-2.3	0.02	0.10
21	*U. deningeri*	EVT7	-15.4	-2.8	0.05	0.23
22	*U. deningeri*	EVT7	-13.9	-2.2	0.04	0.06
23	*U. deningeri*	EVT7	-14.0	-2.5	0.01	0.05
24	*U. deningeri*	EVT7	-14.1	-1.2	0.10	0.14
25	*U. deningeri*	EVT7	-13.7	-2.9	0.04	0.04
26	*U. deningeri*	EVT7	-12.1	-3.2	0.06	0.02
27	*D. vallonnetensis*	EVT7	-11.9	-1.4	0.02	0.07
28	*S. hundsheimensis*	EVT12	-12.8	-3.5	0.00	0.05
29	*D. vallonnetensis*	EVT7	-12.4	-3.1	0.01	0.03
30	*D. vallonnetensis*	EVT7	-11.6	-2.4	0.01	0.06
31	*D. vallonnetensis*	EVT7	-12.0	-3.5	0.01	0.02
32	*D. vallonnetensis*	EVT12	-11.7	-1.1	0.06	0.07
33	*D. vallonnetensis*	EVT7	-9.5	0.0	0.03	0.06
34	*E. altidens*	EVT7	-12.2	-3.1	0.03	0.03
35	*M. meridionalis*	EVT7	-13.6	-4.2	0.05	0.08

36	*D. vallonnetensis*	EVT7	-12.0	-0.8	0.03	0.02
37	*D. vallonnetensis*	EVT12	-11.5	-1.4	0.08	0.10
38	*M. meridionalis*	EVT7	-12.6	-1.4	0.02	0.10
39	*S. hundsheimensis*	EVT12	-12.4	-4.0	0.01	0.02
40	*D.vallonnetensis*	EVT7	-12.1	-1.6	0.03	0.02
41	*D. vallonnetensis*	EVT12	-12.0	-4.3	0.03	0.06
42	*S. hundsheimensis*	EVT7	-11.7	-3.3	0.06	0.11
43	*S. hundsheimensis*	EVT7	-11.4	-4.4	0.02	0.04
44	*S. hundsheimensis*	EVT7	-12.1	-4.5	0.04	0.08
45	*S. hundsheimensis*	EVT7	-12.0	-4.2	0.01	0.03
46	*M. meridionalis*	EVT7	-11.3	-3.5	0.05	0.12
47	*S. hundsheimensis*	EVT7	-11.6	-3.2	0.01	0.03
48	*S. hundsheimensis*	EVT7	-11.9	-2.7	0.01	0.01
49	*B. schoetensacki*	EVT7	-12.5	-1.5	0.01	0.05
50	*B. schoetensacki*	EVT7	-10.8	-3.7	0.04	0.07
51	*S. hundsheimensis*	EVT12	-12.0	-3.8	0.01	0.04
52	*B. schoetensacki*	EVT7	-12.3	0.4	0.02	0.08
53	*B. schoetensacki*	EVT7	-10.0	-3.9	0.04	0.07
54	*E. altidens*	EVT7	-12.8	-1.5	0.02	0.04
55	*E. altidens*	EVT7	-12.1	-2.3	0.01	0.06
56	*E. altidens*	EVT7	-11.7	-2.4	0.01	0.02
57	*S. hundsheimensis*	EVT12	-11.8	-2.8	0.00	0.04
58	*B. schoetensacki*	EVT12	-11.7	-4.2	0.03	0.06
59	*E. altidens*	EVT7	-11.7	-2.9	0.03	0.06
60	*U. deningeri*	EVT12	-13.7	-2.8	0.02	0.11
61	*U. deningeri*	EVT12	-14.2	-3.2	0.01	0.02
62	*U. deningeri*	EVT12	-13.4	-2.2	0.03	0.06
63	*U. deningeri*	EVT12	-14.0	-1.7	0.03	0.05
64	*P. brevirostris*	EVT12	-13.0	-1.5	0.03	0.05
65	*U. deningeri*	EVT12	-13.7	-2.1	0.03	0.05
66	*P. brevirostris*	EVT12	-12.8	-3.2	0.03	0.06
67	*P. brevirostris*	EVT12	-12.4	-3.9	0.03	0.02
68	*S. hundsheimensis*	EVT12	-12.7	-4.2	0.02	0.02
69	*D. vallonnetensis*	EVT12	-13.0	-4.6	0.04	0.07
70	*P. brevirostris*	EVT12	-13.2	-3.6	0.06	0.06
71	*P. brevirostris*	EVT12	-12.2	-3.8	0.01	0.02
72	*P. brevirostris*	EVT12	-13.1	-3.8	0.05	0.03
73	*H. antiquus*	EVT12	-12.8	-4.4	0.05	0.04
74	*P. brevirostris*	EVT12	-12.4	-3.3	0.02	0.03
75	*C. mosbachensis*	EVT12	-13.1	-2.8	0.02	0.09
76	*C. mosbachensis*	EVT12	-12.5	0.4	0.02	0.01
77	*P. brevirostris*	EVT7	-12.0	-2.9	0.04	0.05
78	*C. mosbachensis*	EVT12	-12.6	-2.4	0.02	0.11
79	*P. brevirostris*	EVT7	-11.5	-4.4	0.03	0.17
80	*P. brevirostris*	EVT7	-11.9	-3.5	0.02	0.01
81	*C. mosbachensis*	EVT12	-12.7	0.3	0.03	0.03

82	*C. mosbachensis*	EVT12	-12.2	1.6	0.04	0.04
83	*P. brevirostris*	EVT7	-13.2	-3.1	0.04	0.07
84	*C. mosbachensis*	EVT7	-11.8	-0.1	0.01	0.01
85	*C. mosbachensis*	EVT7	-11.9	-1.1	0.03	0.03
86	*P. brevirostris*	EVT7	-10.1	-4.2	0.01	0.04
87	*C. mosbachensis*	EVT7	-12.6	-1.9	0.01	0.06
88	*C. mosbachensis*	EVT7	-12.2	-2.3	0.03	0.09
89	*P. brevirostris*	EVT7	-10.3	-4.6	0.01	0.01
90	*C. mosbachensis*	EVT7	-13.1	-2.8	0.01	0.04
91	*C. mosbachensis*	EVT7	-12.3	-2.5	0.02	0.01
92	*E. altidens*	EVT12	-12.6	-5.3	0.15	0.24
93	*E. altidens*	EVT12	-12.9	-3.7	0.05	0.02
94	*B. schoetensacki*	EVT12	-12.3	-4.4	0.03	0.25
95	*E. altidens*	EVT12	-12.1	-3.3	0.06	0.19
96	*E. altidens*	EVT12	-8.3	-3.1	0.03	0.03
97	*D. vallonnetensis*	EVT12	-12.1	-2.3	0.01	0.07
98	*B. schoetensacki*	EVT12	-8.7	-2.5	0.03	0.01
99	*B. schoetensacki*	EVT12	-8.2	-3.1	0.03	0.02
100	*B. schoetensacki*	EVT12	-7.8	-2.5	0.01	0.05
101	*M. meridionalis*	EVT7	-11.4	-3.6	0.01	0.02
102	*E. altidens*	EVT12	-13.3	-4.9	0.01	0.07
103	*H. antiquus*	EVT7	-13.3	-4.8	0.02	0.18
104	*H. antiquus*	EVT7	-12.1	-4.3	0.01	0.01
105	*H. antiquus*	EVT7	-12.9	-5.0	0.04	0.11
106	*M. meridionalis*	EVT7	-12.9	-3.2	0.03	0.04
107	*B. schoetensacki*	EVT7	-9.7	-2.4	0.02	0.03
108	*B. schoetensacki*	EVT7	-10.8	-2.9	0.03	0.04
109	*H. antiquus*	EVT7	-12.8	-4.6	0.01	0.01
110	*H. antiquus*	EVT7	-13.3	-3.7	0.04	0.05
111	*E. altidens*	EVT12	-12.7	-3.3	0.01	0.05
112	*M. meridionalis*	EVT7	-11.7	-5.0	0.03	0.02

Table 3. Univariate statistics of $\delta^{13}C$ values from EVT7 samples.

	N	**Min**	**Max**	**Mean**	**Std. error**	**Variance**	**Stand. dev**
U. deningeri	25	-15.6	-12.1	-13.7	0.18	0.83	0.91
S. hundsheimensis	6	-12	-11.4	-11.8	0.1	0.06	0.25
D. vallonnetensis	7	-12.4	-9.5	-11.6	0.36	0.92	0.96
B. schoetensacki	6	-12.5	-9.7	-11	0.48	1.4	1.18
P. brevirostris	6	-13.2	-10	-11.5	0.47	1.34	1.16
H. antiquus	5	-13.3	-12	-12.9	0.22	0.25	0.5
C. mosbachensis	6	-13.1	-11.8	-12.3	0.2	0.23	0.48
E. altidens	5	-12.8	-11.7	-12.1	0.2	0.19	0.44
M. meridionalis	6	-13.6	-11.3	-12.2	0.38	0.88	0.94

Table 4. Univariate statistics of $\delta^{13}C$ values from EVT12 samples.

	N	Min	Max	Mean	Std. error	Variance	Stand. dev
U. deningeri	6	-14.2	-13.4	-13.8	0.12	0.08	0.29
S. hundsheimensis	5	-12.8	-11.8	-12.3	0.19	0.18	0.42
D. vallonnetensis	5	-13	-11.5	-12.1	0.25	0.31	0.55
B. schoetensacki	5	-12.3	-7.8	-9.7	0.93	4.33	2.08
P. brevirostris	7	-13.2	-12.2	-12.7	0.14	0.14	0.38
H. antiquus	1	-12.8	-12.8	-12.8	0	0	0
C. mosbachensis	5	-13.1	-12.2	-12.6	0.14	0.1	0.32
E. altidens	6	-13.3	-8.3	-12	0.76	3.45	1.86

Table 5. Univariate statistics of $\delta^{18}O$ values from EVT7 samples.

	N	Min	Max	Mean	Std. Error	Variance	Stand. Dev
U. deningeri	25	-5.1	-0.8	-3	0.21	1.07	1.03
S. hundsheimensis	6	-4.5	-2.7	-3.7	0.3	0.56	0.75
D. vallonnetensis	7	-3.5	0	-1.8	0.48	1.61	1.27
B. schoetensacki	6	-3.9	0.4	-2.3	0.65	2.54	1.59
P. brevirostris	6	-4.6	-2.9	-3.8	0.29	0.51	0.71
H. antiquus	5	-5	-3.7	-4.5	0.23	0.27	0.52
C. mosbachensis	6	-2.8	-0.1	-1.8	0.41	1.02	1.01
E. altidens	5	-3.1	-1.5	-2.4	0.29	0.41	0.64
M. meridionalis	6	-5	-1.4	-3.5	0.49	1.46	1.21

Table 6. Univariate statistics of $\delta^{18}O$ values from EVT12 samples.

	N	Min	Max	Mean	Std. error	Variance	Stand. dev
U. deningeri	6	-3.2	-1.7	-2.4	0.23	0.31	0.55
S. hundsheimensis	5	-4.2	-2.8	-3.7	0.25	0.32	0.56
D. vallonnetensis	5	-4.6	-1.1	-2.7	0.73	2.68	1.64
B. schoetensacki	5	-4.4	-2.4	-3.3	0.41	0.86	0.93
P. brevirostris	7	-3.9	-1.5	-3.3	0.31	0.68	0.83
H. antiquus	1	-4.4	-4.4	-4.4	0	0	0
C. mosbachensis	5	-2.8	1.6	-0.6	0.86	3.67	1.91
E. altidens	6	-5.3	-3.1	-3.9	0.38	0.87	0.93

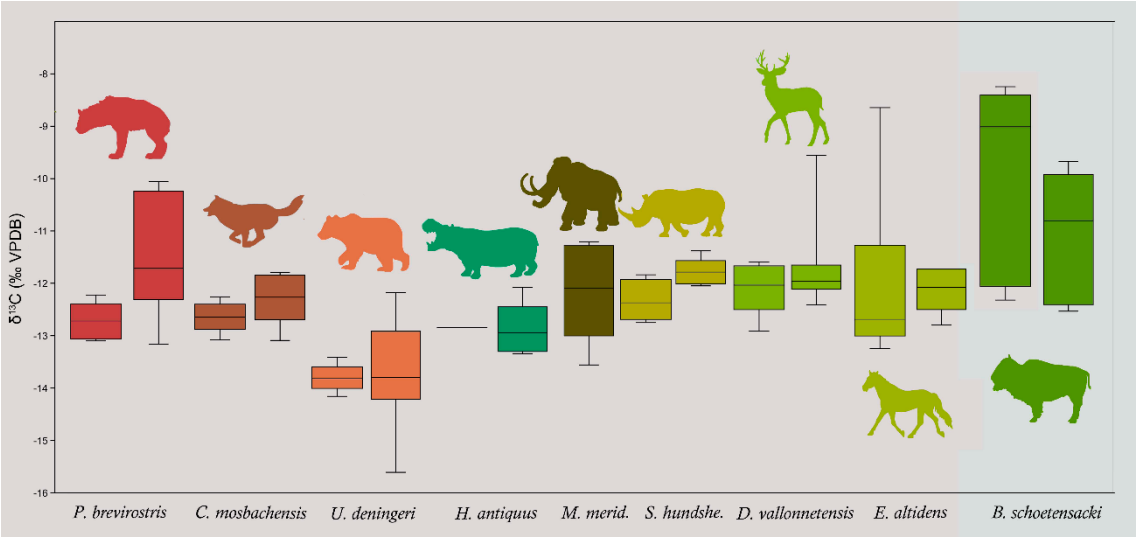

Fig. 16. Isotopic signatures of $\delta^{13}C$ values from EVT12 (left) and EVT7 (right) samples. Reddish colours belonging to carnivores, greenish colours belonging to herbivores.

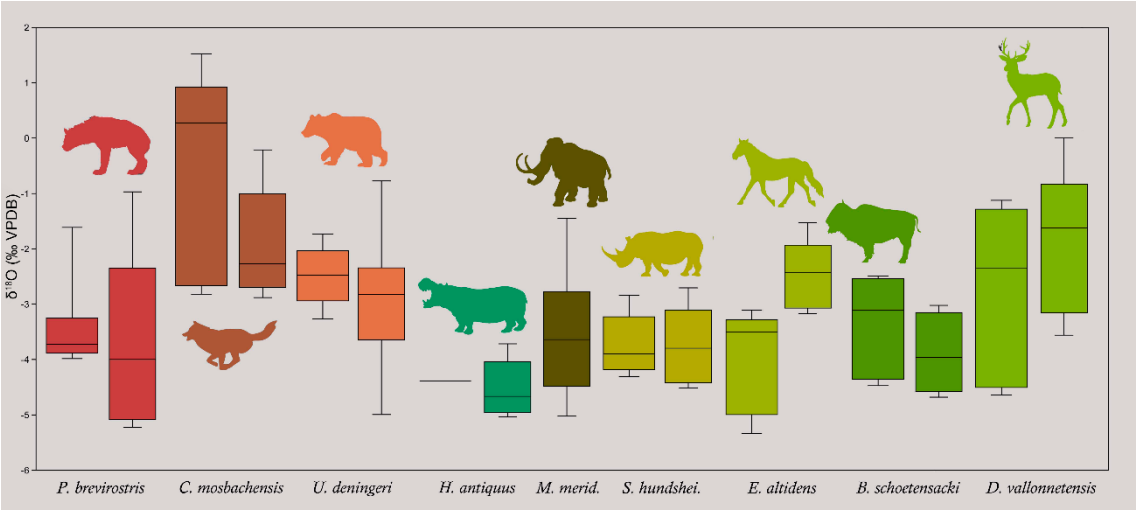

Fig. 17. Isotopic signatures of $\delta^{18}O$ values from EVT12 (left) and EVT7 (right) samples. Reddish colours belonging to carnivores, greenish colours belonging to herbivores.

4.2. Dental microwear analyses

The dental microwear analyses has been performed on 5 lower first molars, in both facets and non-facets surfaces when it has been possible. The first results we can observe are the clear difference regarding the number of pits and scratches depending on the type of surface (Fig. 18). The total number of scratches is higher in the facet surfaces than in the non-facet surfaces, which present a higher number of pits. For the

analysis we have selected the non-facets surfaces, since the specimen IPS14950 does not present facet surfaces.

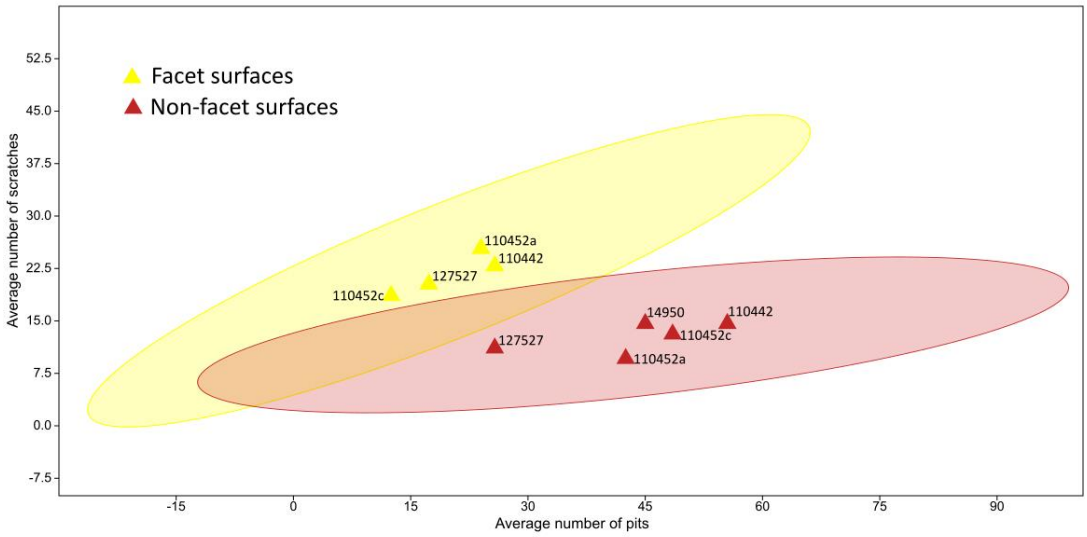

Fig. 18. Bivariate plot of number of pits and scratches in the 5 samples used for dental microwear analyses, considering both facet and non-facet surfaces, with 95% confidence ellipses.

The dental microwear values for *Ursus deningeri* display an equative number of scratches and pits. The average number of scratches for the 5 studied specimens show a huge range of values from 12.5 to 25.8 scratches, with a mean of 19.8 ± 6.2 scratches. The average number of pits show a range of values from 18 to 25.8 pits, with a mean of 21.9 ± 3.3 pits (Tables 7 and 8).

Providing context for our data and comparing it to dental microwear reference data of extant species from Pappa et al., (2019), we find a clear difference between *U. deningeri* and specialized diet ursids (Fig. 19 and 20). In the case of *Ailuropoda melanoleuca*, it presents an average number of total scratches of 19.2, and a much higher average number of total pits of 57. This is attributed to its strictly herbivorous diet based on bamboo stems and leaves. In the other hand, if we observe the values of *Ursus maritimus*, another specialist bear, we find an average number of total scratches of 16.3, and an average number of total pits of 20.9. The low number of scratches is assigned to a poor consumption of abrasive food, given its hypercarnivorous specialized diet. *Melursus ursinus*, which has an insectivorous diet, show an average number of total scratches of 16, and 36.7 for the average number of total pits.

Regarding the number of pits of these 3 specialist species, which present an increasing number of pits for, in sequence, *U. maritimus*, *M. ursinus*, and *A. melanoleuca*, our *U. deningeri* specimens are placed between *U. maritimus* and *M. ursinus*, with values much closer to the last one.

The comparison with other extant bears with a more generalist diet, shows a more equative number of pits and scratches, but with a remarkable difference between the average number of total pits of *Ursus arctos* and Vallparadís ursids. The first one has a number of scratches of 20.3, and a number of pits of 31.2.

Table 7. Raw data from dental microwear of *U. deningeri*. Abbreviations: TS = total number of scratches; FS = fine scratches; CS = coarse scratches; HCS = hypercoarse scratches; SWS = scratch width score; XS = cross scratches; TP = total number of pits; SP = small pits; LP = large pits; PP = puncture pits; G = gouges.

Specimen	TS	FS	CS	HCS	SWS	XS	TP	SP	LP	PP	G
110452a_faceta1_1	11	7	4	0	1	0	40	25	15	0	0
110452a_faceta1_2	11	7	4	0	1	0	47	29	18	0	0
110452a_faceta2_1	11	9	2	0	0	0	45	38	7	0	0
110452a_faceta2_2	7	6	1	0	0	0	38	34	4	2	2
110452a_nofaceta1_1	20	14	6	0	0	2	19	15	4	3	2
110452a_nofaceta1_2	25	12	13	0	1	3	26	14	12	0	0
110452a_nofaceta2_1	35	27	8	0	0	5	33	26	7	0	0
110452a_nofaceta2_2	23	16	7	0	0	3	18	14	4	1	0
110452c_faceta1_1	20	14	5	1	0	1	54	34	20	0	0
110452c_faceta1_2	16	13	3	0	0	0	47	42	5	2	0
110452c_faceta2_1	9	2	7	0	2	0	48	34	14	0	0
110452c_faceta2_2	9	3	6	0	1	0	45	30	12	0	3
110452c_nofaceta1_1	24	19	4	1	1	4	15	11	4	0	0
110452c_nofaceta1_2	14	11	2	1	1	0	10	9	1	0	0
127527_faceta1_1	14	11	3	0	1	2	24	22	2	0	0
127527_faceta1_2	17	14	3	0	1	1	23	23	0	0	0
127527_faceta2_1	8	5	2	1	1	1	23	23	0	0	0
127527_faceta2_2	7	5	2	0	1	0	33	31	2	0	0
127527_nofaceta1_1	28	24	4	0	0	3	15	14	0	0	1
127527_nofaceta2_1	18	16	2	0	0	3	14	14	0	0	0
127527_nofaceta2_2	16	14	2	0	0	5	23	23	0	0	0
14950_faceta1_1	11	9	2	0	0	2	62	62	0	0	0
14950_faceta1_2	19	15	4	0	1	5	28	28	0	0	0
110442_faceta1_1	13	12	1	0	0	1	62	62	0	0	4
110442_faceta1_2	17	16	1	0	0	7	49	49	0	0	0
110442_nofaceta1_1	24	18	5	1	1	7	25	24	1	0	0
110442_nofaceta1_2	32	30	2	0	0	11	25	25	0	0	0
110442_nofaceta2_1	18	10	8	0	1	8	32	31	1	0	2
110442_nofaceta2_2	19	15	4	0	0	6	21	20	1	0	0

Table 8. Average number of analysed variables in the surface used for this work. Abbreviations: TS = total number of scratches; FS = fine scratches; CS = coarse scratches; HCS = hypercoarse scratches; SWS = scratch width score; XS = cross scratches; TP = total number of pits; SP = small pits; LP = large pits; PP = puncture pits; G = gouges.

Specimen	**110452a**	**110452c**	**127527**	**110442**
Area	no_facetas	no_facetas	no_facetas	no_facetas
Layer	EVT12	EVT12	EVT7	EVT7
TS	25.75	19	20.67	23.25
FS	17.25	15	18	18.25
CS	8.5	3	2.67	4.75
HCS	0	1	0	0.25
SWS	0.25	1	0	0.5
XS	2.67	2	3.67	8
TP	24	12.5	17.33	25.75
SP	17.25	10	17	25
LP	6.75	2.5	0	0.75
PP	1	0	0	0
G	0.5	0	0.33	0.5

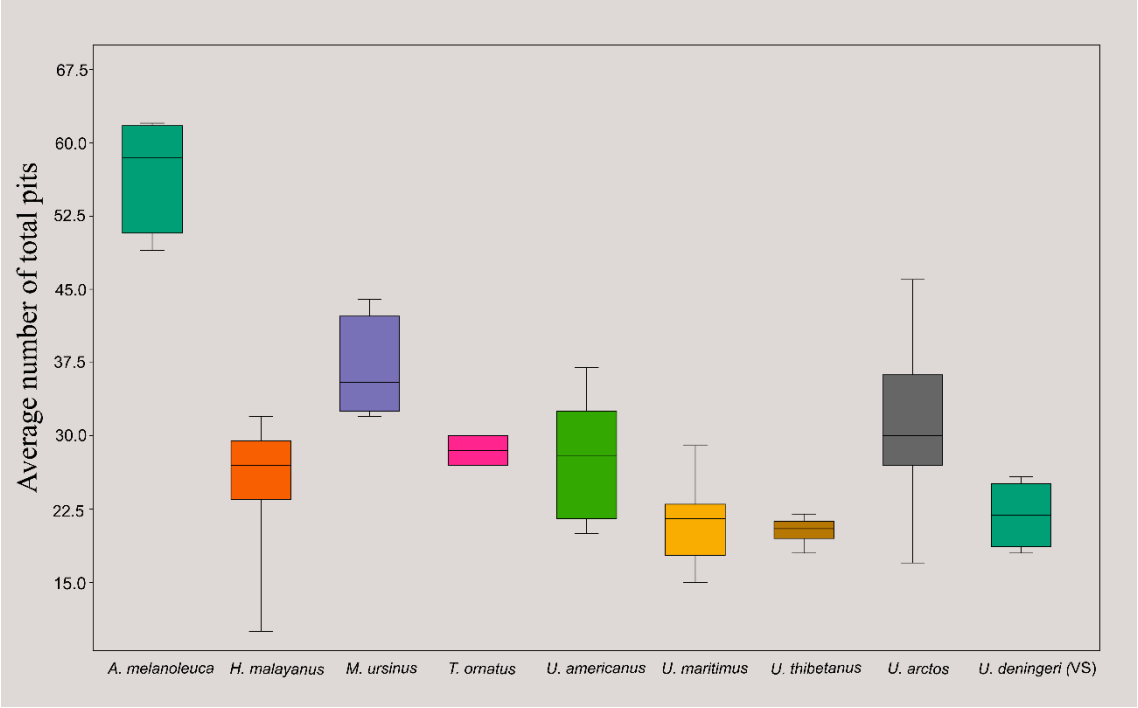

Fig. 19. Boxplots indicating average number of total pits of *U. deningeri* from Vallparadís Section (VS) compared to extant bears. Reference data from Pappa et al., (2019).

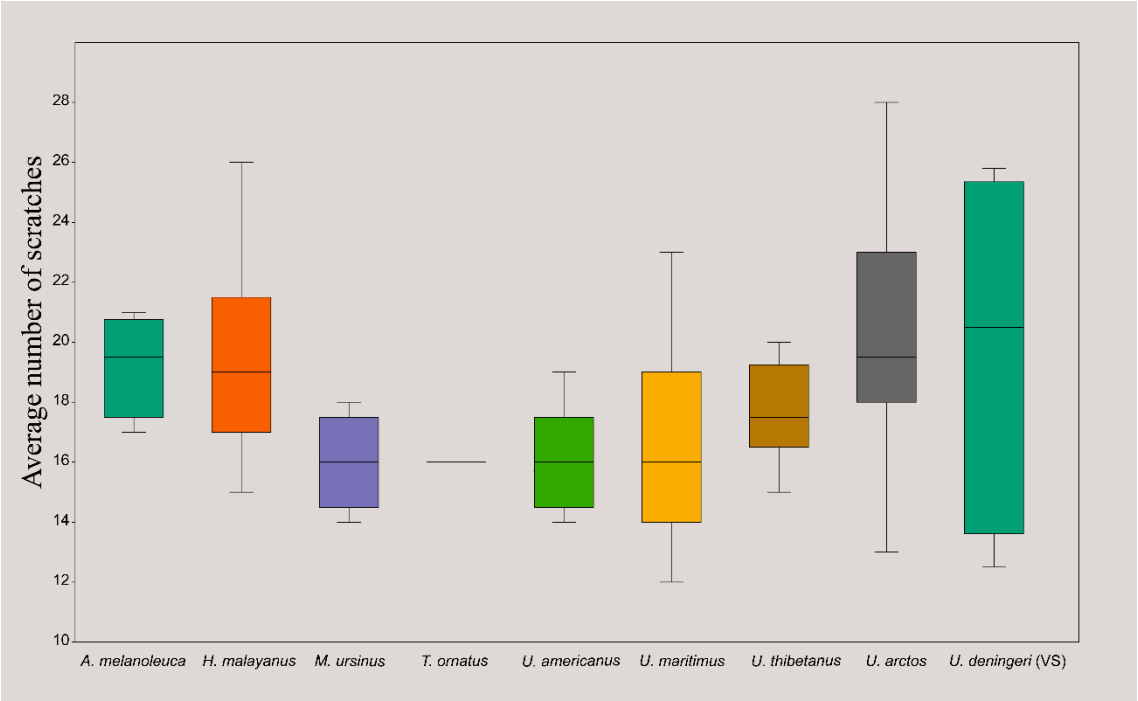

Fig. 20. Boxplots indicating average number of total scratches of *U. deningeri* from Vallparadís Section (VS) compared to extant bears. Reference data from Pappa et al., (2019).

A comparison with *U. arctos* from different geographic locations and latitudes and *U. americanus* has been performed in a correspondence analysis (CA) considering five dental microwear variables (LP = large pits; SP = small pits; FS = fine scratches; CS = coarse scratches; SWS = scratches width score) (Fig. 21; Table 9). The results places *U. deningeri* values far from those of *U. arctos* from South Europe.

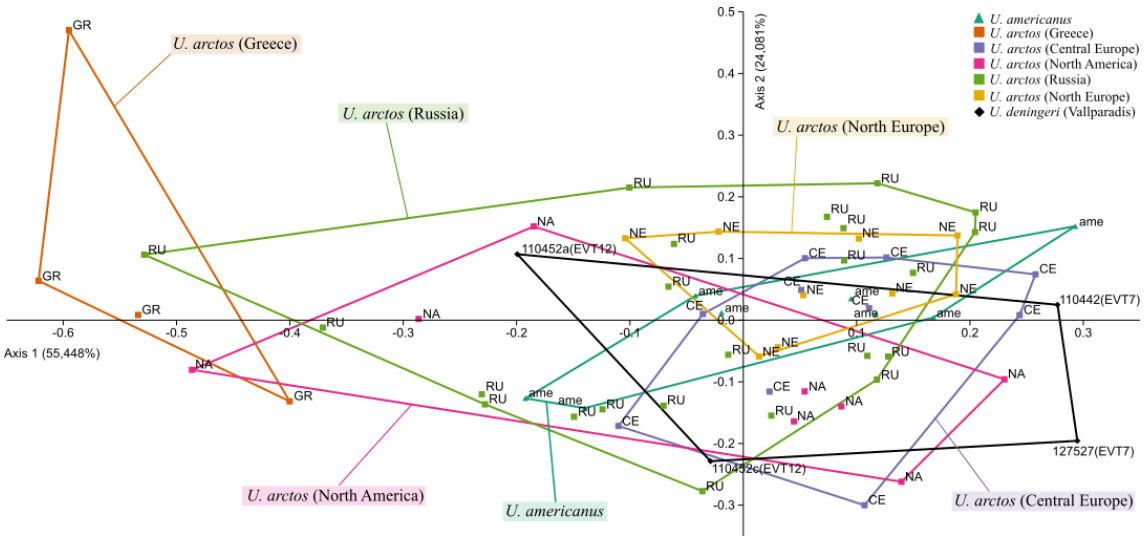

Fig. 21. Correspondence analysis based on five dental microwear variables (LP = large pits; SP = small pits; FS = fine scratches; CS = coarse scratches; SWS = scratches width score). Reference data of extant bears from Pappa et al., (2019).

Table 9. Eigenvalues and percentages of total and cumulative variance for the different axis in the Correspondance Analyses (CA).

Axis	Eigenvalue	% of total	Cumulative
1	0.0423886	55.448	55.448
2	0.0184096	24.081	79.529
3	0.0136471	17.851	97.38
4	0.00200267	2.6196	100

5. Discussion

5.1. Stable isotopes analyses

Regarding the stable isotopes analyses, we obtained enough valid results to make different interpretations for both different studied layers and species. Given the large number of samples used for stables isotopes analyses, the conclusion for each result is related to each species, so we have not interpreted the results as a simple answer to the question previously made in the beginning of this work. Instead, we obtained several answers for several questions.

5.1.1. Carbon stable isotopes

We have used the enamel-diet enrichment factor of +14.1 ± 0.5‰ for ungulates (Cerling & Harris, 1999; Passey et al., 2005) to interpret tooth enamel $\delta^{13}C$ values and estimate potential consumption of C_3- or C_4-plant. These isotopic enrichment factor values for C_3 and C_4 plants are assumed to provide tooth enamel values of < −15.9‰ for closed canopy diets, < −11.4‰ for pure C_3 diets, < −7.4‰ for C_3-dominated diets, from −7.4 to +1.6‰ for C_3–C_4 mixed feeders, > +1.6‰ for C_4-dominated diets and > +3.6‰ for pure C_4 diets in ungulates, which is the one followed for this paper.

In terms of general interpretation of diet and habitat of the species from the assemblage, we can consider that divergence in layers EVT12 and EVT7 of δ13C values between ungulates is marked. From a point of view of variation in results, the two most sensitive herbivores in this analysis are *E. altidens* and, especially, *B. schoetensacki*, since the first one presents a more constant range of values. These ungulates appear to be

grazers, following the relatively high $\delta^{13}C$ signal values for both species. However, it is possible to observe the decrease in the signatures when dealing with the layer EVT7. This demonstrates that either *E. altidens* or *B. schoetensacki* were more grazers in the Jaramillo subchron, corresponding to the layer EVT12 (MIS31), than in the post-Jaramillo subchron, corresponding to the layer EVT7 (MIS21). This is both in agreement with the previous results obtained for Strani et al., (2019) and Sorbelli et al., (2021), who in one side show both ungulates were purely grazers in EVT12 and mixed feeders in EVT7 and on the other side have more stouter postcranial bones in EVT12 as compared with EVT7. Unpublished results of Cirilli and Madurell-Malapeira for equid post-cranial bones also go to the same direction.

In the case of *Dama vallonnetensis*, the $\delta^{13}C$ values show the ubiquity of this species. It is known the cervids are a family with an outstanding plasticity. We could have expected lower values from EVT7 layer than in EVT12, given the new array of options that opened in that moment, leading it to a more C_3-plant feeding behaviour. Instead, we obtained similar values for both layers, demonstrating both the plasticity and ubiquity that the species can display, as well as the ability they have for adapting to new environments. In Strani et al., (2019), the dental microwear data of *D. vallonnetensis* shows a grazer diet in EVT12 and a mixed feeder one in EVT7 for the former taxon. *Hippopotamus antiquus* show low values in both EVT12 and EVT7 layers, putatively related to a wide accessibility to aquatic plants. The $\delta^{13}C$ values of and *Mammuthus meridionalis* display that the species had a grazing diet behaviour in EVT7, since we only provide specimens from the mentioned layer. Surprisingly, *Stephanorhinus hundsheimensis* appears to have been more grazer in EVT7 than in EVT12 on the contrary to the results obtained for microwear for Strani et al., (2019) pointing to a grazer diet in EVT12 and a mixed feeder one in EVT7.

Other researchers have reached the same conclusion regarding the environment change from EVT12 to EVT7, although by using different methodologies. Sorbelli et al., (2021) made a review on *B. schoetensacki* through the early-Middle Pleistocene Transition, focusing on the samples from Vallparadís Section, which is the largest collection of the species together with that from Isernia la Pineta. In the mentioned work, a taxonomical study is carried out, in order to attribute the species to the

specimens, and a morphological analysis of cranial and post-cranial material is also performed. The morphological study included the observation of multiple remains belonging to different parts of the body of the species, leading the researchers to a consensus in which they decided to assign the big number of samples to the species *Bison schoetensacki*, and to differentiate different ecomorphotypes. During the morphological study of metapodials, they observed a change in size and dimensions in those from the layer EVT12 compared to those from the layer EVT7. The first ones were found to be stout and robust, while the other ones appeared to be slender. The robust and stout limb bones are directly related to open habitats as grasslands, and slender limb bones are associated with closed habitats.

In Strani et al., (2019), a mesowear study is complemented with a microwear analysis of ungulates from Vallparadís Section although they different timescale results. They conclude there is a climate shift that leads to a more mixed feeding behaviour on the Vallparadís Section during the post-Jaramillo subchron (EVT7), compared to that from EVT12 on all the analysed species were considered grazers.

5.1.1.1. Physiological behaviour

While fossil ungulates are good indicators to reconstruct their diets and environments they inhabited, carbon isotopic data from the carnivore guild allow the researchers to know about behaviours beyond the dietary habits. Thus, carnivorans physiological conducts can be related to $\delta^{13}C$ values, with inferences on issues of their lives that, in addition of paleodiet studies, help the scientific community to comprehend in a better way the paleoecology of fossil species (Liden & Angerbjörn, 1999; Fernández-Mosquera et al., 2001)

Concerning the $\delta^{13}C$ values for *U. deningeri*, in both layers, we have observed that the ursids present the lowest values from all analysed taxa. We have related these signatures with the phenomenon of hibernation. Bears, when hibernating, go through several changes in their metabolism, which change some energetic factors linked to several physiological adaptations to this period. For example, during dormancy, bears do not urinate nor defecate, they reuse the urea for synthetising aminoacids, they do

not eat or drink, their core temperature decreases, and their main energetic source is their own fat reserves (Nelson, 1980; Bocherens, 2004). Although this has been already tested for N values, its influence on C values is also suggested from these new results.

As the female profits this moment to give birth and breastfeed her cubs, the isotopic data from the mother is reflected on the signature from the cub. This allows the researchers to open the range of usable samples regarding the age of the individual, since it is known the suffered signature increase or decrease in each stage of life of the individual.

Through the literature, these physiological adaptations regarding the period of dormancy in bears, has widely been attributed to an isotopic signature record of high $\delta^{15}N$ values (Torres & García, 1997; Nelson et al., 1998; Liden & Angerbjörn, 1999; Fernández-Mosquera et al., 2001), justifying this increase with the recycling of wasted nitrogen into aminoacids (Bocherens, 2004). However, this is not the only stable isotope which has been related to a possible interpretation linked to the hibernation of bears.

In addition to $\delta^{15}N$, $\delta^{13}C$ signature is also capable of giving insights from dormancy period. As the individual uses its fat reserves as an energetic source during winter dormancy, there is a greater discrimination of heavy isotope ^{13}C, resulting in a decrease in $\delta^{13}C$ values, which is also reflected in the cubs due to the transference via milk consumption (Jenkins et al., 2001; Bocherens, 2004).

Probably this evidence of *U. deningeri* can represent the first evidence of hibernation in fossil ursids, in accordance with the changing environmental conditions associated with the EMPT and the concomitant limitations of food during winters. Previously recorded species, namely *U. etruscus*, display smaller sizes, the absence of sexual dimorphism and more omnivorous diet making the fossils coeval to the EMPT the first cave bears of the fossil record as previously suggested our team in previous publications (Madurell-Malapeira et al., 2010, 2014, 2017; Medin et al, 2017, 2019). In fact, previous climatic conditions in the period from 1.8 to 1.2 Ma were probably the most warm and humid of all the Pleistocene (Head & Gibbard, 2015). Additionally, the bears from the Vallparadís Section shows a tendency to the herbivorism and an increase in size and

sexual dimorphism from 1.2 to 0.8 Ma (MIS35 to MIS21; Madurell-Malapeira, unpublished data)

The carbon stable isotopes values from *Pachycrocuta brevirostris* allow us to make another insight of physiological behavior. The high values of $\delta^{13}C$, aside from showing an increase in EVT7 compared to EVT12, could be indicators of bone mineral fraction consumption, assuming the widely assigned bone-cracking behavior (Palmqvist et al., 2011; Iannucci et al., 2021). The bone mineral fraction fixed in tooth enamel during its consumption is reflected in the carbon isotopic values and makes them grow. The case of *Canis mosbachensis*, instead, does not display this behavior having more stable values, making a clear distinction between the canid species and the giant hyena regarding physiological behaviors.

The putative increase in consumption of bones for *P. brevirostris* from EVT12 to EVT7 could be also related with the evidence of their activity recorded in these layers. In fact, the scavenging activity of the former taxon in EVT7 was widely recorded and more than 500 coprolites were unearthed, on the contrary their activity was scarce, and no coprolites were recovered from EVT12 (Madurell-Malapeira et al., 2017; unpublished data).

5.1.2. Oxygen stable isotopes

Concerning the $\delta^{18}O$, these isotopic data allow us, more accurately than just using $\delta^{13}C$ signatures, to know about the ecological niche that the analysed species from the Vallparadís Section assemblage could have filled during the "*Early-Middle Pleistocene Transition*". Specifically, we obtained results from oxygen stable isotopes since its signal values reflect the dependence on water from a species (Bocherens et al., 1996; Clementz & Koch, 2001; Levin et al., 2006; Grohé et al., 2022).

With the results of oxygen isotopic data, it has been possible to distinct between obligate and non-obligate drinking animals. Obligate drinkers are considered animals that must obtain water directly from surface water, and they have lower $\delta^{18}O$ values than non-obligate drinkers, which are animals that obtain water mainly from plant

consumption (Roberts et al., 2018). By measuring the difference in $\delta^{18}O$ values in tooth enamel in the mentioned dichotomy, it is possible to make inferences on the environmental conditions, the larger the difference the higher the estimated aridity (Levin et al., 2006; Blumenthal et al., 2017).

Here we selected *Hippopotamus antiquus*, *Equus altidens*, and *Bison schoetensacki* as obligate drinkers, and *Dama vallonnetensis* as a non-obligate drinker. Carnivore oxygen stable isotopes values does not give reliable information, given that their increase depends on the previously consumed prey (Hopley et al., 2023). Considering the previous classification, we can interpretate the results of $\delta^{18}O$ values to make determinate the aridity of both EVT12 and EVT7 layers, observing the difference between obligate and non-obligate drinkers oxygen values.

For EVT12 layer, the mean of $\delta^{18}O$ of *D. vallonnetensis* is -2.7 ± 1.6‰. Concerning the obligate drinkers selected, *B. schoetensacki* has a mean of -3.3 ± 0.9‰, *E. altidens* presents a mean of -3.9 ± 0.9‰, and *H. antiquus* has a unique value of -4.4‰. We can estimate an average value for obligate drinkers of -3.9 ± 0.5‰. This makes a difference of 1.2‰ between obligate and non-obligate drinking animals.

For EVT7 layer, the mean of $\delta^{18}O$ of *D. vallonnetensis* is -1.8 ± 1.3‰. Concerning the obligate drinkers selected, *B. schoetensacki* has a mean of -2.3 ± 1.6‰, *E. altidens* presents a mean of -2.4 ± 0.6‰, and *H. antiquus* has a mean of -4.5 ± 0.5‰. We can estimate an average value for obligate drinkers of -2.9 ± 1.4‰. This makes a difference of 1.1‰ between obligate and non-obligate drinking animals.

Surprisingly, these data poorly evidence the higher aridity in MIS31, corresponding to EVT12 layer, than in MIS21, corresponding to EVT7 layer, which is confirmed with both carbon stable isotopes analyses here presented and other studies focused on the Iberian Peninsula (E.g. in Quibas site, in Piñero et al., (2020)).

It is remarkable to note that, although ungulates are better indicators than carnivores regarding oxygen stable isotopes, using bulk stable isotopes ratios on a same hypsodont species can lead to a misunderstanding of the data obtained because of the seasonality. In $\delta^{18}O$ values, the variation of a sample according to it comes from one or the other

season is remarkable. In contrast, in $\delta^{13}C$ values, the variation concerning seasonality is far less important than in oxygen values.

Further isotopic analyses would be fundamental to a more complete interpretation of Early-Middle Pleistocene ursid paleoecology, starting with the stable isotopes analyses of Dmanisi or Vallonnet collections.

5.2. Dental microwear analyses

The dental microwear analysis allows us to compare *U. deningeri* from Vallparadís Section to both extant ursids and fossil ursids. Regarding the comparison with extant bears, *U. deningeri* appears to have had an omnivorous diet, but placed in some point between *U. arctos*, with a fully omnivorous diet, and *A. melanoleuca*, with a fully herbivorous diet. The high number of pits of *U. arctos* can be attributed to the consumption of fruits, so that the difference between *U. arctos* and *U. deningeri* does not allow to just make insights about the herbivorism. As for genetics and diet, the analyzed species falls well short of the specialists. (Macdonald, 2009; Pappa et al., 2019; Ramírez-Pedraza, personal communication). Thus, a more accurate comparison has required to put our data in the background of *U. arctos* from different geographic locations and latitudes and *U. americanus*.

U. arctos and *U. americanus* show similar feeding behavior, with an omnivorous diet. For the brown bear specimens of reference here used, we can distinguish between their geographic location, which are North America, North Europe, Central Europe, Greece, and Russia. Given the huge range obtained for our data, it is not easy to discern what is the latitude containing resources that best fit with the necessities of *U. deningeri*, beyond that discarding Greece.

There is a divergence between the values of the specimens coming from EVT12 layer and EVT7 layer, and it can be related with the environmental changes that took place between MIS31 and MIS21, reaffirming the results obtained in the other proxy here applied, the stable isotopes analyses, and other works which reach the same conclusions.

Regarding the dental microwear in fossil species (Fig. 22 and 23), in particular the cases of Orce (Medin et al., 2017) and Dmanisi (Medin et al., 2019), we have observed that whether the average number of total scratches or pits, the Vallparadís Section specimens appear to have lower values than the other two sites. The values for *Ursus etruscus* would have had an omnivorous diet in both Dmanisi (1.8 Ma) and Orce sites (1.6-1.2 Ma). However, if we compare both sites, the values from Orce are a bit lower than in Dmanisi. It can be related to a start of the change in dietary habits evidenced in the speleaoid bears that find their origin in *U. etruscus*, as well as the arctoid lineage (Kurtén, 1976; Mazza & Rustioni, 1994; Rabeder et al., 2000; Argant, 2001).

In addition, we compared the Vallparadís Section data with other fossil species. Regarding cave bears from Eastern Europe, we selected *U. ingressus* (Shiriaevo 1 cave), *U. kanivetz* (Secrets cave), and *U. rossicus* (Kizel cave), with dental microwear data taken from Ramírez-Pedraza et al., (2022). Late Pleistocene *Ursus spelaeus* from NE Iberian Peninsula (sites: Coves del Toll, Cova de les Teixoneres, l'Arbreda, Mollet, Llenes and Ermitons) (Ramírez-Pedraza et al., 2020) and *U. arctos* and *U. spelaeus* from Hohle Fels (Münzel et al., 2014) are also compared to our data. The *U. deningeri* values show a similar number of pits and scratches to those from Eastern Europe cave bears (*U. ingressus*, *U. kanivetz,* and *U. rossicus*), indicating a similar diet. In contrast, in front of the mainly herbivore dietary habits of *U. spelaeus*, our data fall in a higher position whether dealing with number of pits or number of scratches.

Our results expose the mid-point where *U. deningeri* from Vallparadís Section is placed on, concerning the feeding behavior. The advanced forms of *U. etruscus* from Dmanisi and Orce sites are more generalist and fully omnivore in comparison to the Vallparadís Section specimens. Moreover, the posterior cave bears in Late Pleistocene (*Ursus spelaeus*) from Western Europe, show an even more specialized diet based on plants, culminating the herbivorism started in older forms such as *U. deningeri* from Vallparadís Section site.

The small number of samples for dental microwear analyses may make harder the interpretation of the results, being necessary an increase of samples to obtain more reliable values, although the selection of the here studied specimens has been made according to the availability of the collection.

In addition, comparisons with other coeval *U. deningeri* specimens from sites such as Grotte de La Carrière (Réseau Lachambre, Têt Valley, Eastern Pyrenees) and Pirro Nord (Puglia, Southeastern Italy) would be interesting and helpful to a better comprehension of our results.

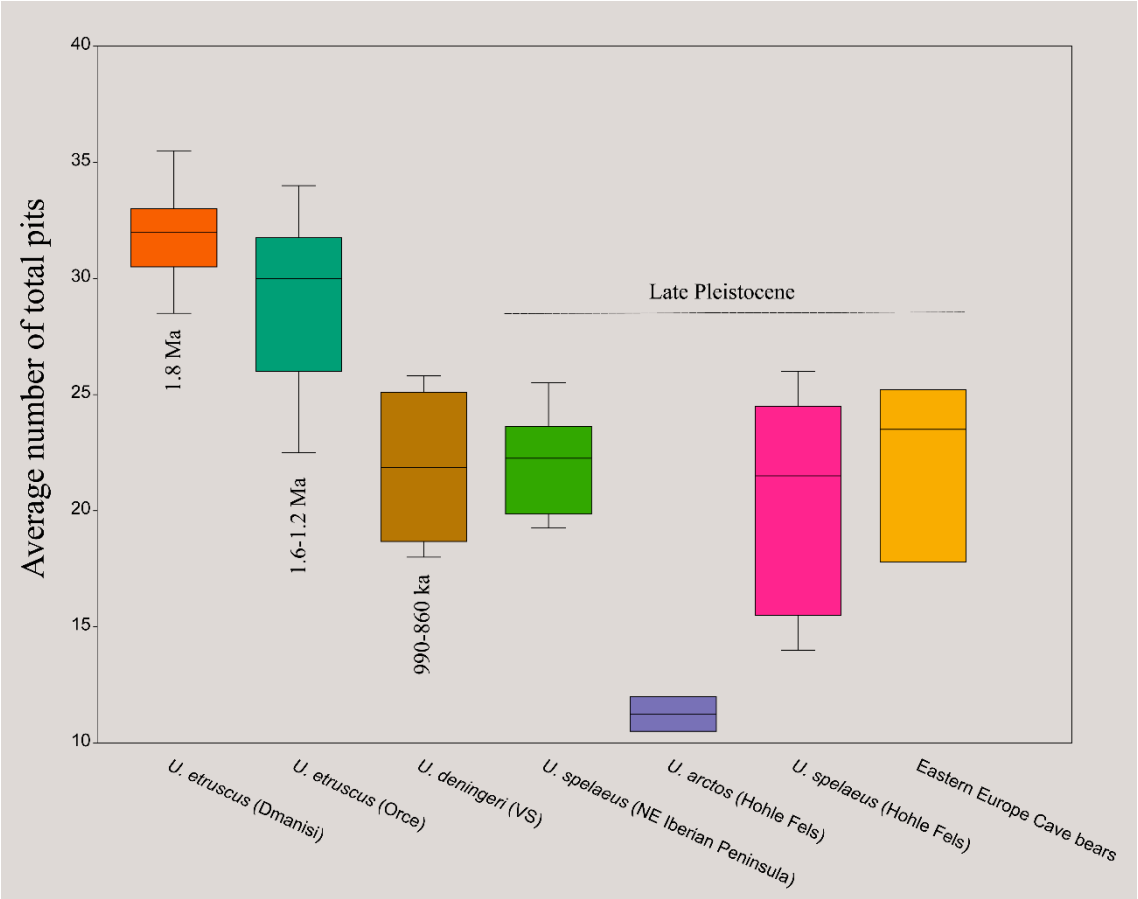

Fig. 22. Boxplot indicating average number of total pits of *U. deningeri* from Vallparadís Section (VS) in comparison to previously published data of fossil ursids. Data from Münzel et al., (2014), Medin et al., (2017, 2019) and Ramírez-Pedraza et al., (2020; 2022):

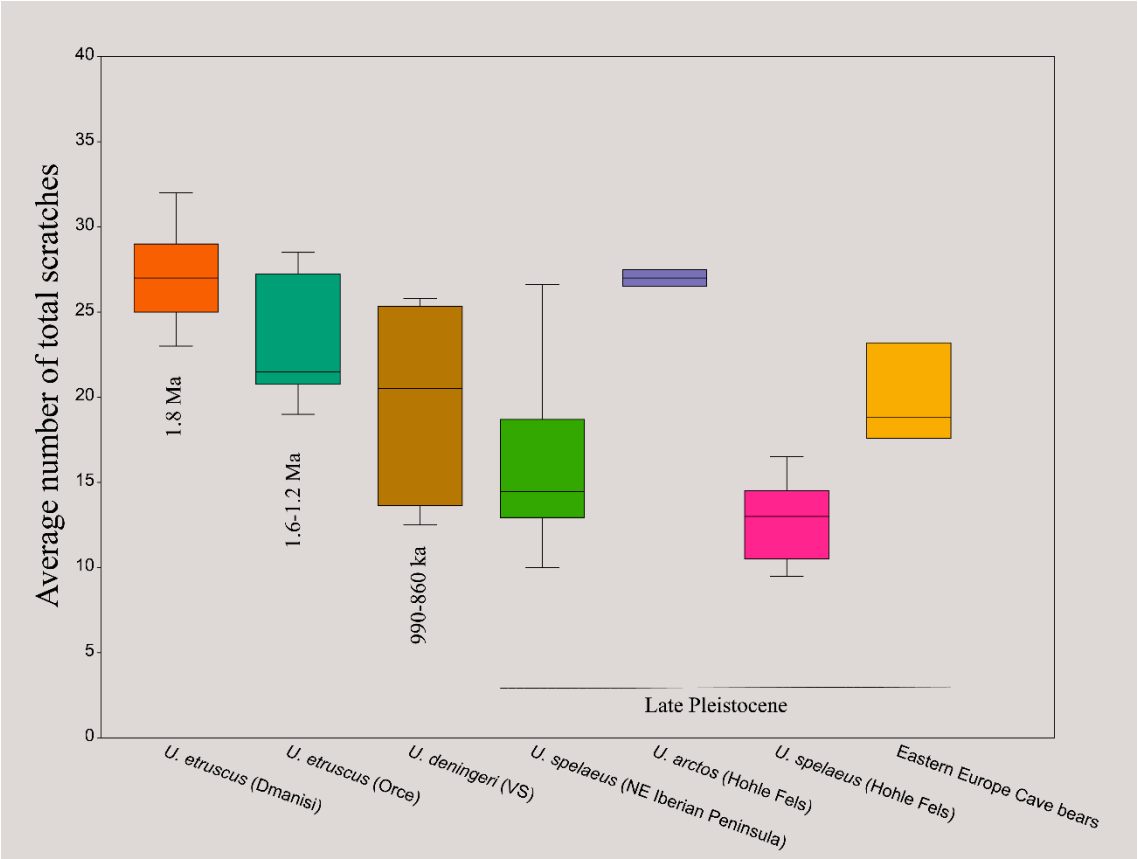

Fig. 23. Boxplot indicating average number of total scratches of *U. deningeri* from Vallparadís Section (VS) in comparison to previously published data of fossil ursids. Data from Münzel et al., (2014), Medin et al., (2017, 2019) and Ramírez-Pedraza et al., (2020; 2022).

5.3. Paleoenvironmental conditions and hominin occupation

As mentioned previously, the Vallparadís Section site presents a huge chronological range, which goes from 1.2 to 0.6 Ma. This period is coeval with the so-called "*Early-Middle Pleistocene Transition*" (ca. 1.4-0.4 Ma) (Head & Gibbard, 2015). Glacial-interglacial cycles progressively changed from a period of 41 ka to 100 ka, resulting in the first major accumulation of global ice volume at MIS24-22, the so-called "*0.9 Ma event*" (Strani et al., 2019). These change in climatic shifts strongly influenced ecosystems, with a tendency of increase in both seasonality and aridity. The paleoenvironmental conditions at the Vallparadís Section changed from humid temperate ecosystems during MIS35, to an increase in aridity and grasslands at MIS31 to another time humid and temperate ecosystems at MIS21 but with an increase in seasonality (Madurell-Malapeira & Fidalgo, unpublished data).

The former data supporting harsh ecosystems around MIS31 are also documented in the Quibas site associated with the presence of arid species like *Praeobivos* and *Hemitragus* (Piñero et al., 2020; Madurell-Malapeira, unpublished data). In fact, no hominin records were documented in Europe around the Jaramillo subchron or slightly before, favoring our interpretations of open and environments with strong seasonality which could be not favorable for hominin dispersals.

Certainly, fossil hominins record in Africa and Eurasia is scarce around the Jaramillo subchron only being common after MIS22 with few findings in Eritrea, Ethiopia and Algeria (Abbate et al., 1998; Mounier et al., 2009; Profico et al., 2016), in Iberian Peninsula (Bermúdez de Castro et al., 1997; Bermúdez-de-Castro et al., 2017), and in East Asia (Bahain et al., 2017). Recently, in a genetic study, Hu et al., (2023) suggested this gap in hominin settlement can be related with a bottleneck in hominin paleopopulations which lasted approximately 117 ka, from 930 to 813 ka. The number of breeding individuals during this period could have reached 1280, with about 98.7% of humans lost at the first stages of the bottleneck.

This former bottleneck could be related to the above-mentioned climatic change and concomitant environmental instability during "*Early-Middle Pleistocene Transition*". Moreover, Margari et al., (2023) present a climatic study based on Portuguese data which highlights the depopulation of Europe slightly before the Jaramillo subchron. Specifically, the change from stable interstadial conditions before 1.15 Ma to a strong glacial event from 1.154 to 1.123 Ma probably conditioned the depopulation of Europe around the MIS31.

Our results reinforce, partially, these recently published studies about a depopulation of Europe driven by climatic conditions. Considering the complementary information that both stable isotopes and dental microwear analyses give us (the first one reflects growth time of crown, the second one the last days/weeks before death of the individual), both consequent interpretations lead us to a paradigm where fossil hominins are not found. The aridity of MIS31 reflected in oxygen stable isotopic data, together with the feeding behaviors of ungulates during this period, resulting in a diet based on C_4 plants, enhances the idea of a tough period to go through occupations in Europe. Moreover, dental microwear analyses, although indicating an omnivorous

feeding behavior, show a trend towards the herbivorism in *U. deningeri*, thus avoiding an overlapping in resource requirements between the ursids and hominins. This leaves the changes in climatic shifts during "*Early-Middle Pleistocene Transition"* as the most probable unique responsible of the depopulation of Europe during that time.

6. Conclusions

Here we present a multiproxy analysis on the dietary habits of *Ursus deningeri* and insights on the paleoecology of a well-preserved fossil large mammal assemblage unearthed from the Vallparadís Section site, the only European Pleistocene section coeval with the "*Early-Middle Pleistocene Transition"* (EMPT).

We have studied the EVT12 (MIS31) and the EVT7 (MIS21) layers of the former section in order to continue chronologically the previously published dietary studies focused on the ursids from Dmanisi (1.8 Ma) and Orce sites (1.6-1.2 Ma) by Medin et al., (2017, 2019). Both carbon and oxygen isotopic data indicate a higher aridity regime during MIS31 as compared with MIS21, since $\delta^{13}C$ values show a more grazing behaviour (enriches C values) in ungulates of the older layer (EVT12) while $\delta^{18}O$ values indicate a slightly higher difference in obligate and non-obligate drinkers values in EVT12. For the carnivoran guild, the stable isotopes reflect specific physiological behaviours such as the probably earlier evidence of hibernation in ursids and consequently the starting point of the cave bear lineage, and an increase on bone mineral consumption from MIS31 to MIS21 in the hyaena *P. brevirostris*. Dental microwear analyses place *U. deningeri* in a mid-point between the generalist omnivore *U. etruscus* from Dmanisi and Orce and the herbivore Late Pleistocene *U. spelaeus* from Western Europe. That indicates that *U. deningeri* started a trend towards the herbivorism, culminating it in the later Late Pleistocene iconic cave bears. The start of hibernating behaviour and the tendency to herbivorism documented here in the Vallparadís Section bears, i.e., the first steps towards the cave bear lineage, could be prompted by the environmental instability associated with the EMPT and more specifically with the concomitant increase in aridity and seasonality since MIS31.

This is one of the first studies based on stable isotopes obtained from the hydroxilapatite (or bioapatite) of Mediterranean Early Pleistocene large mammals. In addition, this work represents the first time that *U. deningeri* dental microwear is studied using low-magnification microwear. Our results have allowed us to shed new light on the dietary behaviour of the Vallparadís Section large mammals in congruence with previously published data (Strani et al., 2019; Sorbelli et al., 2021), suggesting a strong aridity phase at the Jaramillo subchron (MIS31) and more suitable conditions around MIS21.

Finally, it is noteworthy our data agree with recently published research on the consequences of the "*Early-Middle Pleistocene Transition*" in hominin populations. In fact, no European site around MIS31 display hominin direct or indirect records, nor the Vallpardís Section, Bòvila Ordis, Quibas, Collecurti or Untermassfeld. Genetic bottlenecks are supposed by hominin populations at that time and strong glacial pulses around MIS35 justified by their absence. Further research is obviously needed to improve all these assumptions, however the increase in aridity, open grasslands and seasonality are well-documented around 1.0 Ma in Mediterranean Europe.

7. Acknowledgements

Field surveys and research on the different localities of the Vallparadís Section has been performed thanks to the financial support of the Departament de Cultura de la Generalitat de Catalunya with three consecutive quadrennial research projects leaded by J. Madurell-Malapeira (2014-2025). The isotopic analyses presented in this work had been possible thanks to the financial support of the Palarq Foundation (2022) with a project leaded by J. Madurell-Malapeira and C. Tornero.

8. References

Abbate, E., Albianelli, A., Azzaroli, A., Benvenuti, M., Tesfamariam, B., Bruni, P., Cipriani, N., Clarke, R. J., Ficcarelli, G., Macchiarelli, R., Napoleone, G., Papini, M., Rook, L., Sagri, M., Tecle, T. M., Torre, D., & Villa, I. (1998). A one-million-year-old Homo cranium from the Danakil (Afar) Depression of Eritrea. *Nature*, *393*(6684), 458–460.

Agustí, J., Cabrera, L., Garces, M., & Parés, J. M. (1997). The Vallesian mammal succession in the Vallès-Penedès basin (northeast Spain): Paleomagnetic calibration and correlation with global events. *Palaeogeography, Palaeoclimatology, Palaeoecology*, *133*(3–4), 149–180.

Alba, D. M., Moyà-Solà, S., Madurell, J., & Aurell, P. (2008). Dentognathic remains of Macaca (Primates, Cercopithecidae) from the late early pleistocene of Terrassa (Catalonia, Spain). *Journal of Human Evolution*, *55*(6), 1160–1163.

Alba, D. M., Aurell, J., Madurell, J., Gómez, M., Moyà-Solà, S., & Berasategui, X. (2008). Paleontologia i geologia del jaciment del Pleistocè inferior de Vallparadís (Terrassa, Vallès Occidental). *Tribuna d'arqueologia*, *2008*, 29–44.

Anyonge, W. (1996). Microwear on canines and killing behavior in large carnivores: saber function in Smilodon fatalis. *Journal of Mammalogy*, *77*(4), 1059–1067.

Argant, A. (2001). Cave bear ancestors. *Cadernos Do Laboratorio Xeolòxico de Laxe*, *26*, 341–348.

Bahain, J.-J., Shao, Q., Han, F., Sun, X., Voinchet, P., Liu, C., Yin, G., & Falgueres, C. (2017). Contribution des méthodes ESR et ESR/U-Th à la datation de quelques gisements pléistocènes de Chine. *Anthropologie*, *121*(3), 215–233.

Baker, G., Jones, L. H. P., & Wardrop, I. D. (1959). Cause of wear in sheeps' teeth. *Nature*, *184*(4698), 1583–1584.

Balasse, M. (2002). Reconstructing dietary and environmental history from enamel isotopic analysis: time resolution of intra-tooth sequential sampling. *International Journal of Osteoarchaeology*, *12*(3), 155–165.

Balasse, M., Evin, A., Tornero, C., Radu, V., Fiorillo, D., Popovici, D., Andreescu, R., Dobney, K., Cucchi, T., & Bălăşescu, A. (2016). Wild, domestic and feral? Investigating the status of suids in the Romanian Gumelniţa (5th mil. cal BC) with biogeochemistry and geometric morphometrics. *Journal of Anthropological Archaeology*, *42*, 27–36.

Barnicoat, C. R. (1957). Wear in sheep's teeth. *New Zealand Journal of Science and Technology, Section A*, *38*, 583–632.

Bedaso, Z. K., Wynn, J. G., Alemseged, Z., & Geraads, D. (2013). Dietary and paleoenvironmental reconstruction using stable isotopes of herbivore tooth enamel from middle Pliocene Dikika, Ethiopia: Implication for Australopithecus afarensis habitat and food resources. *Journal of Human Evolution*, *64*(1), 21–38.

Bermúdez de Castro, J. M., Arsuaga, J. L., Carbonell, E., Rosas, A., Martınez, I., & Mosquera, M. (1997). A hominid from the Lower Pleistocene of Atapuerca, Spain: possible ancestor to Neandertals and modern humans. *Science*, *276*(5317), 1392–1395.

Bermúdez-de-Castro, J.-M., Martinón-Torres, M., Martín-Francés, L., Modesto-Mata, M., Martínez-de-Pinillos, M., García, C., & Carbonell, E. (2017). Homo antecessor: The state of the art eighteen years later. *Quaternary International*, *433*, 22–31.

Bibi, F., Souron, A., Bocherens, H., Uno, K., & Boisserie, J.-R. (2013). Ecological change in the lower Omo Valley around 2.8 Ma. *Biology Letters*, *9*(1), 20120890.

Blumenthal, S. A., Levin, N. E., Brown, F. H., Brugal, J.-P., Chritz, K. L., Harris, J. M., Jehle, G. E., & Cerling, T. E. (2017). Aridity and hominin environments. *Proceedings of the National Academy of Sciences*, *114*(28), 7331–7336.

Bocherens, H. (2004). Cave bear palaeoecology and stable isotopes: checking the rules of the game. *Publications Du Musée Des Confluences*, *2*(1), 183–188.

Bocherens, H. (2015). Isotopic tracking of large carnivore palaeoecology in the mammoth steppe. *Quaternary Science Reviews*, *117*, 42–71.

Bocherens, H. (2019). Isotopic insights on cave bear palaeodiet. *Historical Biology*, *31*(4), 410–421.

Bocherens, H., Stiller, M., Hobson, K. A., Pacher, M., Rabeder, G., Burns, J. A., Tütken, T., & Hofreiter, M. (2011). Niche partitioning between two sympatric genetically distinct cave bears (Ursus spelaeus and Ursus ingressus) and brown bear (Ursus arctos) from Austria: isotopic evidence from fossil bones. *Quaternary International*, *245*(2), 238–248.

Bocherens, H., Koch, P. L., Mariotti, A., Geraads, D., & Jaeger, J.-J. (1996). Isotopic biogeochemistry (13 C, 18 O) of mammalian enamel from African Pleistocene hominid sites. *Palaios*, 306–318.

Bocherens, H., Fizet, M., & Mariotti, A. (1994). Diet, physiology and ecology of fossil mammals as inferred from stable carbon and nitrogen isotope biogeochemistry: implications for Pleistocene bears. *Palaeogeography, Palaeoclimatology, Palaeoecology*, *107*(3–4), 213–225.

Bocherens, H., Fizet, M., & Mariotti, A. (1990). Mise en évidence du régime alimentaire végétarien de l'ours des cavernes (Ursus spelaeus) par la biogéochimie isotopique (13C, 15N) du collagène des Vertébrés fossiles. *Comptes Rendus de l'Académie Des Sciences. Série 2, Mécanique, Physique, Chimie, Sciences de l'univers, Sciences de La Terre*, *311*(10), 1279–1284.

Bocherens, H., Billiou, D., Patou-Mathis, M., Bonjean, D., Otte, M., & Mariotti, A. (1997). Paleobiological implications of the isotopic signatures (13C, 15N) of fossil mammal collagen in Scladina Cave (Sclayn, Belgium). *Quaternary Research*, *48*(3), 370–380.

Bocherens, H., Drucker, D. G., Billiou, D., Geneste, J.-M., & van Der Plicht, J. (2006). Bears and humans in Chauvet Cave (Vallon-Pont-d'Arc, Ardeche, France): insights from stable

isotopes and radiocarbon dating of bone collagen. *Journal of Human Evolution*, *50*(3), 370–376.

Bocherens, H., Bridault, A., Drucker, D. G., Hofreiter, M., Münzel, S. C., Stiller, M., & Van Der Plicht, J. (2014). The last of its kind? Radiocarbon, ancient DNA and stable isotope evidence from a late cave bear (Ursus spelaeus ROSENMÜLLER, 1794) from Rochedane (France). *Quaternary International*, *339*, 179–188.

Bojarska, K., & Selva, N. (2012). Spatial patterns in brown bear Ursus arctos diet: the role of geographical and environmental factors. *Mammal Review*, *42*(2), 120–143.

Boscaini, A. (2014). *Plio-Pleistocene lynxes from the Iberian Peninsula. Taxonomy and phylogenetic relationships with the extant and fossil species* [PhD Thesis]. Master dissertation, Universitat Autonoma de Barcelona and Universitat de ….

Butler, P. M. (1952). The milk-molars of Perissodactyla, with remarks on molar occlusion. *Proceedings of the Zoological Society of London*, *121*(4), 777–817.

Cabrera, L., & Calvet, F. (1996). *Tertiary basins of Spain: Onshore Neogene record in NE Spain: Vallès–Penedès and El Camp half-grabens (NW Mediterranean)*.

Cabrera, L., Roca, E., Garcés, M., & de Porta, J. (2004). Estratigrafía y evolución tectonosedimentaria oligocena superior-neógena del sector central del margen catalán (Cadena Costero-Catalana). *Geología de España*, 569–572.

Cerling, T. E., & Harris, J. M. (1999). Carbon isotope fractionation between diet and bioapatite in ungulate mammals and implications for ecological and paleoecological studies. *Oecologia*, *120*, 347–363.

Cerling, T. E., Andanje, S. A., Blumenthal, S. A., Brown, F. H., Chritz, K. L., Harris, J. M., Hart, J. A., Kirera, F. M., Kaleme, P., & Leakey, L. N. (2015). Dietary changes of large herbivores in the Turkana Basin, Kenya from 4 to 1 Ma. *Proceedings of the National Academy of Sciences*, *112*(37), 11467–11472.

Cerling, T. E., Harris, J. M., Ambrose, S. H., Leakey, M. G., & Solounias, N. (1997). Dietary and environmental reconstruction with stable isotope analyses of herbivore tooth enamel from the Miocene locality of Fort Ternan, Kenya. *Journal of Human Evolution*, *33*(6), 635–650.

Clark, P. U., Archer, D., Pollard, D., Blum, J. D., Rial, J. A., Brovkin, V., Mix, A. C., Pisias, N. G., & Roy, M. (2006). The middle Pleistocene transition: characteristics, mechanisms, and implications for long-term changes in atmospheric pCO2. *Quaternary Science Reviews*, *25*(23–24), 3150–3184.

Clementz, M. T. (2012). New insight from old bones: stable isotope analysis of fossil mammals. *Journal of Mammalogy*, *93*(2), 368–380.

Clementz, M. T., & Koch, P. L. (2001). Differentiating aquatic mammal habitat and foraging ecology with stable isotopes in tooth enamel. *Oecologia*, *129*, 461–472.

Cutress, T. W., & Healy, W. B. (1965). Wear of sheep's teeth: II. Effects of pasture juices on dentine. *New Zealand Journal of Agricultural Research*, *8*(4), 753–762.

Dahlberg, A. A., & Kinzey, W. (1962). Etude microscopique de l'abrasion et de l'attrition sur la surface des dents. *Bulletin Du Groupement International Pour La Recherche Scientifique En Stomatologie et Odontologie (Bruxelles)*, *5*, 242–251.

de Mas, D. (1984). *L'Evolució geomorfològica quaternària del Vallès Occidental* [PhD Thesis]. Universitat de Barcelona.

Dewar, E. (2004). Microwear of carnivorous mammals described by low-magnification dental stereomicroscopy. *Journal of Vertebrate Paleontology*, *24*(3), 52A-52A.

Donohue, S. L., DeSantis, L. R., Schubert, B. W., & Ungar, P. S. (2013). Was the giant short-faced bear a hyper-scavenger? A new approach to the dietary study of ursids using dental microwear textures. *PLoS One*, *8*(10), e77531.

Duval, M., Falguères, C., Bahain, J.-J., Grün, R., Shao, Q., Aubert, M., Dolo, J.-M., Agusti, J., Martinez-Navarro, B., & Palmqvist, P. (2012). On the limits of using combined U-

series/ESR method to date fossil teeth from two Early Pleistocene archaeological sites of the Orce area (Guadix-Baza basin, Spain). *Quaternary Research*, *77*(3), 482–491.

Duval, M., Bahain, J.-J., Falgueres, C., Garcia, J., Guilarte, V., Grün, R., Martínez, K., Moreno, D., Shao, Q., & Voinchet, P. (2015a). Revisiting the ESR chronology of the Early Pleistocene hominin occupation at Vallparadís (Barcelona, Spain). *Quaternary International*, *389*, 213–223.

Duval, M., Bahain, J.-J., Falgueres, C., Garcia, J., Guilarte, V., Grün, R., Martínez, K., Moreno, D., Shao, Q., & Voinchet, P. (2015b). Revisiting the ESR chronology of the Early Pleistocene hominin occupation at Vallparadís (Barcelona, Spain). *Quaternary International*, *389*, 213–223.

Farquhar, G. D., Ehleringer, J. R., & Hubick, K. T. (1989). Carbon isotope discrimination and photosynthesis. *Annual Review of Plant Biology*, *40*(1), 503–537.

Fernández-Mosquera, D., Vila-Taboada, M., & Grandal-d'Anglade, A. (2001). Stable isotopes data (δ13C, δ15N) from the cave bear (Ursus spelaeus): a new approach to its palaeoenvironment and dormancy. *Proceedings of the Royal Society of London. Series B: Biological Sciences*, *268*(1472), 1159–1164.

Field, A. C., & Purves, D. (1964). The intake of soil by the grazing sheep. *Proceedings of the Nutrition Society, 23, Pp24-25*.

Frary, V. J., Duchamp, J., Maehr, D. S., & Larkin, J. L. (2011). Density and distribution of a colonizing front of the American black bear Ursus americanus. *Wildlife Biology*, *17*(4), 404–416.

Fredriksson, G. M. (2012). *Effects of El Niño and large-scale forest fires on the ecology and conservation of Malayan sun bears (Helarctos malayanus) in East Kalimantan, Indonesian Borneo*.

Fredriksson, G. M., & Wich, S. A. (2006). Frugivory in sun bears (Helarctos malayanus) is linked to El Niño-related fluctuations in fruiting phenology, East Kalimantan, Indonesia. *Biological Journal of the Linnean Society*, *89*(3), 489–508.

Furusaka, S., Kozakai, C., Nemoto, Y., Umemura, Y., Naganuma, T., Yamazaki, K., & Koike, S. (2017). The selection by the Asiatic black bear (Ursus thibetanus) of spring plant food items according to their nutritional values. *ZooKeys*, *672*, 121.

Gabunia, L., Vekua, A., Lordkipanidze, D., Swisher III, C. C., Ferring, R., Justus, A., Nioradze, M., Tvalchrelidze, M., Antón, S. C., & Bosinski, G. (2000). Earliest Pleistocene hominid cranial remains from Dmanisi, Republic of Georgia: taxonomy, geological setting, and age. *Science*, *288*(5468), 1019–1025.

García-Aguilar, J. M., Guerra-Merchán, A., Serrano, F., Palmqvist, P., Flores-Moya, A., & Martínez-Navarro, B. (2014). Hydrothermal activity and its paleoecological implications in the latest Miocene to Middle Pleistocene lacustrine environments of the Baza Basin (Betic Cordillera, SE Spain). *Quaternary Science Reviews*, *96*, 204–221.

García-Aguilar, J. M., Guerra-Merchan, A., Serrano, F., Flores-Moya, A., Delgado-Huertas, A., Espigares, M. P., Ros-Montoya, S., Martinez-Navarro, B., & Palmqvist, P. (2015). A reassessment of the evidence for hydrothermal activity in the Neogene-Quaternary lacustrine environments of the Baza basin (Betic Cordillera, SE Spain) and its paleoecological implications. *Quaternary Science Reviews*, *112*, 230–235.

Gende, S. M., & Quinn, T. P. (2004). The relative importance of prey density and social dominance in determining energy intake by bears feeding on Pacific salmon. *Canadian Journal of Zoology*, *82*(1), 75–85.

Goillot, C., Blondel, C., & Peigné, S. (2009). Relationships between dental microwear and diet in Carnivora (Mammalia) — Implications for the reconstruction of the diet of extinct taxa. *Palaeogeography, Palaeoclimatology, Palaeoecology*, *271*(1–2), 13–23. https://doi.org/10.1016/j.palaeo.2008.09.004

González-Guarda, E., Domingo, L., Tornero, C., Pino, M., Fernández, M. H., Sevilla, P., Villavicencio, N., & Agustí, J. (2017). Late Pleistocene ecological, environmental and climatic reconstruction based on megafauna stable isotopes from northwestern Chilean Patagonia. *Quaternary Science Reviews*, *170*, 188–202.

Grine, F. E. (1986). Dental evidence for dietary differences in Australopithecus and Paranthropus: a quantitative analysis of permanent molar microwear. *Journal of Human Evolution*, *15*(8), 783–822.

Grine, F. E. (1981). Trophic differences between'gracile'and'robust'australopithecines: a scanning electron microscope analysis of occlusal events. *South African Journal of Science*, *77*(5), 203–230.

Grohé, C., Uno, K., & Boisserie, J.-R. (2022). Lutrinae Bonaparte, 1838 (Carnivora, Mustelidae) from the Plio-Pleistocene of the Lower Omo Valley, southwestern Ethiopia: systematics and new insights into the paleoecology and paleobiogeography of the Turkana otters. *Comptes Rendus. Palevol*, *30*.

Head, M. J., & Gibbard, P. L. (2015). Early–Middle Pleistocene transitions: linking terrestrial and marine realms. *Quaternary International*, *389*, 7–46.

Healy, W. B. (1967). *Ingestion of soil by sheep*.

Healy, W. B., & Ludwig, T. G. (1965). Wear of sheep's teeth: I. The role of ingested soil. *New Zealand Journal of Agricultural Research*, *8*(4), 737–752.

Healy, W. B., Cutress, T. W., & Michie, C. (1967). Wear of sheep's teeth: IV. Reduction of soil ingestion and tooth wear by supplementary feeding. *New Zealand Journal of Agricultural Research*, *10*(2), 201–209.

Hopley, P. J., Cerling, T. E., Crété, L., Werdelin, L., Mwebi, O., Manthi, F. K., & Leakey, L. N. (2023). Stable isotope analysis of carnivores from the Turkana Basin, Kenya: Evidence for temporally-mixed fossil assemblages. *Quaternary International*, *650*, 12–27.

Hu, W., Hao, Z., Du, P., Vincenzo, F. D., Manzi, G., Cui, J., Fu, Y.-X., Pan, Y.-H., & Li, H. (2023). Genomic inference of a severe human bottleneck during the Early to Middle Pleistocene transition. *Science*, *381*, 979–984.

Huygens, O. C., Miyashita, T., Dahle, B., Carr, M., Izumiyama, S., Sugawara, T., & Hayashi, H. (2003). Diet and feeding habits of Asiatic black bears in the Northern Japanese Alps. *Ursus*, 236–245.

Iannucci, A., Mecozzi, B., Sardella, R., & Iurino, D. A. (2021). The extinction of the giant hyena Pachycrocuta brevirostris and a reappraisal of the Epivillafranchian and Galerian Hyaenidae in Europe: Faunal turnover during the Early–Middle Pleistocene Transition. *Quaternary Science Reviews*, *272*, 107240.

Jenkins, S. G., Partridge, S. T., Stephenson, T. R., Farley, S. D., & Robbins, C. T. (2001). Nitrogen and carbon isotope fractionation between mothers, neonates, and nursing offspring. *Oecologia*, *129*, 336–341.

Jones, D. B., & DeSantis, L. R. (2016). Dietary ecology of the extinct cave bear: evidence of omnivory as inferred from dental microwear textures. *Acta Palaeontologica Polonica*, *61*(4), 735–741.

Joshi, A. R., Garshelis, D. L., & Smith, J. L. (1997). Seasonal and habitat-related diets of sloth bears in Nepal. *Journal of Mammalogy*, *78*(2), 584–597.

Koch, P. L. (1998). Isotopic reconstruction of past continental environments. *Annual Review of Earth and Planetary Sciences*, *26*(1), 573–613.

Koch, P. L., Tuross, N., & Fogel, M. L. (1997). The effects of sample treatment and diagenesis on the isotopic integrity of carbonate in biogenic hydroxylapatite. *Journal of Archaeological Science*, *24*(5), 417–429.

Kohn, M. J. (2010). Carbon isotope compositions of terrestrial C3 plants as indicators of (paleo) ecology and (paleo) climate. *Proceedings of the National Academy of Sciences*, *107*(46), 19691–19695.

Kohn, M. J. (1996). Predicting animal δ18O: accounting for diet and physiological adaptation. *Geochimica et Cosmochimica Acta*, *60*(23), 4811–4829.

Kohn, M. J., & Cerling, T. E. (2002). Stable isotope compositions of biological apatite. *Reviews in Mineralogy and Geochemistry*, *48*(1), 455–488.

Koike, S., Kozakai, C., Nemoto, Y., Masaki, T., Yamazaki, K., Abe, S., Nakajima, A., Umemura, Y., & Kaji, K. (2012). Effect of hard mast production on foraging and sex-specific behavior of the Asiatic black bear (Ursus thibetanus). *Mammal Study*, *37*(1), 21–28.

Krajcarz, M., Pacher, M., Krajcarz, M. T., Laughlan, L., Rabeder, G., Sabol, M., Wojtal, P., & Bocherens, H. (2016). Isotopic variability of cave bears (δ15N, δ13C) across Europe during MIS 3. *Quaternary Science Reviews*, *131*, 51–72.

Krueger, H. W., & Sullivan, C. H. (1984). *Models for carbon isotope fractionation between diet and bone*. ACS Publications.

Kubo, M. O., Yamada, E., Kubo, T., & Kohno, N. (2017). Dental microwear texture analysis of extant sika deer with considerations on inter-microscope variability and surface preparation protocols. *Biosurface and Biotribology*, *3*(4), 155–165.

Kurtén, B. (1976). *The cave bear story: life and death of a vanished animal*. Columbia University Press.

Levin, N. E., Cerling, T. E., Passey, B. H., Harris, J. M., & Ehleringer, J. R. (2006). A stable isotope aridity index for terrestrial environments. *Proceedings of the National Academy of Sciences*, *103*(30), 11201–11205.

Levin, N. E., Simpson, S. W., Quade, J., Cerling, T. E., & Frost, S. R. (2008). Herbivore enamel carbon isotopic composition and the environmental context of Ardipithecus at Gona, Ethiopia. In *The geology of early humans in the Horn of Africa* (Vol. 446, pp. 215–234). Geological Society of America Special Paper.

Liden, K., & Angerbjörn, A. (1999). Dietary change and stable isotopes: a model of growth and dormancy in cave bears. *Proceedings of the Royal Society of London. Series B: Biological Sciences*, *266*(1430), 1779–1783.

Lordkipanidze, D., Jashashvili, T., Vekua, A., De León, M. S. P., Zollikofer, C. P., Rightmire, G. P., Pontzer, H., Ferring, R., Oms, O., & Tappen, M. (2007). Postcranial evidence from early Homo from Dmanisi, Georgia. *Nature*, *449*(7160), 305–310.

Ludwig, T. G., Healy, W. B., & Cutress, T. W. (1966). Wear of sheep's teeth: III. Seasonal variation in wear and ingested soil. *New Zealand Journal of Agricultural Research*, *9*(2), 157–164.

Macdonald, D. (2009). *The encyclopedia of mammals*. OUP Oxford.

Macfadden, B. J., Cerling, T. E., Harris, J. M., & Prado, J. (1999). Ancient latitudinal gradients of C3/C4 grasses interpreted from stable isotopes of New World Pleistocene horse (Equus) teeth. *Global Ecology and Biogeography*, *8*(2), 137–149.

Madurell-Malapeira, J., Ros-Montoya, S., Espigares, M. P., Alba, D. M., & Aurell-Garrido, J. (2014). Villafranchian large mammals from the Iberian Peninsula: paleobiogeography, paleoecology and dispersal events. *Journal of Iberian Geology*, *40*(1), 167–178.

Madurell-Malapeira, J., Minwer-Barakat, R., Alba, D. M., Garcés, M., Gómez, M., Aurell-Garrido, J., Ros-Montoya, S., Moyà-Solà, S., & Berástegui, X. (2010). The Vallparadís section (Terrassa, Iberian Peninsula) and the latest Villafranchian faunas of europe. *Quaternary Science Reviews*, *29*(27–28), 3972–3982.

Madurell-Malapeira, J., Alba, D. M., Espigares, M.-P., Vinuesa, V., Palmqvist, P., Martínez-Navarro, B., & Moyà-Solà, S. (2017). Were large carnivorans and great climatic shifts limiting factors for hominin dispersals? Evidence of the activity of Pachycrocuta brevirostris during the Mid-Pleistocene Revolution in the Vallparadís Section (Vallès-Penedès Basin, Iberian Peninsula). *Quaternary International*, *431*, 42–52. https://doi.org/10.1016/j.quaint.2015.07.040

Madurell-Malapeira, J., Aurell, J., Alba, D. M., & Moyà-Solà, S. (2009). Los niveles fosilíferos epivillafranchienses de Vallparadís (Terrassa, Barcelona, España). *Paleolusitana*, *1*, 237–243.

Margari, V., Hodell, D. A., Parfitt, S. A., Ashton, N. M., Grimalt, J. O., Kim, H., Yun, K.-S., Gibbard, P. L., Stringer, C. B., Timmermann, A., & Tzedakis, P. C. (2023). Extreme glacial cooling likely led to hominin depopulation of Europe in the Early Pleistocene. *Science*, *381*(6658), 693–699. https://doi.org/10.1126/science.adf4445

Martinell, J. (1988). An overview of the marine Pliocene of NE Spain. *Géologie Méditerranéenne*, *15*(4), 227–233.

Martínez-Navarro, B. (1991). Revisión sistemática y estudio cuantitativo de la fauna de macromamíferos del yacimiento de Venta Micena (Orce, Granada). *PhD Universidad de Barcelona*.

Mazza, P., & Rustioni, M. (1994). *On the phylogeny of Eurasian bears*. Schweizerbart.

Medin, T., Martínez-Navarro, B., Madurell-Malapeira, J., Figueirido, B., Kopaliani, G., Rivals, F., Kiladze, G., Palmqvist, P., & Lordkipanidze, D. (2019). The bears from Dmanisi and the first dispersal of early Homo out of Africa. *Scientific Reports*, *9*(1), 17752. https://doi.org/10.1038/s41598-019-54138-6

Medin, T., Martínez-Navarro, B., Rivals, F., Madurell-Malapeira, J., Ros-Montoya, S., Espigares, M.-P., Figueirido, B., Rook, L., & Palmqvist, P. (2017). Late Villafranchian Ursus etruscus and other large carnivorans from the Orce sites (Guadix-Baza basin, Andalusia, southern Spain): Taxonomy, biochronology, paleobiology, and ecogeographical context. *Quaternary International*, *431*, 20–41. https://doi.org/10.1016/j.quaint.2015.10.053

Mendoza, M., Janis, C. M., & Palmqvist, P. (2005). Ecological patterns in the trophic-size structure of large mammal communities: a 'taxon-free'characterization. *Evolutionary Ecology Research*, *7*(4), 505–530.

Merceron, G., Zazzo, A., Spassov, N., Geraads, D., & Kovachev, D. (2006). Bovid paleoecology and paleoenvironments from the Late Miocene of Bulgaria: evidence from dental microwear and stable isotopes. *Palaeogeography, Palaeoclimatology, Palaeoecology*, *241*(3–4), 637–654.

Merceron, G., Kostopoulos, D. S., De Bonis, L., Fourel, F., Koufos, G. D., Lécuyer, C., & Martineau, F. (2013). Stable isotope ecology of Miocene bovids from northern Greece and the ape/monkey turnover in the Balkans. *Journal of Human Evolution*, *65*(2), 185–198.

Metcalfe, J. Z., Longstaffe, F. J., & Hodgins, G. (2013). Proboscideans and paleoenvironments of the Pleistocene Great Lakes: landscape, vegetation, and stable isotopes. *Quaternary Science Reviews*, *76*, 102–113.

Mijarra, J. M. P., Burjachs, F., Manzaneque, F. G., & Morla, C. (2007). A palaeoecological interpretation of the lower–middle Pleistocene Cal Guardiola site (Terrassa, Barcelona, NE Spain) from the comparative study of wood and pollen samples. *Review of Palaeobotany and Palynology*, *146*(1–4), 247–264.

Mills, J. R. E. (1955). Ideal dental occlusion in the primates. *Dent Practit*, *6*, 47–61.

Minwer-Barakat, R., Madurell-Malapeira, J., Alba, D. M., Aurell-Garrido, J., De Esteban-Trivigno, S., & Moyà-Solà, S. (2011). Pleistocene rodents from the Torrent de Vallparadís section (Terrassa, northeastern Spain) and biochronological implications. *Journal of Vertebrate Paleontology*, *31*(4), 849–865.

Mounier, A., Marchal, F., & Condemi, S. (2009). Is Homo heidelbergensis a distinct species? New insight on the Mauer mandible. *Journal of Human Evolution*, *56*(3), 219–246.

Münzel, S. C., Rivals, F., Pacher, M., Döppes, D., Rabeder, G., Conard, N. J., & Bocherens, H. (2014). Behavioural ecology of Late Pleistocene bears (Ursus spelaeus, Ursus ingressus): Insight from stable isotopes (C, N, O) and tooth microwear. *Quaternary International*, *339–340*, 148–163. https://doi.org/10.1016/j.quaint.2013.10.020

Naito, Y. I., Meleg, I. N., Robu, M., Vlaicu, M., Drucker, D. G., Wißing, C., Hofreiter, M., Barlow, A., & Bocherens, H. (2020). Heavy reliance on plants for Romanian cave bears evidenced by amino acid nitrogen isotope analysis. *Scientific Reports*, *10*(1), 6612.

Nelson, D. E., Angerbjörn, A., Lidén, K., & Turk, I. (1998). Stable isotopes and the metabolism of the European cave bear. *Oecologia*, *116*, 177–181.

Nelson, R. A. (1980). Protein and fat metabolism in hibernating bears. *Federation Proceedings*, *39*(12), 2955–2958.

Oms, O., Agustí, J., Gabàs, M., & Anadón, P. (2000). Lithostratigraphical correlation of micromammal sites and biostratigraphy of the Upper Pliocene to Lower Pleistocene in the Northeast Guadix-Baza Basin (southern Spain). *Journal of Quaternary Science: Published for the Quaternary Research Association*, *15*(1), 43–50.

Palmqvist, P., & Arribas, A. (2001). Taphonomic decoding of the paleobiological information locked in a lower Pleistocene assemblage of large mammals. *Paleobiology*, *27*(3), 512–530.

Palmqvist, P., Martínez-Navarro, B., Pérez-Claros, J. A., Torregrosa, V., Figueirido, B., Jiménez-Arenas, J. M., Patrocinio Espigares, M., Ros-Montoya, S., & De Renzi, M. (2011). The giant hyena Pachycrocuta brevirostris: Modelling the bone-cracking behavior of an extinct carnivore. *Quaternary International*, *243*(1), 61–79. https://doi.org/10.1016/j.quaint.2010.12.035

Palmqvist, P., Gröcke, D. R., Arribas, A., & Fariña, R. A. (2003). Paleoecological reconstruction of a lower Pleistocene large mammal community using biogeochemical (δ13C, δ15N, δ18O, Sr: Zn) and ecomorphological approaches. *Paleobiology*, *29*(2), 205–229.

Palmqvist, P., Pérez-Claros, J. A., Janis, C. M., Figueirido, B., Torregrosa, V., & Grocke, D. R. (2008a). Biogeochemical and ecomorphological inferences on prey selection and resource partitioning among mammalian carnivores in an early Pleistocene community. *Palaios*, *23*(11), 724–737.

Palmqvist, P., Pérez-Claros, J. A., Janis, C. M., & Gröcke, D. R. (2008b). Tracing the ecophysiology of ungulates and predator–prey relationships in an early Pleistocene large mammal community. *Palaeogeography, Palaeoclimatology, Palaeoecology*, *266*(1–2), 95–111.

Panthi, S., Aryal, A., & Coogan, S. C. (2019). Diet and macronutrient niche of Asiatic black bear (Ursus thibetanus) in two regions of Nepal during summer and autumn. *Ecology and Evolution*, *9*(7), 3717–3727.

Pappa, S., Schreve, D. C., & Rivals, F. (2019). The bear necessities: A new dental microwear database for the interpretation of palaeodiet in fossil Ursidae. *Palaeogeography, Palaeoclimatology, Palaeoecology*, *514*, 168–188. https://doi.org/10.1016/j.palaeo.2018.10.015

Passey, B. H., Cerling, T. E., Schuster, G. T., Robinson, T. F., Roeder, B. L., & Krueger, S. K. (2005). Inverse methods for estimating primary input signals from time-averaged isotope profiles. *Geochimica et Cosmochimica Acta*, *69*(16), 4101–4116.

Peigné, S., Goillot, C., Germonpré, M., Blondel, C., Bignon, O., & Merceron, G. (2009). Predormancy omnivory in European cave bears evidenced by a dental microwear analysis of *Ursus spelaeus* from Goyet, Belgium. *Proceedings of the National Academy of Sciences*, *106*(36), 15390–15393. https://doi.org/10.1073/pnas.0907373106

Peigné, S., & Merceron, G. (2019). Palaeoecology of cave bears as evidenced by dental wear analysis: a review of methods and recent findings. *Historical Biology*, *31*(4), 448–460.

Pérez-Rama, M., Fernández-Mosquera, D., & Grandal-d'Anglade, A. (2011). Effects of hibernation on the stable isotope signatures of adult and neonate cave bears. *Quaternaire*, *4*, 79–88.

Peyton, B. (1980). Ecology, distribution, and food habits of spectacled bears, Tremarctos ornatus, in Peru. *Journal of Mammalogy*, *61*(4), 639–652.

Piñero, P., Agustí, J., Oms, O., Blain, H.-A., Furió, M., Laplana, C., Sevilla, P., Rosas, A., & Vallverdú, J. (2020). First continuous pre-Jaramillo to Jaramillo terrestrial vertebrate succession from Europe. *Scientific Reports*, *10*(1), 1901.

Pinto Llona, A. C., & Andrews, P. J. (2001). *Dental wear and grit ingestion in extant and extinct bears from Northern Spain*.

Pinto-Llona, A. (2006). Comparative dental microwear analysis of cave bears Ursus spelaeus Rosenmüller, 1794 and brown bears Ursus arctos Linnaeus, 1758. *Sci Ann Sch Geol Aristot Univ Thessalon*, *98*, 103–108.

Pinto-Llona, A. C. (2013). Macrowear and occlusal microwear on teeth of cave bears Ursus spelaeus and brown bears Ursus arctos: Inferences concerning diet. *Palaeogeography, Palaeoclimatology, Palaeoecology*, *370*, 41–50.

Profico, A., Di Vincenzo, F., Lorenza, G., Marcello, P., & Manzi, G. (2016). Filling the gap. Human cranial remains from Gombore II (Melka Kunture, Ethiopia; ca. 850 ka) and the origin of Homo heidelbergensis. *Journal of Anthropological Sciences*, *94*, 41–63.

Rabeder, G., Nagel, D., & Pacher, M. (2000). *Der Höhlenbär*. Thorbecke Stuttgart.

Ramírez Pedraza, I., Baryshnikov, G. F., Prilepskaya, N. E., Belyaev, R. I., Pappa, S., & Rivals, F. (2022). Paleodiet and niche partitioning among the easternmost European cave bears based on tooth wear analysis. *Historical Biology*, *34*(6), 1063–1071. https://doi.org/10.1080/08912963.2021.1960324

Ramírez-Pedraza, I., Tornero, C., Pappa, S., Talamo, S., Salazar-García, D. C., Blasco, R., Rosell, J., & Rivals, F. (2019). Microwear and isotopic analyses on cave bear remains from Toll Cave reveal both short-term and long-term dietary habits. *Scientific Reports*, *9*(1), 5716. https://doi.org/10.1038/s41598-019-42152-7

Ramírez-Pedraza, I., Pappa, S., Blasco, R., Arilla, M., Rosell, J., Millán, F., Maroto, J., Soler, J., Soler, N., & Rivals, F. (2020). Dietary habits of the cave bear from the Late Pleistocene

in the northeast of the Iberian Peninsula. *Quaternary International*, *557*, 63–69. https://doi.org/10.1016/j.quaint.2019.09.043

Rensberger, J. M. (1978). Scanning electron microscopy of wear and occlusal events in some small herbivores. *Development, Function and Evolution of Teeth*, 415–438.

Richards, M. P., Pacher, M., Stiller, M., Quilès, J., Hofreiter, M., Constantin, S., Zilhao, J., & Trinkaus, E. (2008). Isotopic evidence for omnivory among European cave bears: Late Pleistocene Ursus spelaeus from the Peştera cu Oase, Romania. *Proceedings of the National Academy of Sciences*, *105*(2), 600–604.

Rivals, F., & Deniaux, B. (2003). Dental microwear analysis for investigating the diet of an argali population (Ovis ammon antiqua) of mid-Pleistocene age, Caune de l'Arago cave, eastern Pyrenees, France. *Palaeogeography, Palaeoclimatology, Palaeoecology*, *193*(3–4), 443–455.

Rivals, F., Semprebon, G., & Lister, A. (2012). An examination of dietary diversity patterns in Pleistocene proboscideans (Mammuthus, Palaeoloxodon, and Mammut) from Europe and North America as revealed by dental microwear. *Quaternary International*, *255*, 188–195.

Rivals, F., Semprebon, G. M., & Lister, A. M. (2019). Feeding traits and dietary variation in Pleistocene proboscideans: A tooth microwear review. *Quaternary Science Reviews*, *219*, 145–153.

Rivals, F., & Semprebon, G. M. (2017). Latitude matters: an examination of behavioural plasticity in dietary traits amongst extant and Pleistocene Rangifer tarandus. *Boreas*, *46*(2), 254–263.

Roberts, P., Stewart, M., Alagaili, A. N., Breeze, P., Candy, I., Drake, N., Groucutt, H. S., Scerri, E. M., Lee-Thorp, J., & Louys, J. (2018). Fossil herbivore stable isotopes reveal middle Pleistocene hominin palaeoenvironment in 'Green Arabia.' *Nature Ecology & Evolution*, *2*(12), 1871–1878.

Robu, M., Wynn, J. G., Mirea, I. C., Petculescu, A., Kenesz, M., Puşcaş, C. M., Vlaicu, M., Trinkaus, E., & Constantin, S. (2018). The diverse dietary profiles of MIS 3 cave bears from the Romanian Carpathians: insights from stable isotope (δ13C and δ15N) analysis. *Palaeontology*, *61*(2), 209–219.

Robu, M., Fortin, J. K., Richards, M. P., Schwartz, C. C., Wynn, J. G., Robbins, C. T., & Trinkaus, E. (2013). Isotopic evidence for dietary flexibility among European Late Pleistocene cave bears (Ursus spelaeus). *Canadian Journal of Zoology*, *91*(4), 227–234.

Roca, E., Sans, M., Cabrera, L., & Marzo, M. (1999). Oligocene to Middle Miocene evolution of the central Catalan margin (northwestern Mediterranean). *Tectonophysics*, *315*(1–4), 209–229.

Ryan, A. S. (1979). Wear striation direction on primate teeth: a scanning electron microscope examination. *American Journal of Physical Anthropology*, *50*(2), 155–167.

Saarinen, J., Fortelius, M., Bocherens, H., Oms, O., Agustí, J., Carrión, J. S., Ochando, J., Blain, H.-A., DeMiguel, D., & Solano-García, J. (2022). Revisiting the paleoenvironmental reconstruction of the Orce sites and the early Homo habitats in western Europe. A response to Palmqvist et al.(2022). *Quaternary Science Reviews*, *297*, 107730.

Scott, R. S., Ungar, P. S., Bergstrom, T. S., Brown, C. A., Grine, F. E., Teaford, M. F., & Walker, A. (2005). Dental microwear texture analysis shows within-species diet variability in fossil hominins. *Nature*, *436*(7051), 693–695.

Semprebon, G. M., Godfrey, L. R., Solounias, N., Sutherland, M. R., & Jungers, W. L. (2004). Can low-magnification stereomicroscopy reveal diet? *Journal of Human Evolution*, *47*(3), 115–144.

Semprebon, G. M., & Rivals, F. (2010). Trends in the paleodietary habits of fossil camels from the Tertiary and Quaternary of North America. *Palaeogeography, Palaeoclimatology, Palaeoecology*, *295*(1–2), 131–145.

Semprebon, G. M., & Rivals, F. (2007). Was grass more prevalent in the pronghorn past? An assessment of the dietary adaptations of Miocene to recent Antilocapridae (Mammalia: Artiodactyla). *Palaeogeography, Palaeoclimatology, Palaeoecology*, *253*(3–4), 332–347.

Solounias, N., & Semprebon, G. (2002). Advances in the reconstruction of ungulate ecomorphology with application to early fossil equids. *American Museum Novitates*, *2002*(3366), 1–49.

Sorbelli, L., Alba, D. M., Cherin, M., Moullé, P.-É., Brugal, J.-P., & Madurell-Malapeira, J. (2021). A review on Bison schoetensacki and its closest relatives through the early-Middle Pleistocene transition: Insights from the Vallparadís Section (NE Iberian Peninsula) and other European localities. *Quaternary Science Reviews*, *261*, 106933.

Souron, A. (2017). Diet and ecology of extant and fossil wild pigs. *Ecology, Conservation and Management of Wild Pigs and Peccaries. Cambridge University Press, Cambridge*, 29–38.

Souron, A. (2018). Morphology, diet, and stable carbon isotopes: on the diet of Theropithecus and some limits of uniformitarianism in paleoecology. *American Journal of Physical Anthropology*, *166*(1), 261–267.

Souron, A., Balasse, M., & Boisserie, J.-R. (2012). Intra-tooth isotopic profiles of canines from extant Hippopotamus amphibius and late Pliocene hippopotamids (Shungura Formation, Ethiopia): insights into the seasonality of diet and climate. *Palaeogeography, Palaeoclimatology, Palaeoecology*, *342*, 97–110.

Souron, A., Boisserie, J.-R., & White, T. D. (2013). A new species of the suid genus Kolpochoerus from Ethiopia. *Acta Palaeontologica Polonica*, *60*(1), 79–96.

Sponheimer, M., & Lee-Thorp, J. A. (2003). Using carbon isotope data of fossil bovid communities for palaeoenvironmental reconstruction: Research articles: Human origins research in South Africa. *South African Journal of Science*, *99*(5), 273–275.

Steinmetz, R., & Garshelis, D. L. (2008). Distinguishing Asiatic black bears and sun bears by claw marks on climbed trees. *The Journal of Wildlife Management*, *72*(3), 814–821.

Strani, F., DeMiguel, D., Alba, D. M., Moyà-Solà, S., Bellucci, L., Sardella, R., & Madurell-Malapeira, J. (2019). The effects of the "0.9 Ma event" on the Mediterranean ecosystems during the Early-Middle Pleistocene transition as revealed by dental wear patterns of fossil ungulates. *Quaternary Science Reviews*, *210*, 80–89. https://doi.org/10.1016/j.quascirev.2019.02.027

Stynder, D. D., Ungar, P. S., Scott, J. R., & Schubert, B. W. (2012). A dental microwear texture analysis of the Mio-Pliocene hyaenids from Langebaanweg, South Africa. *Acta Palaeontologica Polonica*, *57*(3), 485–496.

Stynder, D. D., DeSantis, L. R., Donohue, S. L., Schubert, B. W., & Ungar, P. S. (2019). A dental microwear texture analysis of the early Pliocene African ursid Agriotherium africanum (Mammalia, Carnivora, Ursidae). *Journal of Mammalian Evolution*, *26*, 505–515.

Szabó, B., Pazonyi, P., Tóth, E., Magyari, E. K., Kiss, G. I., Rinyu, L., Futó, I., & Virág, A. (2021). Pleistocene and holocene palaeoenvironmental reconstruction of the carpathian basin based on multiproxy analysis of cervid teeth. *Historical Biology*, *33*(12), 3307–3325.

Teaford, M. F., & Oyen, O. J. (1989). Differences in the rate of molar wear between monkeys raised on different diets. *Journal of Dental Research*, *68*(11), 1513–1518.

Teaford, M. F., & Walker, A. (1984). Quantitative differences in dental microwear between primate species with different diets and a comment on the presumed diet of Sivapithecus. *American Journal of Physical Anthropology*, *64*(2), 191–200.

Thorp, J. L., & Van der Merwe, N. J. (1987). Carbon isotope analysis of fossil bone apatite. *South African Journal of Science*, *83*(11), 712–715.

Tipple, B. J., Meyers, S. R., & Pagani, M. (2010). Carbon isotope ratio of Cenozoic CO2: A comparative evaluation of available geochemical proxies. *Paleoceanography*, *25*(3).

Tornero, C., Bălăşescu, A., Ughetto-Monfrin, J., Voinea, V., & Balasse, M. (2013). Seasonality and season of birth in early Eneolithic sheep from Cheia (Romania): methodological advances and implications for animal economy. *Journal of Archaeological Science*, *40*(11), 4039–4055. https://doi.org/10.1016/j.jas.2013.05.013

Tornero, C., Aguilera, M., Ferrio, J. P., Arcusa, H., Moreno-García, M., Garcia-Reig, S., & Rojo-Guerra, M. (2018). Vertical sheep mobility along the altitudinal gradient through stable isotope analyses in tooth molar bioapatite, meteoric water and pastures: A reference from the Ebro valley to the Central Pyrenees. *Quaternary International*, *484*, 94–106.

Tornero, C., Balasse, M., Molist, M., & Saña, M. (2016). Seasonal reproductive patterns of early domestic sheep at Tell Halula (PPNB, Middle Euphrates Valley): Evidence from sequential oxygen isotope analyses of tooth enamel. *Journal of Archaeological Science: Reports*, *6*, 810–818.

Toro-Moyano, I., Martínez-Navarro, B., Agustí, J., Souday, C., de Castro, J. M. B., Martinón-Torres, M., Fajardo, B., Duval, M., Falguères, C., & Oms, O. (2013). The oldest human fossil in Europe, from Orce (Spain). *Journal of Human Evolution*, *65*(1), 1–9.

Torres, T. de, & García, N. (1997). Comments on: Diet, physiology and ecology of fossil mammals as inferred from stable carbon and nitrogen isotope biogeochemistry: Implications for Pleistocene bears by H. Bocherens et al. *Palaeogeography Palaeoclimatology Palaeoecology*, *128*(1–4), 359–361.

Ungar, P. S., Scott, J. R., Schubert, B. W., & Stynder, D. D. (2010). *Carnivoran dental microwear textures: comparability of carnassial facets and functional differentiation of postcanine teeth*.

Ungar, P. S., Brown, C. A., Bergstrom, T. S., & Walker, A. (2003). Quantification of dental microwear by tandem scanning confocal microscopy and scale-sensitive fractal analyses. *Scanning: The Journal of Scanning Microscopies*, *25*(4), 185–193.

Uno, K. T., Rivals, F., Bibi, F., Pante, M., Njau, J., & de la Torre, I. (2018). Large mammal diets and paleoecology across the Oldowan–Acheulean transition at Olduvai Gorge, Tanzania from stable isotope and tooth wear analyses. *Journal of Human Evolution*, *120*, 76–91.

van Valkenburgh, B., Teaford, M. F., & Walker, A. (1990). Molar microwear and diet in large carnivores: inferences concerning diet in the sabretooth cat, Smilodon fatalis. *Journal of Zoology*, *222*(2), 319–340.

Vekua, A., Lordkipanidze, D., Rightmire, G. P., Agusti, J., Ferring, R., Maisuradze, G., Mouskhelishvili, A., Nioradze, M., De Leon, M. P., & Tappen, M. (2002). A new skull of early Homo from Dmanisi, Georgia. *Science*, *297*(5578), 85–89.

Walker, A., Hoeck, H. N., & Perez, L. (1978). Microwear of mammalian teeth as an indicator of diet. *Science*, *201*(4359), 908–910.

Wong, S. T. (2002). Food habits of Malayan sun bears in lowland tropical forest of Borneo. *Ursus*, *13*, 127–136.

ANNEXES

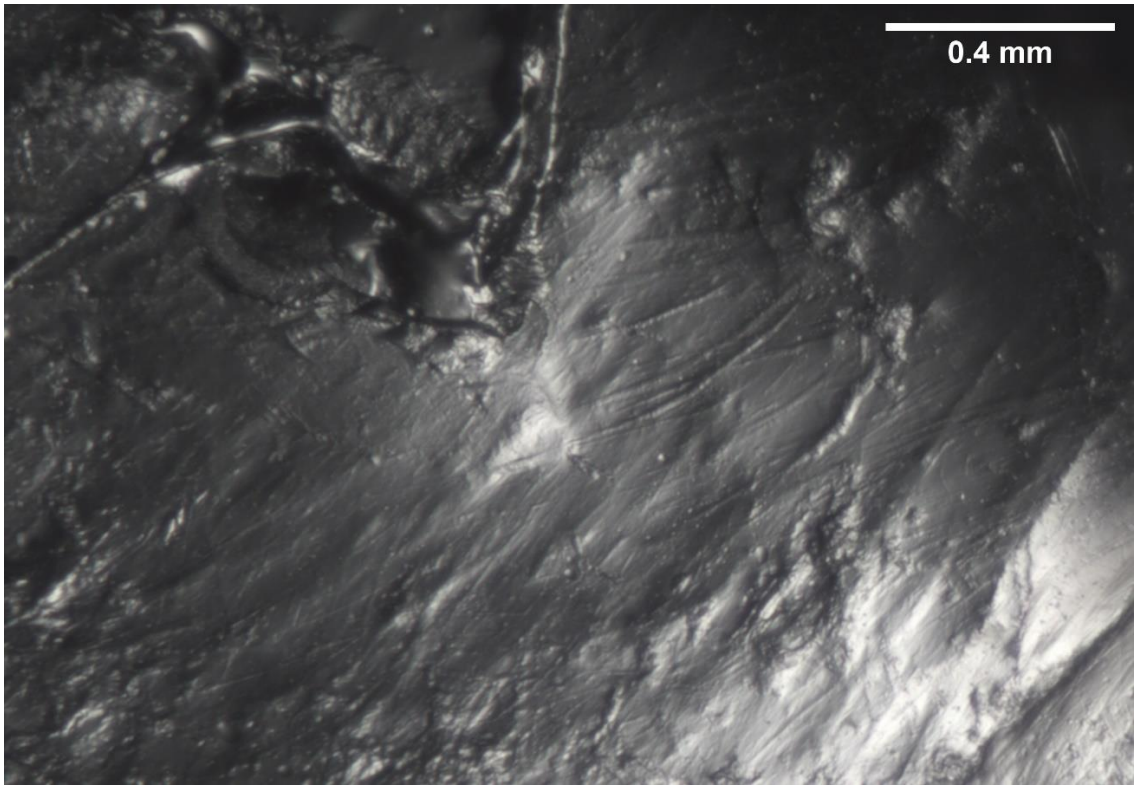

Supplementary Figure 1: Microphotography of sample IPS14950_faceta1_1y2.

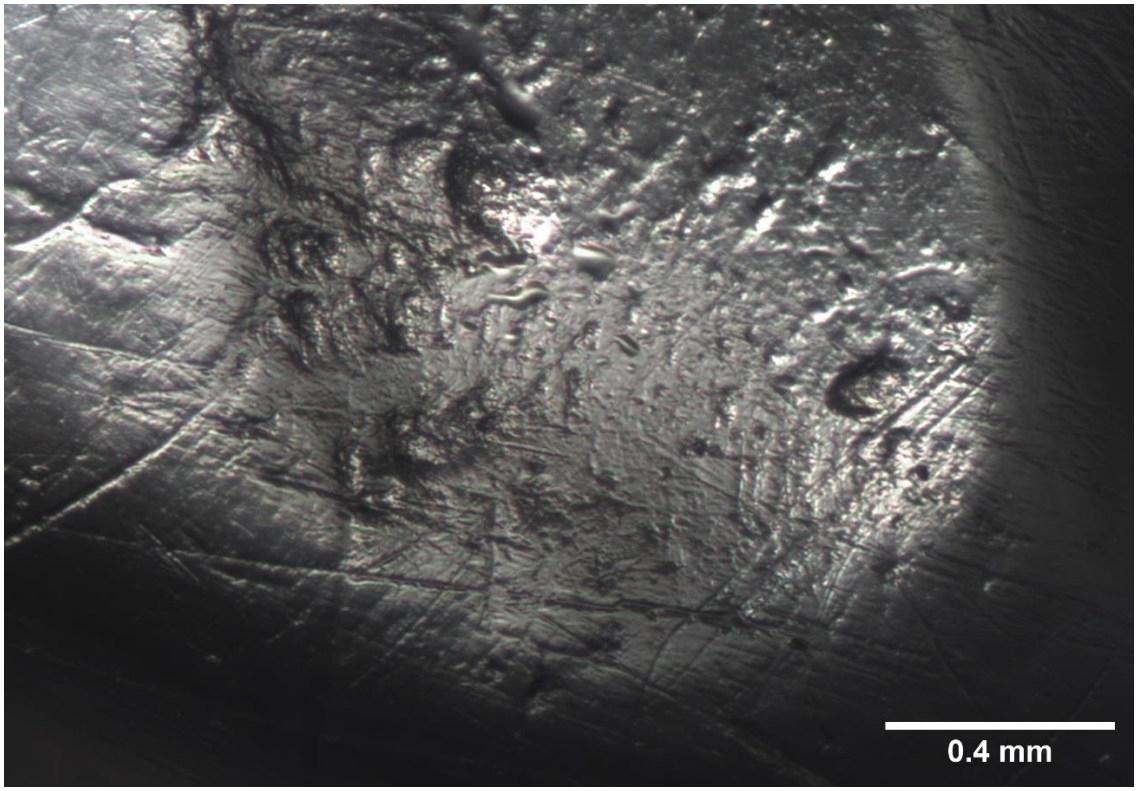

Supplementary Figure 2: Microphotography of sample IPS110442_faceta1_1y2.

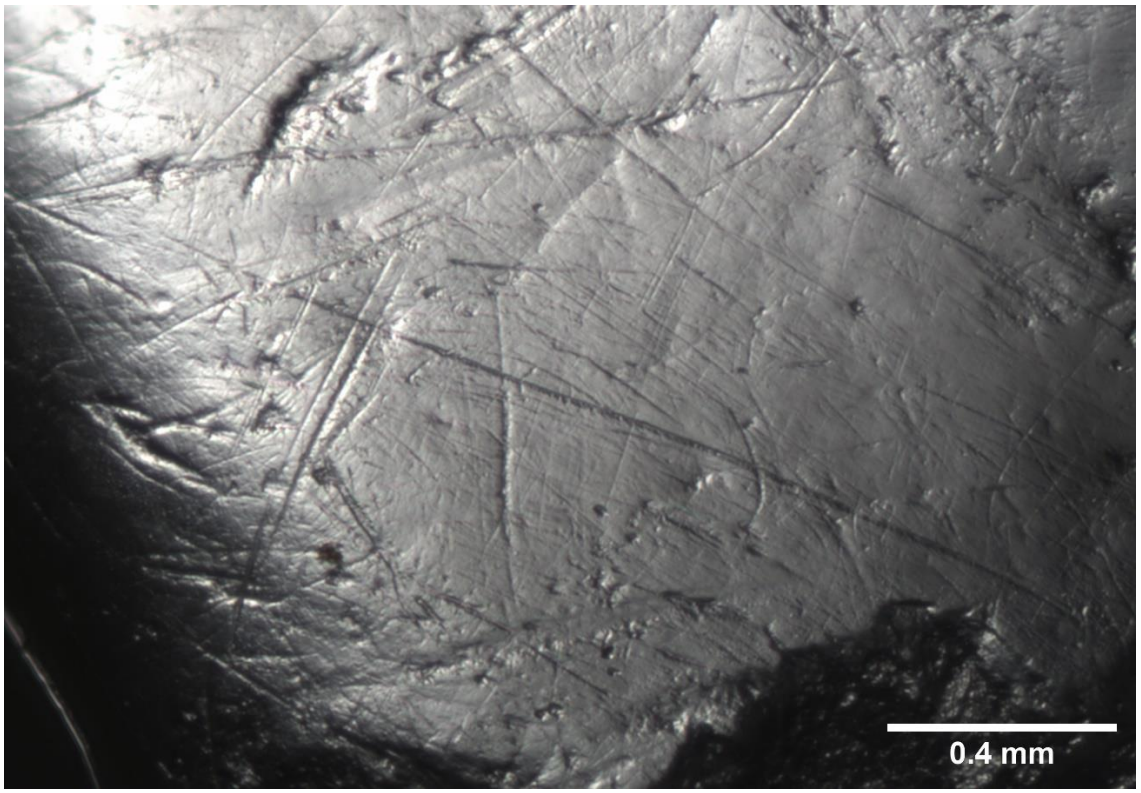

Supplementary Figure 3: Microphotography of sample IPS110442_faceta1_1y2_M1.

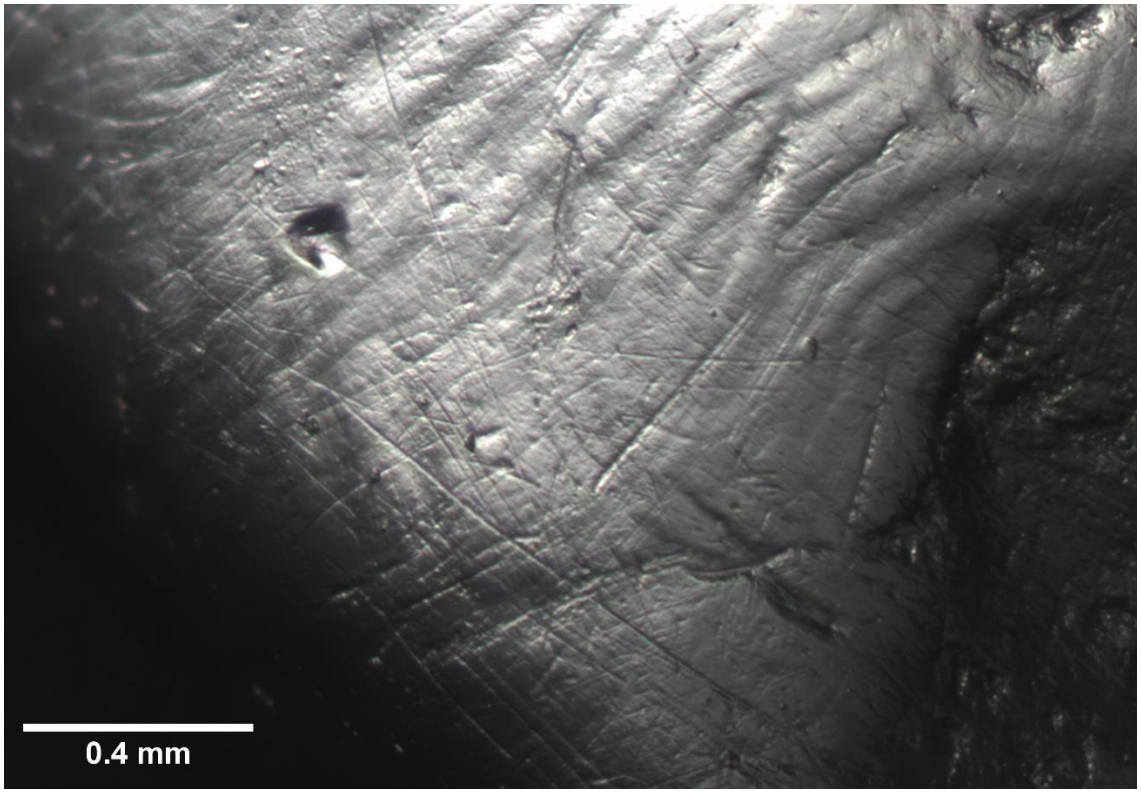

Supplementary Figure 4: Microphotography of sample IPS110442_nofaceta1_1y2.

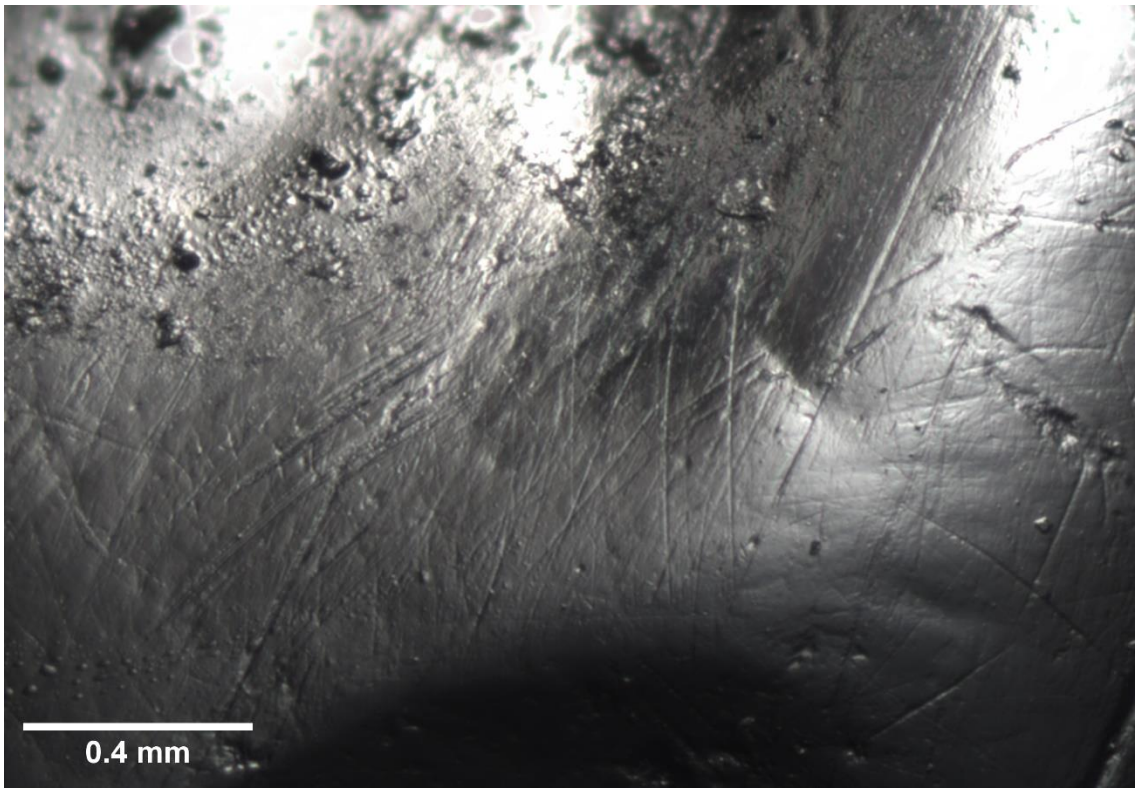

Supplementary Figure 5: Microphotography of sample IPS110442_nofaceta2_1.

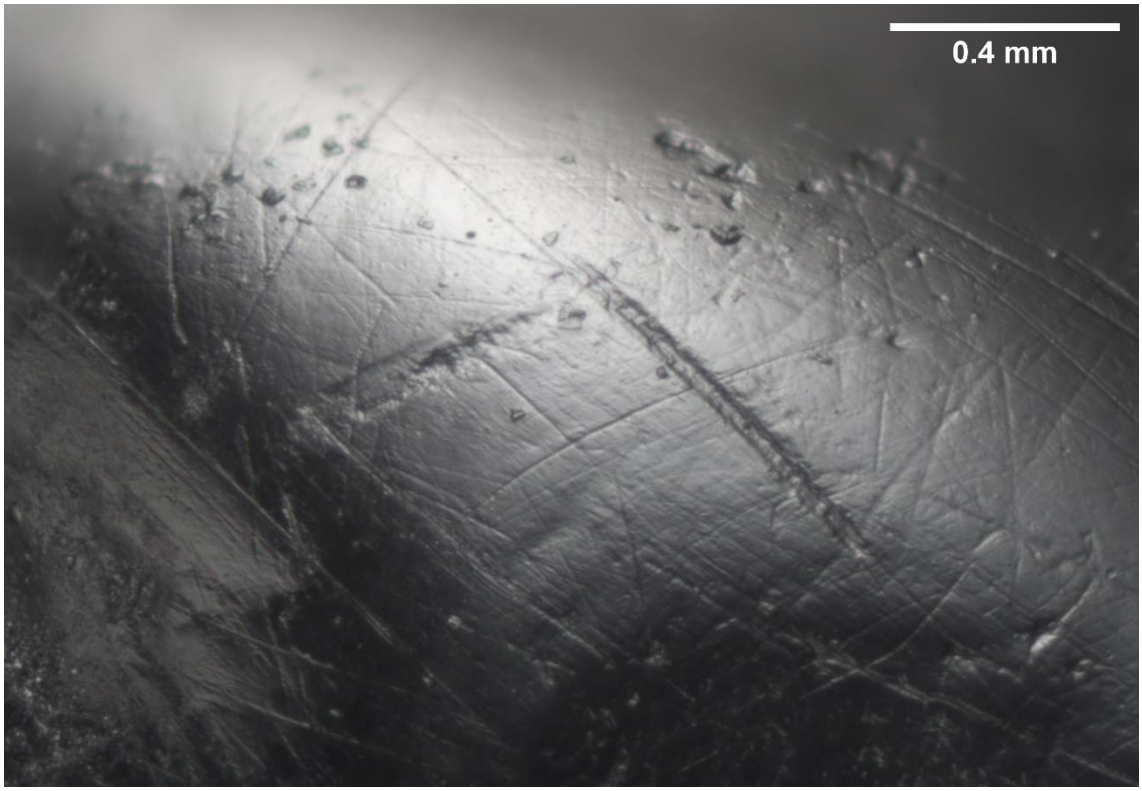

Supplementary Figure 6: Microphotography of sample IPS110442_nofaceta2_2.

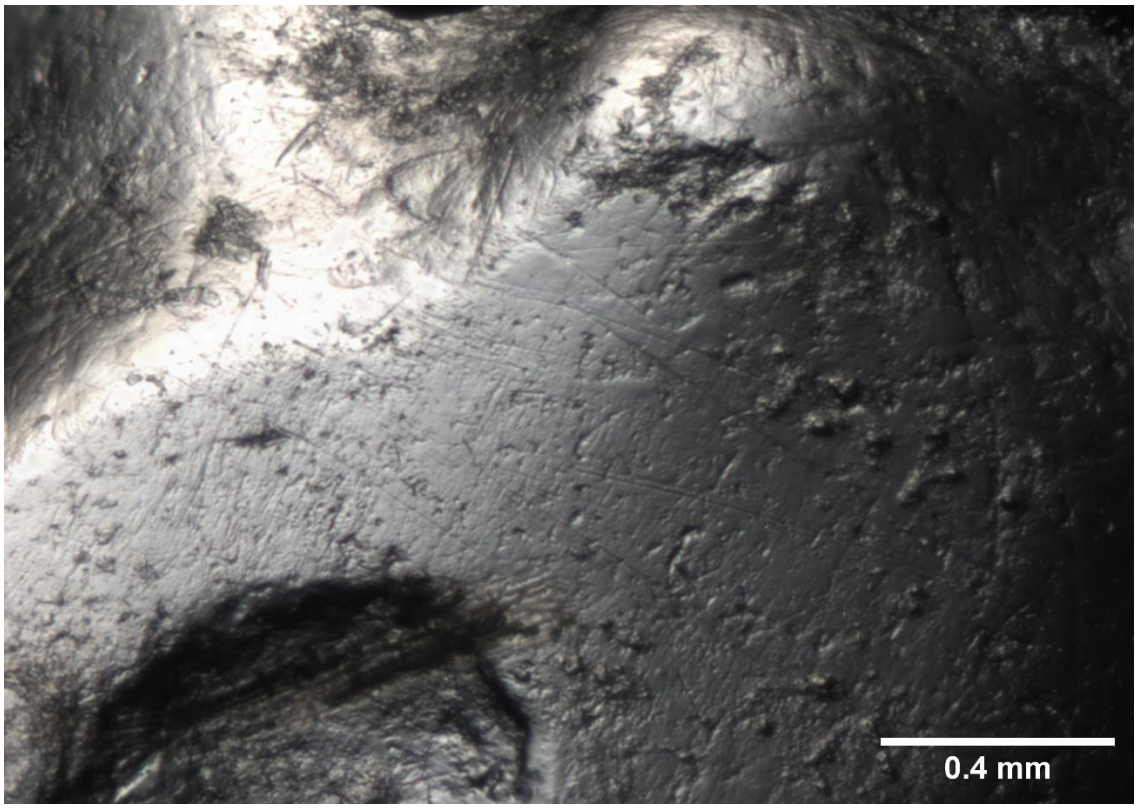

Supplementary Figure 7: Microphotography of sample IPS110452a_faceta1_1.

Supplementary Figure 8: Microphotography of sample IPS110452a_faceta1_2.

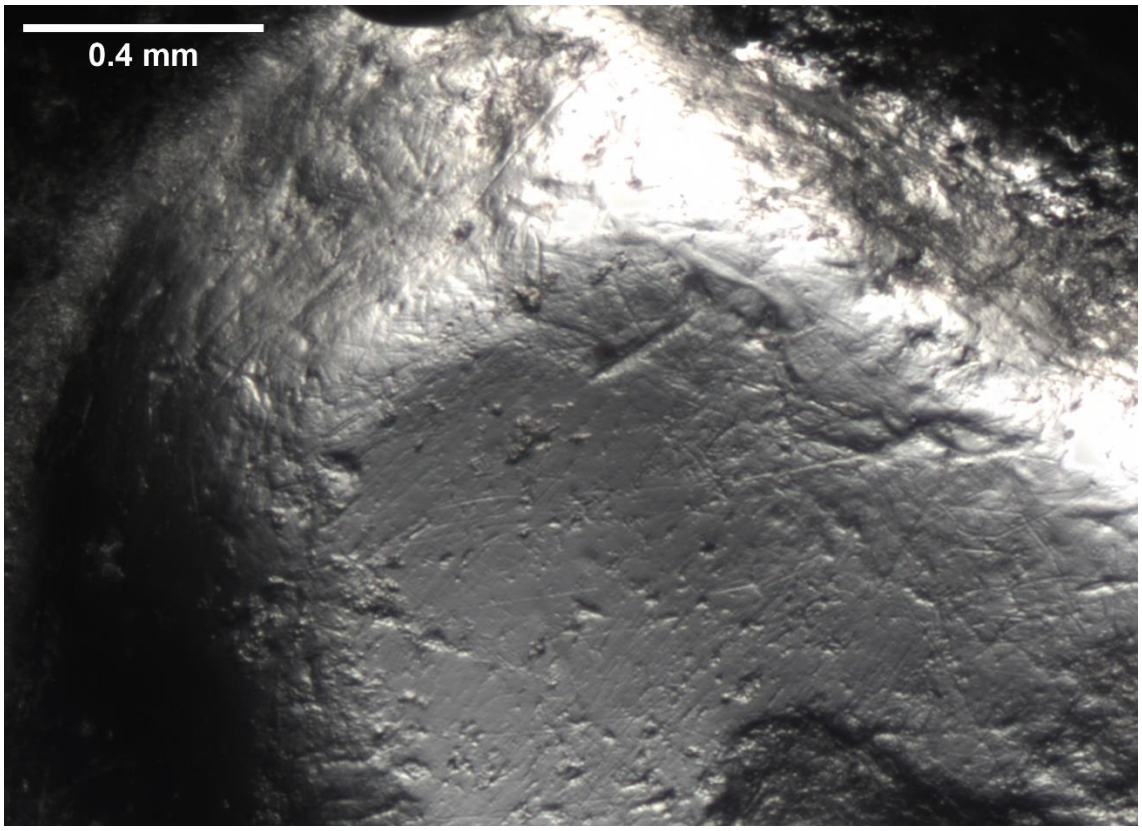

Supplementary Figure 9: Microphotography of sample IPS110452a_faceta2_1.

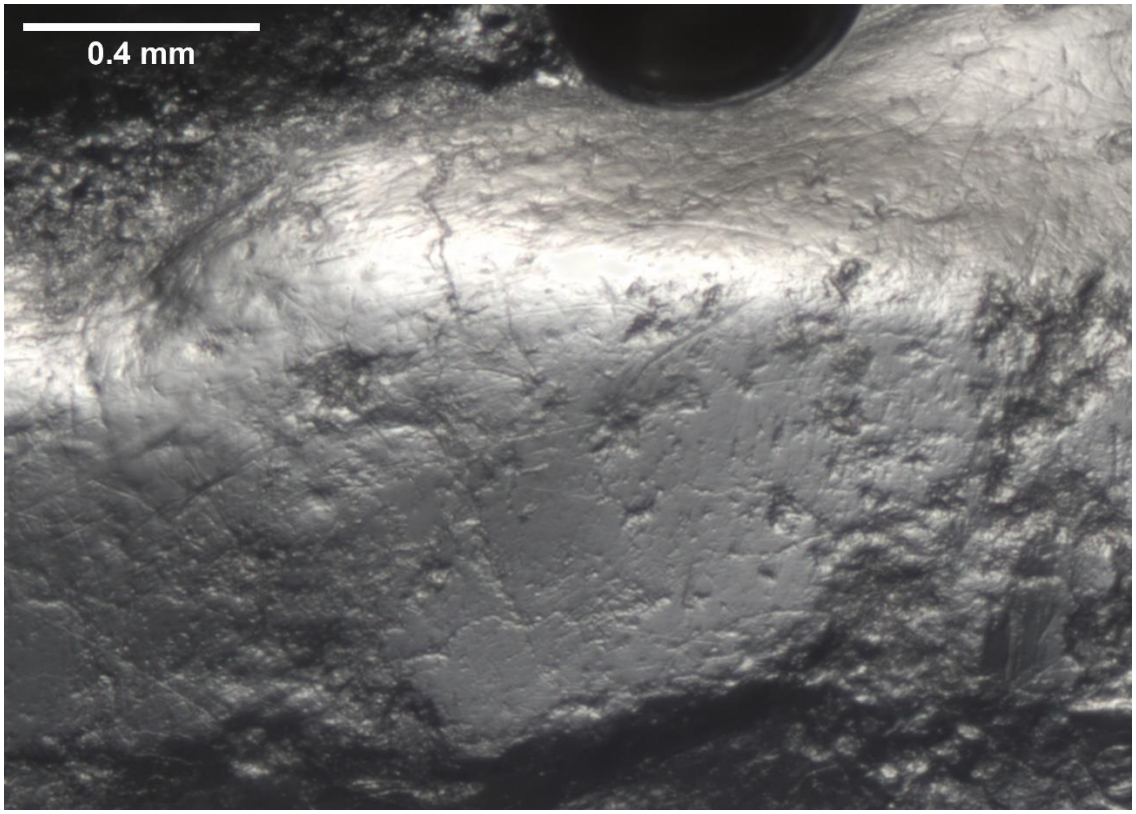

Supplementary Figure 10: Microphotography of sample IPS110452a_faceta2_2.

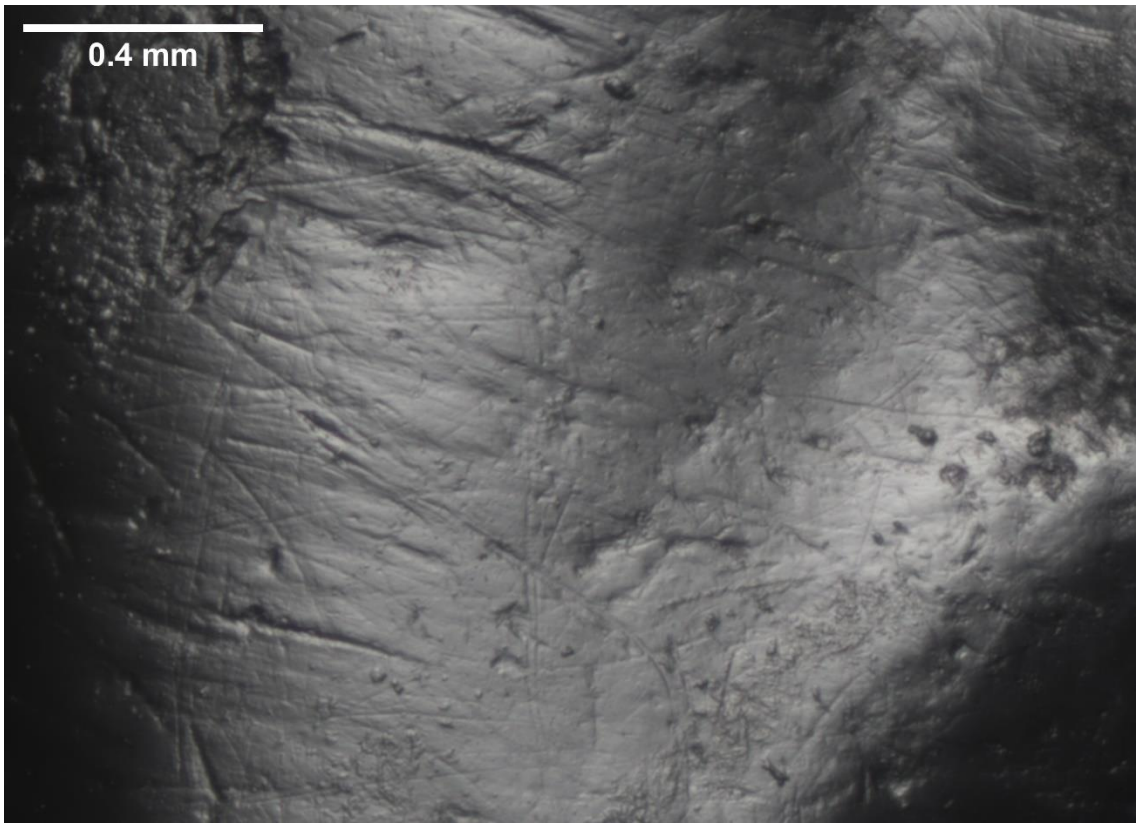

Supplementary Figure 11: Microphotography of sample IPS110452a_no faceta1_1.

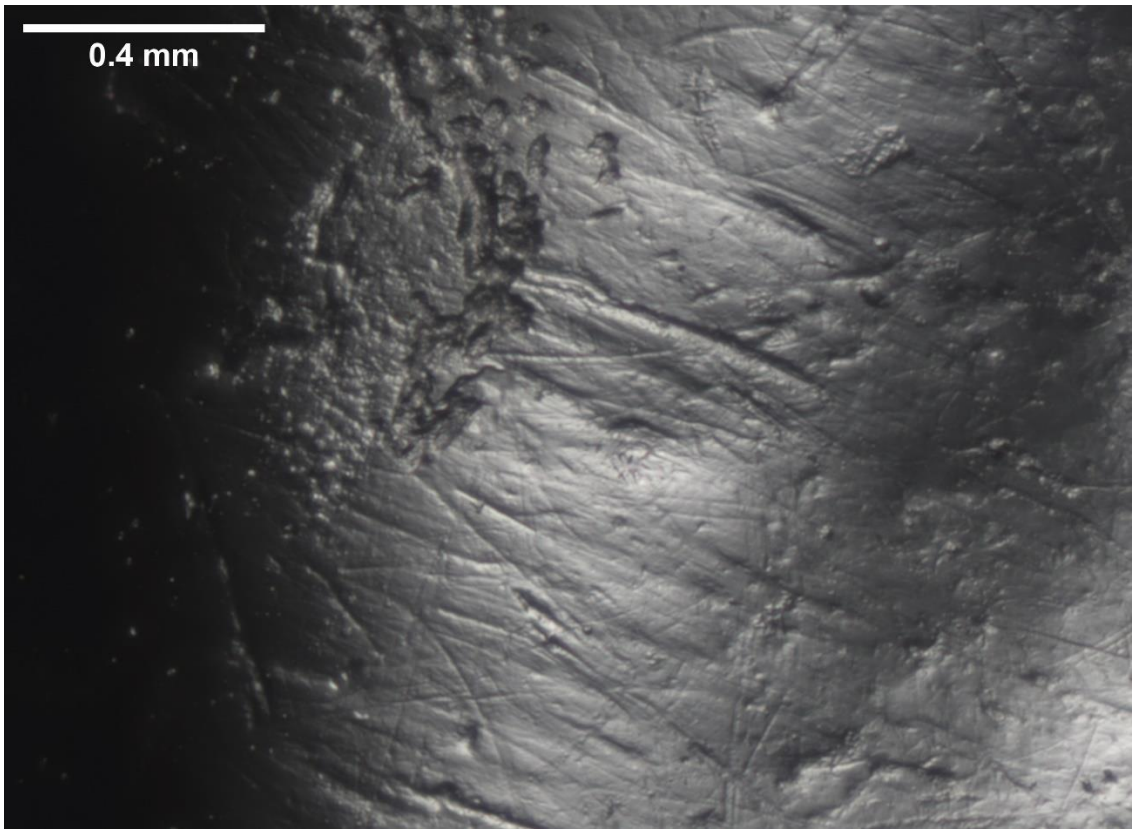

Supplementary Figure 12: Microphotography of sample IPS110452a_no faceta1_2.

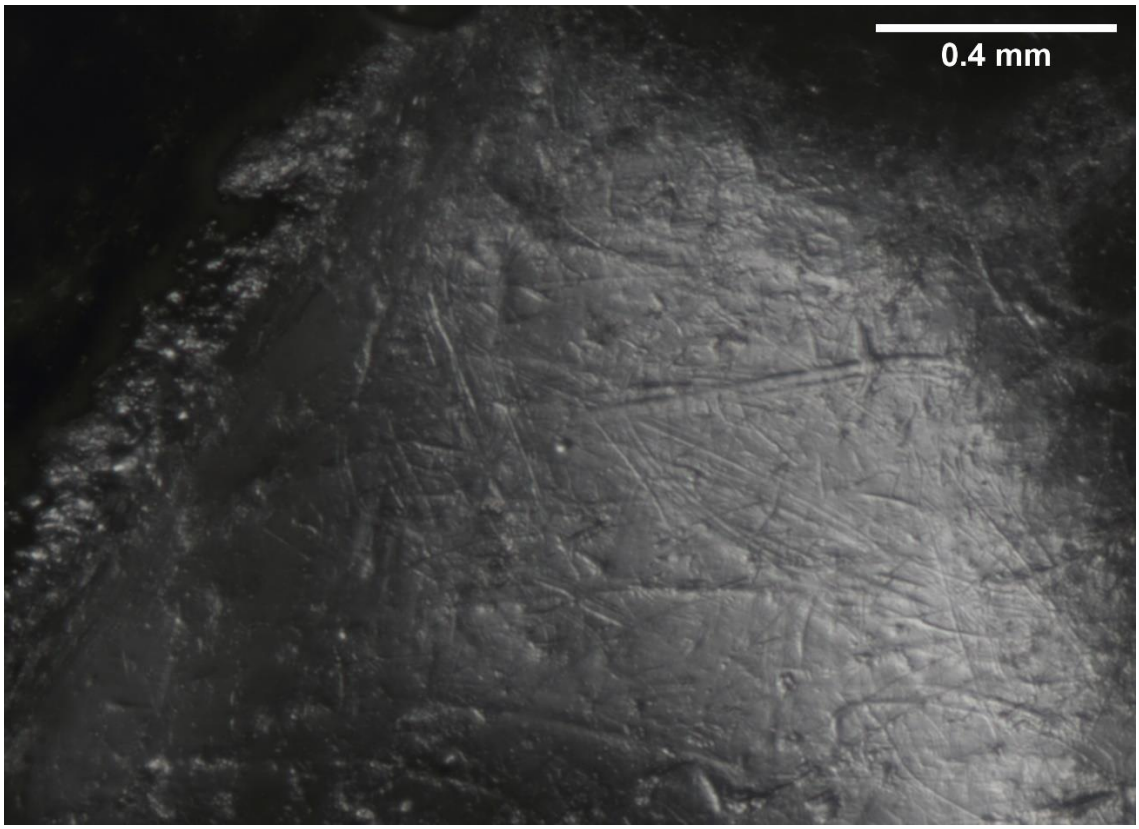

Supplementary Figure 13: Microphotography of sample IPS110452a_no faceta2_1y2.

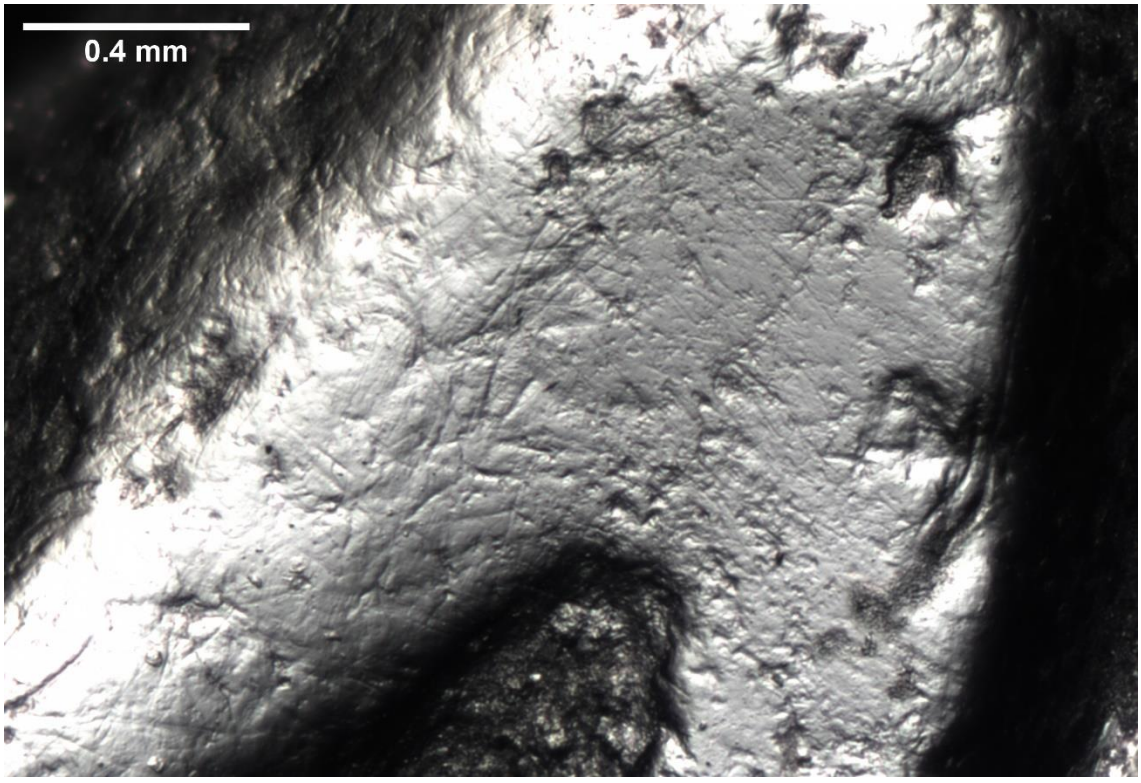

Supplementary Figure 14: Microphotography of sample IPS110452c_faceta1_1.

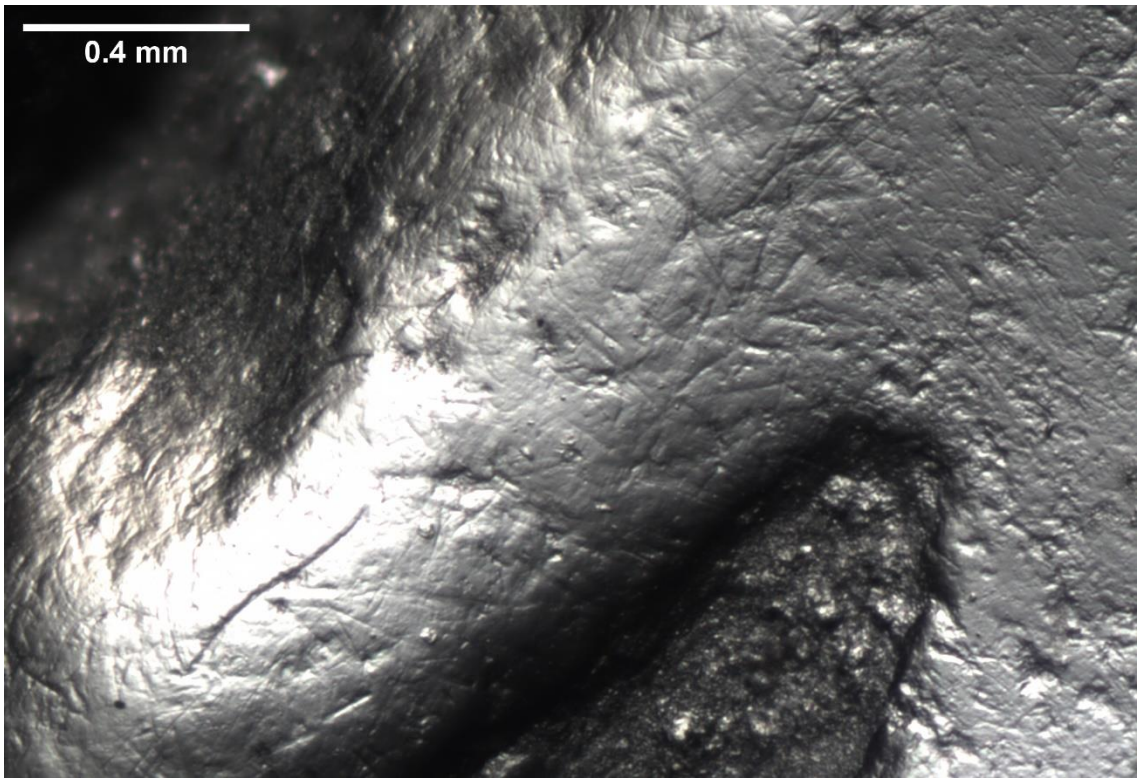

Supplementary Figure 15: Microphotography of sample IPS110452c_faceta1_2.

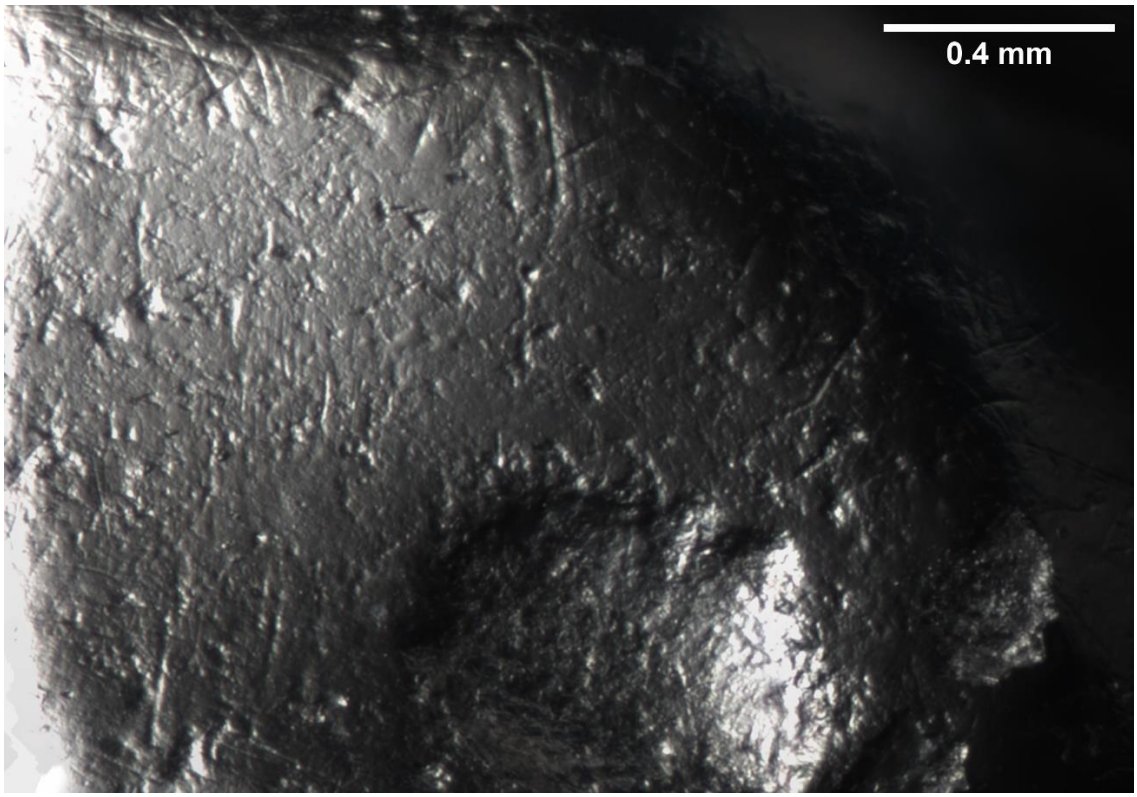

Supplementary Figure 16: Microphotography of sample IPS110452c_faceta2_1y2.

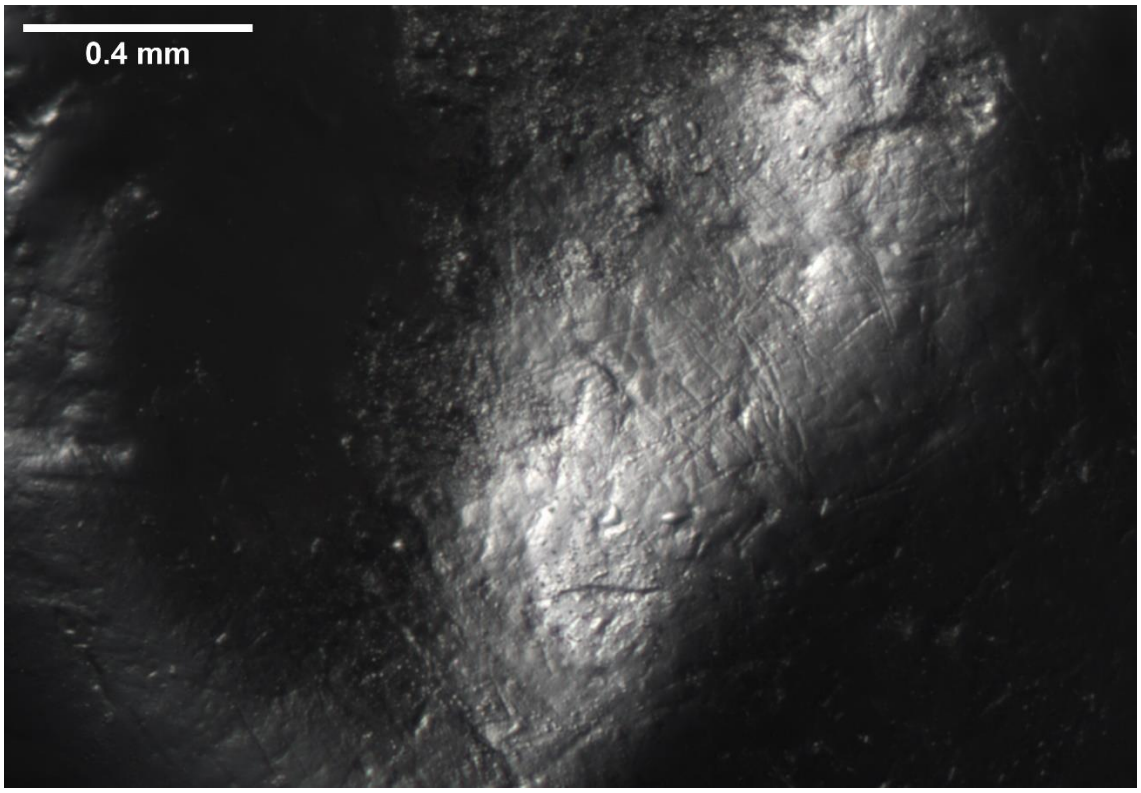

Supplementary Figure 17: Microphotography of sample IPS110452c_nofaceta1_1.

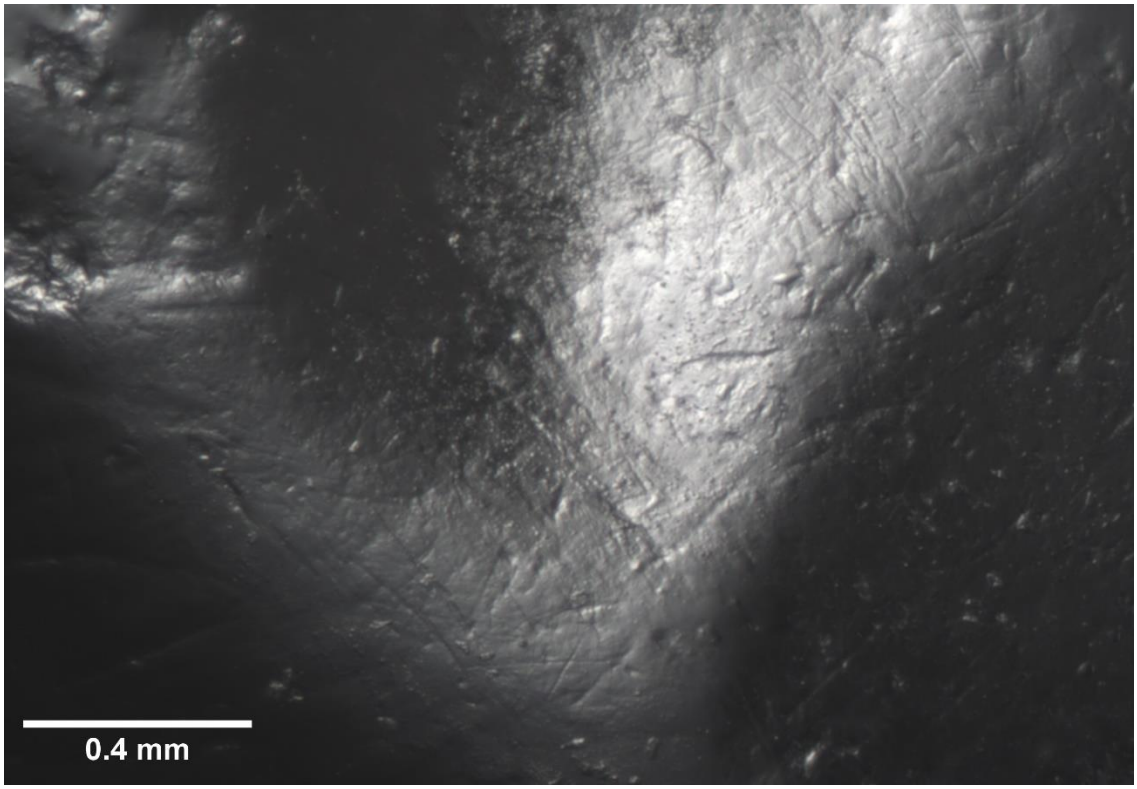

Supplementary Figure 18: Microphotography of sample IPS110452c_nofaceta1_2.

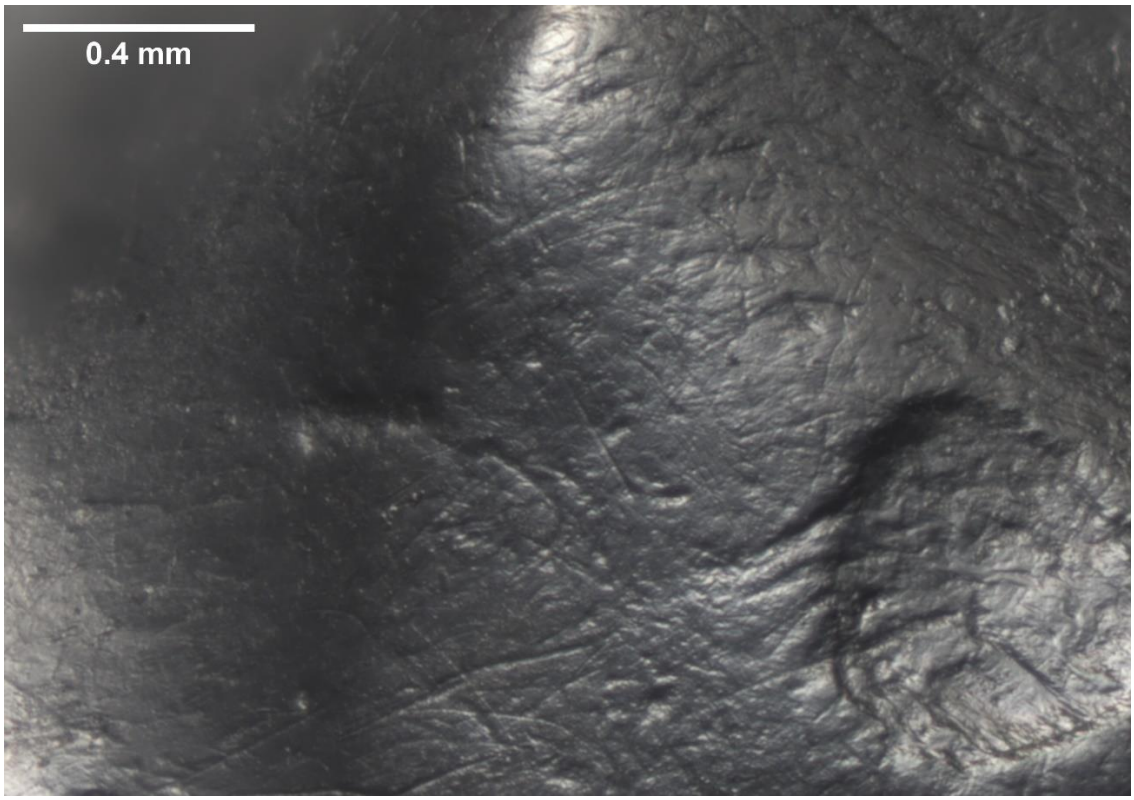

Supplementary Figure 19: Microphotography of sample IPS127527_faceta1_1y2.

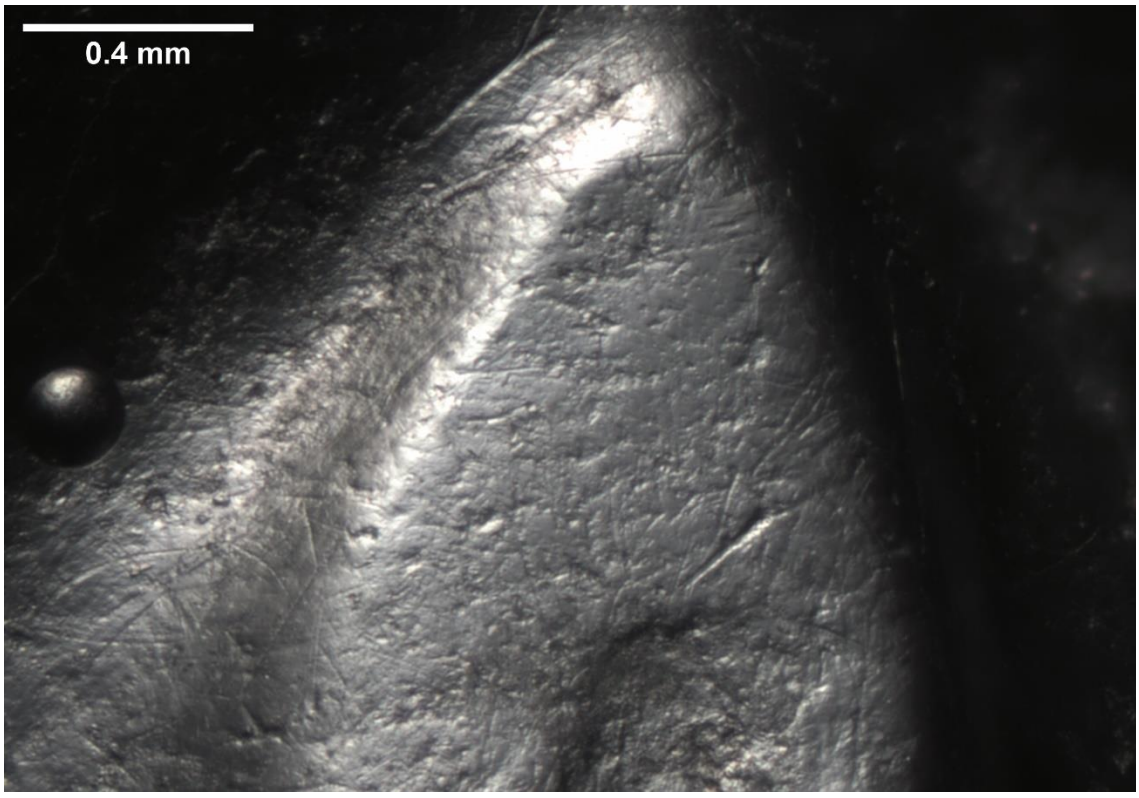

Supplementary Figure 20: Microphotography of sample IPS127527_faceta2_1.

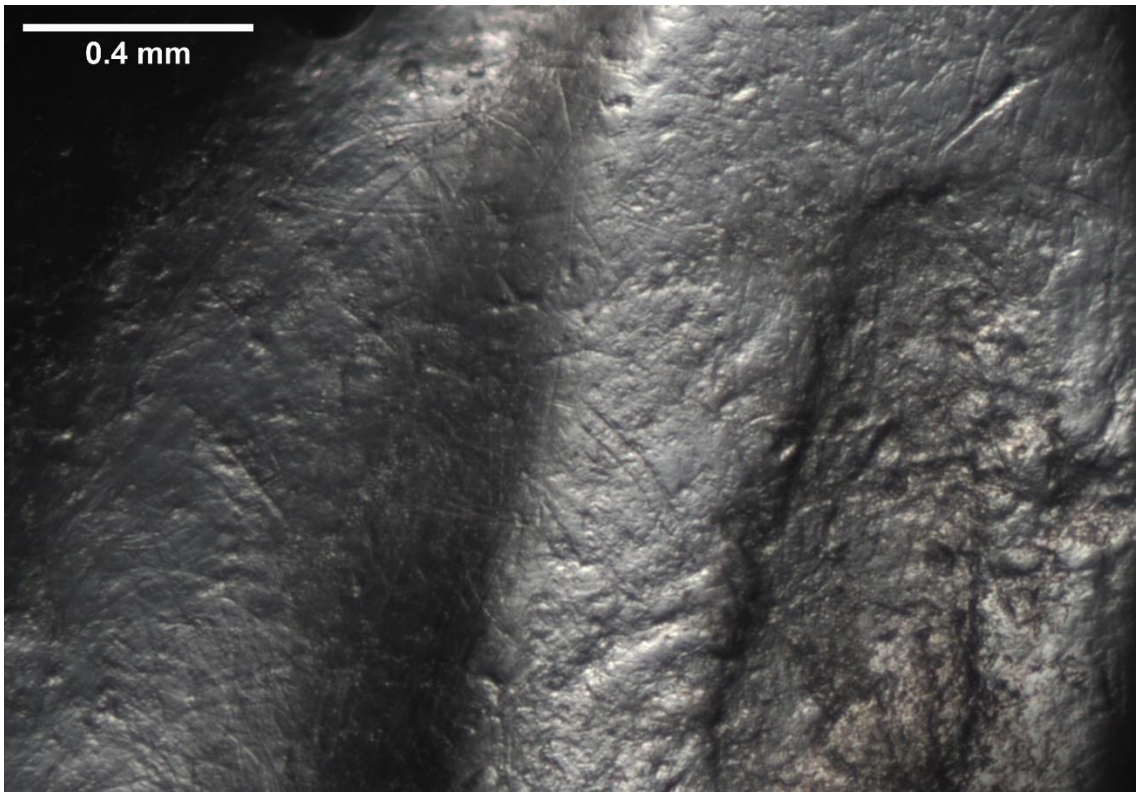

Supplementary Figure 21: Microphotography of sample IPS127527_faceta2_2.

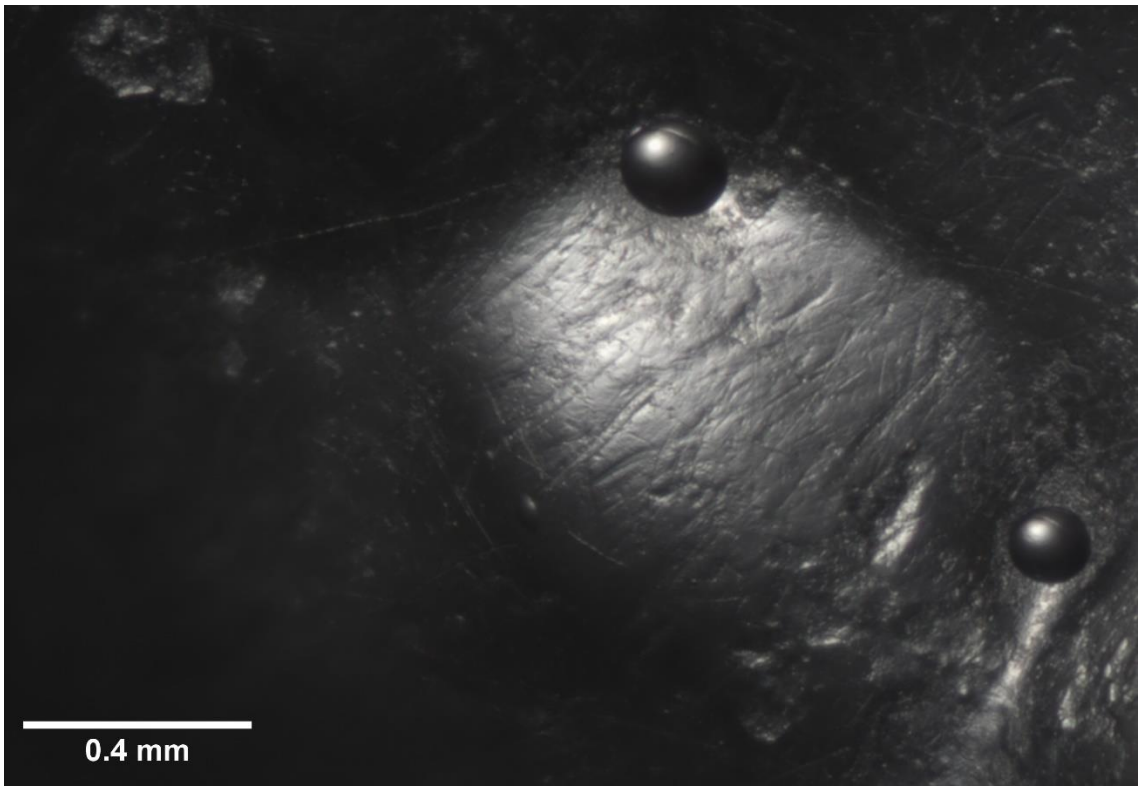

Supplementary Figure 22: Microphotography of sample IPS127527_nofaceta1_1.

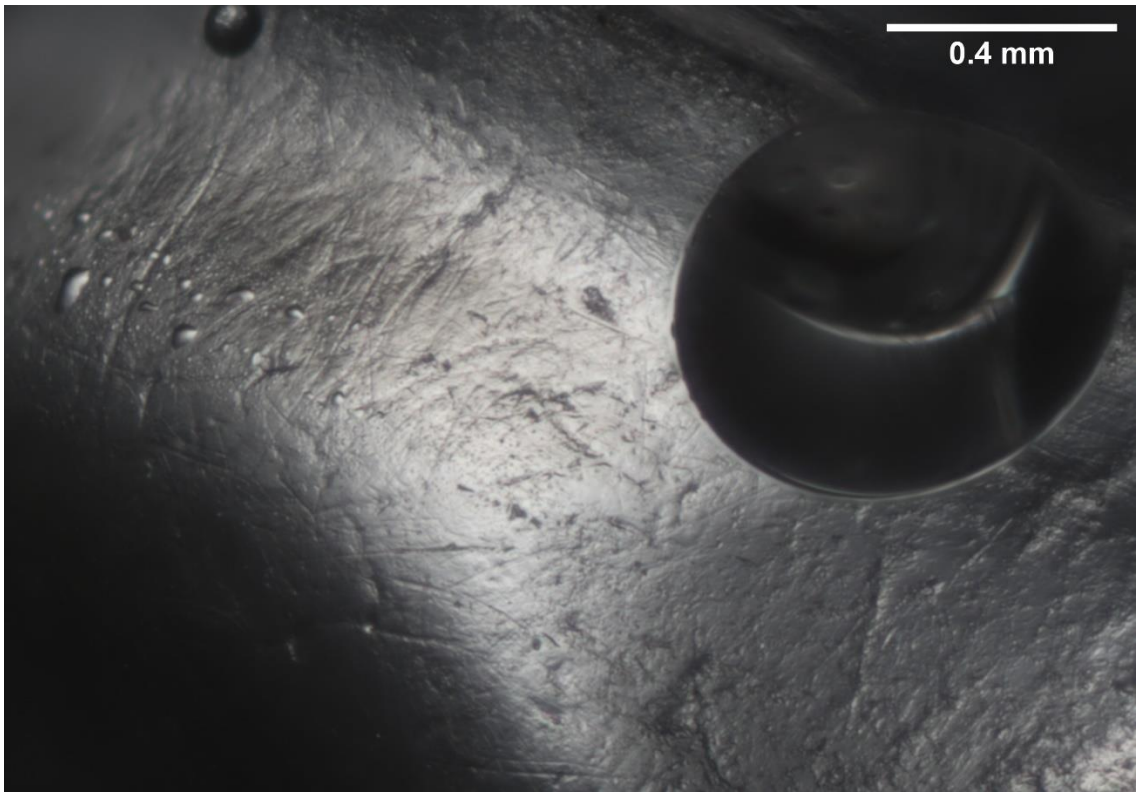

Supplementary Figure 23: Microphotography of sample IPS127527_nofaceta2_1.

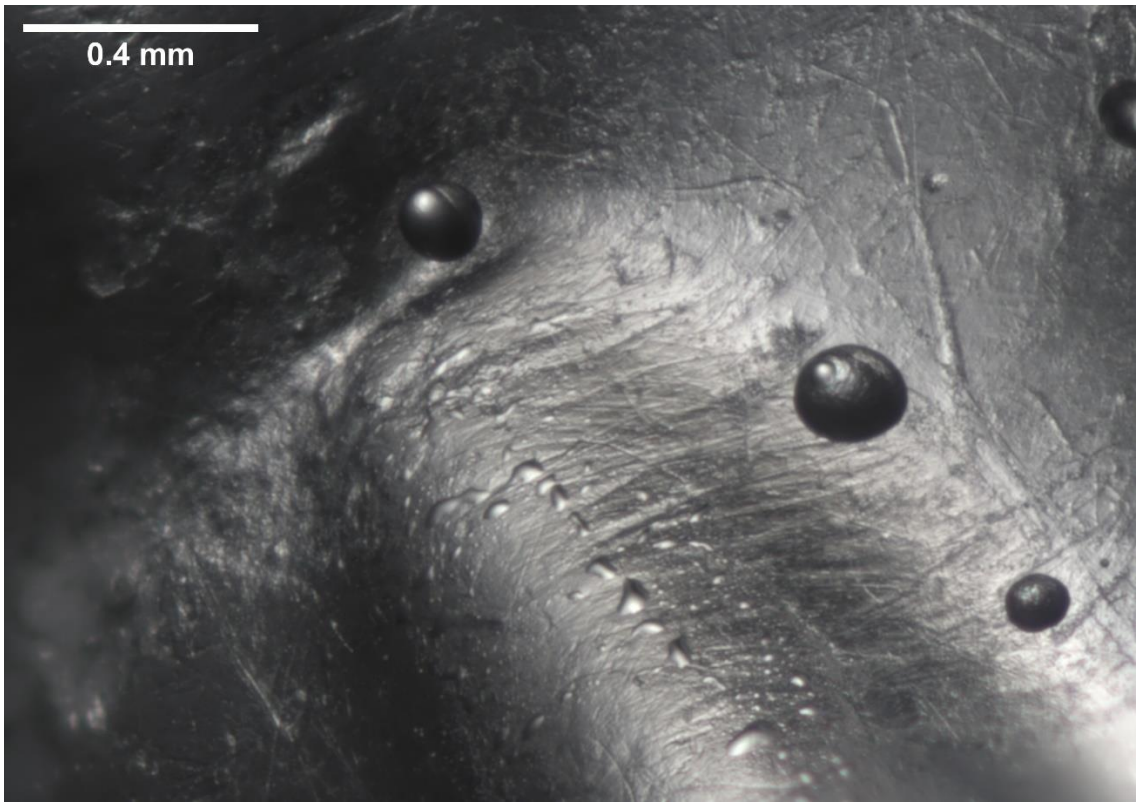

Supplementary Figure 24: Microphotography of sample IPS127527_nofaceta2_2.